Doctoral School of Health Sciences

Faculty of Health Sciences, University of Pécs
Head of the Doctoral School: Prof. Dr. József Bódis MD, Ph.D., DSc

Clinical applications of combined PET/MRI in oncology, head and neck cancer.
Ph.D. Dissertation
Omar Freihat

Program-6*. Oncology – Health Sciences*

Program leader:

Prof. Dr. Istvan Kiss MD, Ph.D., DSc.

Sub-program-6/2*: Diagnostic Medical Imaging*

Sub-program leader: Prof. Dr. Peter Bogner MD, Ph.D.,

Title of research topic*: PET/CT and PET/MRI based treatment modalities in the current Oncology.*

Supervisors:

Dr. habil. Zsolt Cselik MD, Ph.D., Doctoral School of Health Sciences, University of Pécs.

Dr. habil. Arpad Kovacs, MD, Ph.D., Doctoral School of Health Sciences, University of Pécs.

Pécs, 2021

Dedication

To my beloved son

آدم

Adam

TABLE OF CONTENTS

1. THESIS OUTLINES:

In this thesis we studied the use of combined PET/MRI imaging markers in head and neck cancer. The first goal of this thesis was to assess the ability of the DWI for discriminating between benign and malignant lymph node in HNSCC, especially sub-centimeters lymph nodes, since there is an argument weather DWI can differentiate between small lymph nodes <10mm shortest axial diameter. In our work we found that DWI is a useful imaging technique to differentiate between benign and malignant lymph nodes. **Appendix 1.**

The second goal was to compare the diagnostical role of PET/MRI imaging parameters (ADC, SUV, TLG, and MTV) to evaluate patients with OPSCC in reference to their ability to predict HPV as a non-invasive technique and their ability to predict treatment response to chemo/radiotherapy. Based on our results, we have demonstrated through the clinical investigations that DWI is able to play an important role as a non-invasive technique to differentiate between HPV-positive and HPV-negative oropharyngeal cancer as well as the ability of DWI and PET parameters to predict tumors treatment response to therapy. **Appendix 2.**

The third goal was assessing the correlation between the imaging biomarkers from PET and MRI and their ability to prospectively predicting tumor aggressiveness and wither these modalities provide similar information or it can provide complementary information about tumor environment. We found that there is significant correlation between ADC and any of PET imaging parameters, as a result, both imaging parameters are complementary to each other in HNC assessment. **Appendix 3.**

Published and accepted papers within the topic:

1. **Freihat, O**., Pinter, T., Kedves, A. *et al.* Diffusion-Weighted Imaging (DWI) derived from PET/MRI for lymph node assessment in patients with Head and Neck Squamous Cell Carcinoma (HNSCC). *Cancer Imaging* **20,** 56 (2020). https://doi.org/10.1186/s40644-020-00334-x. ***Q1, 2.3 IF.***

2. *Freihat O*, Tóth Z, Pintér T, Kedves A, Sipos D, Cselik Z, Lippai N, Repa I, Kovács Á. Pre-treatment PET/MRI based FDG and DWI imaging parameters for predicting HPV status and tumor response to chemoradiotherapy in primary oropharyngeal squamous cell carcinoma (OPSCC). Oral Oncol. 2021 Feb 25;116:105239. doi: 10.1016/j.oraloncology.2021.105239. Epub ahead of print. PMID: 33640578. ***Q1, 3.99 IF.***

3. Kedves A, Tóth Z, Emri M, Fábián K, Sipos D, **Freihat O**, Tollár J, Cselik Z, Lakosi F, Bajzik G, Repa I and Kovács Á (2020) Predictive Value of Diffusion, Glucose Metabolism Parameters of PET/MR in Patients With Head and Neck Squamous Cell Carcinoma Treated With Chemoradiotherapy. *Front. Oncol.* 10:1484. doi: 10.3389/fonc.2020.01484. ***Q1, 4.98 IF.***

4. Predictive value of PET/CT based metabolic information in the modern 3D based radiotherapy treatment of head and neck cancerpatients – single institute study. Zsolt Cselik[1,2] MD, PhD, Zoltán Tóth[2,8] MD, András Kedves[2,3,6] MSc, Dávid Sipos[2,3,6] MSc, **Omar Freihat**[2] MSc, Tímea Vecsera[3], Gábor Lukács[2,4] MD, PhD, Miklós Emri[5] MD, PhD, Gábor Bajzik[2,6] MD, PhD, Janaki Hadjiev[6] MD, PhD, Imre Repa[2,6] MD, PhD, Mariann Moizs[6] MD, PhD, Árpád Kovács[2,3,7] MD, PhD
Q3, 1.0 IF

Published papers related to topic:

1. Sipos D, Freihat O, Pandur AA, Tollár J, Kedves A, Repa I, Kovács Á, Csima MP. Possible predictors of burnout among radiographers in Hungary: demographic and work related characteristics.
    DOI:https://dea.lib.unideb.hu/dea/bitstream/handle/2437/297151/FILE_UP_1_Knt_0006 24_fin-0002.pdf?sequence=1.

Under review papers within the dissertation topic:

1. Correlation between tissue cellularity and metabolism represented by diffusion weighted imaging (DWI) and 18F-FDG PET/MRI in head and neck cancer (HNC).
    Omar FREIHAT[1*], Zoltán TÓTH MD[1,3], Tamas PINTER MD[2,3], András KEDVES[1,2,5], Dávid SIPOS[1,2,5], Cselik ZSOLT MD PhD[1,4], Imre REPA MD PhD[1,2,3], Árpád KOVÁCS MD PhD[1,6]. BMC Cancer journal, **Q1, 3.3 IF**

3. ABBREVIATIONS:

DWI: Diffusion Weighted Imaging

ADC: Apparent Diffusion Coefficient

AUC: Area Under the Curve

ROI: Region of Interest

PET/MRI: Positron Emission Tomography/Magnetic Resonance Imaging

PET/CT: Positron Emission Tomography/Computed Tomography

HNSCC: Head and Neck Squamous Cell Carcinoma

HPSCC: Hypopharangeal Squamous Cell Carcinoma

LSCC: Laryngeal Squamous Cell Carcinoma

NPC: Nasopharyngeal Carcinoma

OPSCC: Oropharyngeal Squamous Cell Carcinoma

AJCC: American Joint Committee on Cancer

SUV: Standardized Uptake Value

MTV: Metabolic Tumor Volume

TLG: Total Lesion Glycolysis

CRT: Chemo-Radiotherapy

HNC: Head and Neck Cancer

FDG: Fluorodeoxyglucose

(G): Tumor Grade.

HPV: Human papilloma virus

4. INTRODUCTION

4.1. HEAD AND NECK CANCER EPIDIMIOLOGY

Head and neck cancer originates in the upper aerodigestive tract, from the level From the skull base to the thoracic outlet. Head and Neck cancers are a heterogeneous group of cancers that existed anatomically close to each other, but different in terms of etiology, histology, diagnostic, and treatment approaches. (Society for Medical Oncology, 2017) About 91% of all H&N cancer are squamous cell carcinomas, 2% are sarcomas and the other 7% are adenocarcinomas, melanomas, and not well-specified tumors. (European crude and age-adjusted incidence by cancer, years of diagnosis 2000 and 2007 analysis based on 83 population-based cancer registries * 2014). Head and neck squamous cell carcinoma (HNSCC) evolves an assortment of cancers arising in the lip, oral cavity, hypopharynx, oropharynx, nasopharynx, or larynx. (Society for Medical Oncology, 2017). Alcohol and tobacco are known risk factors for most head and neck cancers, and incidence rates are found to be higher in regions with high rates of alcohol and tobacco consumption. (Hashibe et al., 2011)

In 2017, the Global Burden of Disease has been estimated a number of 890,000 new head and neck cancers (HNCs) worldwide, illustrating 5.3% of all cancers. (Fitzmaurice et al., 2019) Based on the most recent epidemiological studies, it has been found that HNC's was attributed to annual 507,000 death's representing 5.3% of all cancer deaths. (Aupérin, 2020). In Hungary, according to the International Agency for Research on Cancer (IARC), there was a total of 70,454 new caners cases in 2018, 6,772 (9.6%) of the total new cancer cases were from HNC as the third most type of cancers incidence. (Globocan, 2019) There were a total of 33,010 deaths due to all types of cancers as the second leading cause of deaths after cardiovascular diseases in Hungary (OECD et al., 2017). HNC cancer deaths were 2,610 deaths representing (7.9%) of all cancer deaths. **Table (1).**

According to data from the Hungarian Central Statistical Office, mortality rate of head and neck cancers has been increased significantly since the 1970s. The number of these cancers has trebled and their mortality has become nearly five-fold. (Tamás, 2018)

Incidence, Mortality and Prevalence by cancer site

Cancer	New cases				Deaths				5-year prevalence (all ages)	
	Number	Rank	(%)	Cum.risk	Number	Rank	(%)	Cum.risk	Number	Prop.
Lung	11 004	1	15.6	7.00	8 893	1	26.9	5.58	11 723	120.99
Breast	8 215	2	11.7	9.20	2 212	3	6.7	2.00	31 217	614.75
Colon	7 065	3	10.0	3.89	3 290	2	10.0	1.52	18 513	191.08
Prostate	5 508	4	7.8	7.75	1 225	7	3.7	1.07	18 340	397.75
Rectum	3 715	5	5.3	2.27	1 768	5	5.4	0.93	10 611	109.52
Bladder	3 391	6	4.8	2.01	950	8	2.9	0.43	10 355	106.88
Pancreas	2 326	7	3.3	1.29	2 078	4	6.3	1.12	1 403	14.48
Kidney	2 296	8	3.3	1.44	831	11	2.5	0.43	5 907	60.97
Stomach	2 089	9	3.0	1.09	1 523	6	4.6	0.74	3 014	31.11
Corpus uteri	1 919	10	2.7	2.21	413	20	1.3	0.35	6 874	135.37
Melanoma of skin	1 724	11	2.4	1.08	351	22	1.1	0.19	5 561	57.40
Non-Hodgkin lymphoma	1 583	12	2.2	0.97	585	17	1.8	0.30	4 538	46.84
Leukaemia	1 451	13	2.1	0.87	872	10	2.6	0.45	3 891	40.16
Cervix uteri	1 312	14	1.9	1.71	499	19	1.5	0.57	4 096	80.66
Lip, oral cavity	1 310	15	1.9	0.89	606	15	1.8	0.42	3 891	40.16
Ovary	1 305	16	1.9	1.48	777	12	2.4	0.79	3 547	69.85
Thyroid	1 191	17	1.7	0.85	95	26	0.29	0.04	4 477	46.21
Larynx	1 099	18	1.6	0.81	526	18	1.6	0.37	3 378	34.86
Liver	1 087	19	1.5	0.66	920	9	2.8	0.54	748	7.72
Brain, nervous system	840	20	1.2	0.55	696	13	2.1	0.44	2 311	23.85
Gallbladder	756	21	1.1	0.34	608	14	1.8	0.26	729	7.52
Oesophagus	746	22	1.1	0.52	592	16	1.8	0.41	799	8.25
Oropharynx	734	23	1.0	0.55	340	23	1.0	0.25	2 468	25.47
Testis	554	24	0.79	0.83	42	29	0.13	0.06	2 392	51.88
Hypopharynx	526	25	0.75	0.40	359	21	1.1	0.27	906	9.35
Multiple myeloma	449	26	0.64	0.28	280	24	0.85	0.15	1 110	11.46
Vulva	251	27	0.36	0.23	106	25	0.32	0.07	779	15.34
Hodgkin lymphoma	221	28	0.31	0.17	38	31	0.12	0.02	900	9.29
Salivary glands	165	29	0.23	0.11	60	28	0.18	0.03	435	4.49
Penis	113	30	0.16	0.17	31	33	0.09	0.04	358	7.76
Nasopharynx	108	31	0.15	0.08	61	27	0.18	0.04	346	3.57
Vagina	68	32	0.10	0.06	32	32	0.10	0.02	189	3.72
Mesothelioma	47	33	0.07	0.03	41	30	0.12	0.03	55	0.57
Anus	29	34	0.04	0.02	18	34	0.05	0.01	83	0.86
Kaposi sarcoma	10	35	0.01	0.00	3	35	0.01	0.00	26	0.27
All cancer sites	70 454	-	-	35.10	33 010	-	-	16.85	185 277	1912.27

Table 1: Incidence, Mortality and Prevalence by cancer site in Hungary 2018.
(Source: https://gco.iarc.fr/today/data/factsheets/populations/348-hungary-fact-sheets.pdf)

4.2.   RISK FACTORS:

Smoking, alcohol consumption are the most important risk factors for developing cancer (Blot et al., 1988), human papillomavirus (HPV) infection, and Epstein-Barr virus (EBV) infection (nasopharyngeal cancers in Asia) are also associated risk factors with head and neck cancer. (Cruz et al., 1997; Sankaranarayanan et al., 1998). Herpes simplex virus (HSV) is another risk factor but is less strongly correlated with the development of oral carcinomas than EBV or HPV. (Larsson et al., 1991) Immunodeficiency is also found to be an important risk factor for developing head and neck cancer, which may increase the incidence by threefold. (Deeken et al., 2012; Grulich et al., 2007) As well as other but less relevant risk factors that may play a role in HNC development such as occupational exposure, radiation, genetic factors, betel nut chewing, poor oral hygiene and periodontal disease, which has been linked with carcinoma of the oral cavity. (Guha et al., 2014; Hashim et al., 2016; Lacko et al., 2014; Sale et al., 2004; Vaughan et al., 1997).

4.3.   CLINICAL EVALUATION

According to the American Joint Committee on Cancer (AJCC) (Edge & Compton, 2010), head and neck cancer arises in the upper aerodigestive tract lining membranes. The TNM classifications described as; T which represents the extent of the primary tumor for each site in the neck area, size, or both, generally the T classifications are similar from different sites with minimal differences in some specific details for each localization, the major sites include (1) the oral cavity, (2) the oropharynx, (3) the hypopharynx, (4) the larynx, (5) the nasopharynx, and (6) nasal and paranasal sinuses, **Figure 1**. N classification, which describes the lymph nodes metastatic in the adjacent lymphatic system. Regional cervical lymph node status is a very important prognostic factor in head and neck cancer and must be evaluated and assessed in each tumor. M classification describes the absence or presence of distant metastases in other organs in the body, most commonly lungs, liver, and bone. After gathering this clinical information, the specific TNM status of each patient is then tabulated to give a numerical status of Stage I, II, III, or IV.
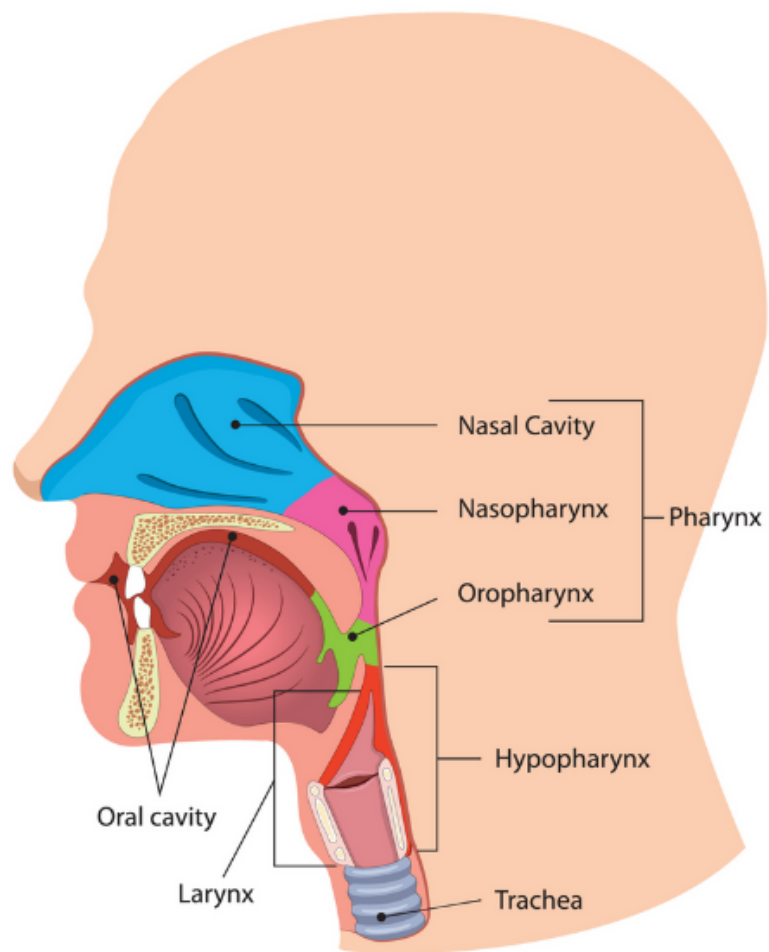
Figure 1: head and neck cancer primary tumor localizations.

(source: https://www.nfcr.org/blog/head-and-neck-cancer-awareness-month/)

Head and neck cancer status of the regional lymph nodes is of such prognostic importance that the cervical nodes must be assessed for each patient and tumor. The lymph nodes may be subdivided into specific anatomic subsites and grouped into seven levels for ease of description. **Figure (2).**
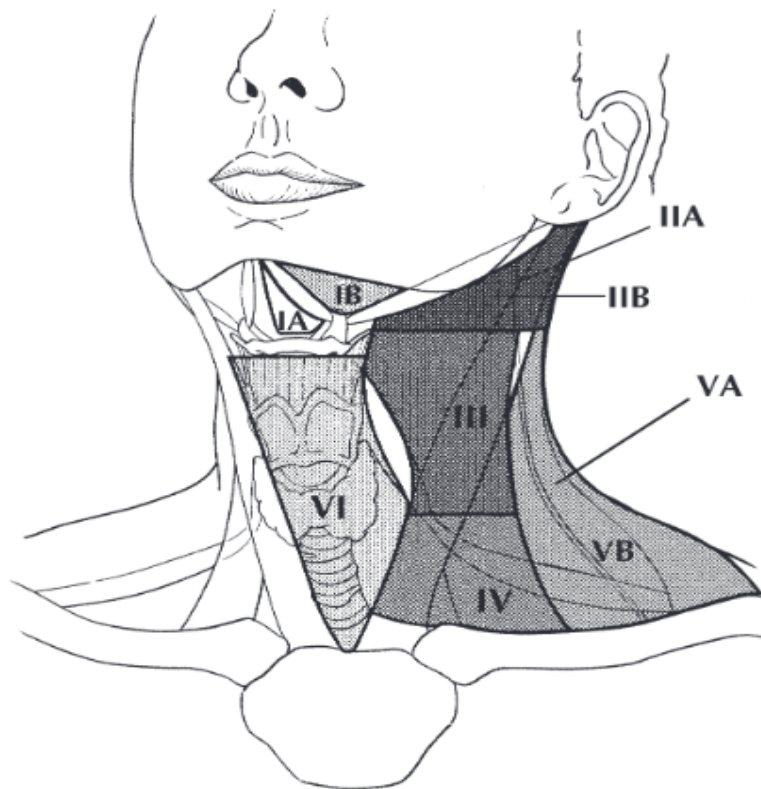

Figure 2: levels of the lymph nodes in the neck area. (Edge & Compton, 2010)

Head and neck cancer lymph node metastases' location plays a significant prognosis role. This has been proved by estimating the survival, which is significantly worse when metastases involve lymph nodes beyond the first echelon of lymphatic drainage and, particularly, lymph nodes in the lower regions of the neck, level IV, and level VB (supraclavicular region).

For a better estimation and assessment of the disease extent before the treatment, imaging modalities and techniques such as computed tomography (CT), magnetic resonance imaging (MRI), positron emission tomography (PET) alone or combined (PET/CT or PET/MRI), as well as Ultrasonography (US), may be applied and, in advanced tumor stages, have added to the accuracy of the primary tumor and lymph node staging, primary localization and regional lymph node involvement. As another useful technique for primary tumor evaluation, Endoscopy, is preferable for a more detailed assessment for T staging. Biopsy, by fine-needle aspiration (FNA) may confirm the presence of the tumor and it's helpful to understand the histopathologic nature of the disease, but, in another context, it can't alone rule out the presence of the disease.

As a new imaging modality, PET/MRI has been had emerged as an effective and accurate imaging modality in oncology. (Partovi et al., 2014) The PET/MRI is expected to be more valuable than PET or CT alone or combined because PET/MRI involves better contrast in soft tissues from the MRI and a lower radiation dose than CT. (Pace L, Nicolai E, Aiello M, Catalano OA, 2013) The superior role of the PET/MRI over other imaging modalities is its ability to perform many functional imaging techniques. (Queiroz et al., 2014) These include DWI which is a widely used technology as a noninvasive diagnosis technology of tissue biology. (Yamauchi H, 2014)

In the clinical field, to discriminate different types of cervical lymph nodes and monitor treatment response imaging technologies have been used, for example, to determine primary tumor and lymph nodes characteristics; such as morphology (shape and size), presences of necrosis, internal cellularity, stage and grade of the primary tumor. (De Bondt et al., 2009; King et al., 2004) These criteria have been succeeded in providing information about the cellularity and the functional aspect of the tumor with the anatomical information, not only for providing information about location and the size of the tumor but also for the tumor functional and biological aspects by monitoring the hypermetabolic areas inside the tumor (Sauter et al., 2013; Veit-Haibach et al., 2013).

Diffusion weighted MRI (DW-MRI) provides information and data on the microscopic motion of water molecules in the tissue, this technique doesn't require contrast media injection to visualize

the structure of the tissue. (Tim Schakel et al., 2013) Water molecules are continuously moving due to thermal equilibrium, which is known as Brownian motion. (Luypaert et al., 2001; Sumi et al., 2006) The diffusion coefficient (expressed in mm2/s) defines the distance water molecules travel, or rather diffuse, over a given time span. (T. Schakel, 2018) The diffusion coefficient in free water at body temperature is 3.0 mm2/s, with a Gaussian distribution. (Tim Schakel et al., 2017) This means that after 50 milliseconds, approximately 32% of the water molecules have traveled 17 meters, while only 5% have traveled 34 meters or more. (Denis Le Bihan & Iima, 2015; Tim Schakel et al., 2017) The free diffusion of water molecules in biological tissues, on the other hand, is hampered by barriers such as cell membranes, macromolecules, and extracellular tortuosity. (Covello et al., 2015) As a consequence, the diffusion coefficient derived from DW-MRI images will no longer represent the water's free diffusion coefficient and will deviate from the Gaussian distribution. (de Figueiredo et al., 2011) To illustrate this effect, the apparent diffusion coefficient (ADC) was developed. (D Le Bihan et al., 1986) Tissues with more barriers limit water movement, resulting in a comparison with the surrounding, less restrictive tissues. (T. Schakel, 2018) Tumors would have more restricted water diffusion due to their increased cellularity and higher degree of tissue disorganization. Tissues that limit diffusion appear bright on diffusion weighted images and have a low ADC value as a result.

Particularly, DWI/MRI, has been suggested as a sensitive sign for differentiating benign from the malignant lesions and monitoring treatment response in head and neck cancer (Kwee et al., 2009; Li et al., 2008; Lin et al., 2010; Maeda et al., 2005; Maeda & Maier, 2008). DW is a non-invasive examination imaging technique that allows characterizing tissues based on the water displacement molecule motion (Herneth et al., 2003; King et al., 2004; Sumi et al., 2006; Taha Ali, 2012), the range of motion is distinguished by its Apparent Diffusion Coefficient (ADC) values (Chawla et al., 2009). The basic concept of DW imaging is exploiting the biologic tissues water indiscriminate motion (Eis et al., 1995; Herneth et al., 2003), the signal loss in the diffusion sequences caused by the water molecule motion which cause phase dispersion of the spin, ADC map can measure the amount of signal loss within the biologic tissue (Herneth et al., 2003; Wu et al., 2011). As a result, the DWI technology shows an ability to differentiate neoplastic tissue from normal tissue, necrotic and inflammatory tissue (Vandecaveye et al., 2010).

Metastatic lymph node in head and neck tumors is a prognostic factor that tends to worsen the prognostics of patients with head and neck neoplasms, the accurate detection and diagnosis will help to optimize the treatment outcomes. (Johnson, 1990) Due to the limitations of the invasive medical interventions (biopsy) which can't always detect heterogeneity of intra-tumor structures from a single attempt, as well as non-rational to perform multiple biopsies for the patient or performing biopsies for all suspected lesions in the individual, (Rasmussen et al., 2017) more realistic diagnostic methods were needed to provide a more inclusive view of tumor texture and biology including internal tumor characteristics. Previous studies have shown that multiparametric imaging can provide precise data for tumor biology and heterogeneity. (Even et al., 2016; Leibfarth et al., 2016) CT and MRI are very useful imaging modalities in the initial assessment and diagnosis of head and neck cancers and it has been widely used for therapy delineation as well as surveillance and post-therapy follow up. (Lee et al., 2013; Razek et al., 2014; Yousem et al., 1992) Morphological characteristics include size, shape, internal biological components and vascularity are important factors associated with the metastatic lymph nodes; although, the accuracy has some limitations.

Moreover, FDG uptake values measured from PET imaging has an important role in head and neck imaging due to its ability to measure the glucose metabolism in the tumors, (Miccò et al., 2014; Toth et al., 2018; Yildirim et al., 2017) which may also reflect the tumor's aggressiveness and the risk of the metastasis to spread to the adjacent structures. (Haerle et al., 2010; Nakajo et al., 2012) Although the SUV is the most common parameter used to estimate glucose metabolism, and it has shown promising results in predicting the presence of lymph nodes metastatic during the primary assessment as well as a predictor of survival and recurrence. (Onal et al., 2013) Recently; new metabolic parameters, TLG and MTV have emerged as new parameters that can measure the glucose metabolism activity of tumors and have been founded to be more effective than SUV because tumor contour is considered when using MTV and TLG. (Kim et al., 2016)

Clinically, there is a periodic and crucial question of whether malignant and normal lesions can be distinguished by DWI/ADC. (Kanmaz & Karavas, 2018) In general, it has been shown that benign lymph nodes have higher ADC values than malignant ones. Nevertheless, for daily use, there is a need for sensible threshold values to help physicians to determine whether the node is malignant

or benign regardless of the invasive procedures followed to determine the nature of these nodes. DWI/ADC offers this non-invasive medical intervention.

BIBLIOGRAPHY

Aupérin, A. (2020). Epidemiology of head and neck cancers: an update. *Current Opinion in Oncology*, *32*(3), 178–186. https://doi.org/10.1097/CCO.0000000000000629

Blot, W. J., McLaughlin, J. K., Winn, D. M., Austin, D. F., Greenberg, R. S., Preston-Martin, S., Bernstein, L., Schoenberg, J. B., Stemhagen, A., & Fraumeni, J. F. J. (1988). Smoking and drinking in relation to oral and pharyngeal cancer. *Cancer Research*, *48*(11), 3282–3287.

Chawla, S., Kim, S., Wang, S., & Poptani, H. (2009). Diffusion-weighted imaging in head and neck cancers. *Future Oncology*, *5*(7), 959–975. https://doi.org/10.2217/fon.09.77

Covello, M., Cavaliere, C., Aiello, M., Cianelli, M. S., Mesolella, M., Iorio, B., Rossi, A., & Nicolai, E. (2015). Simultaneous PET/MR head-neck cancer imaging: Preliminary clinical experience and multiparametric evaluation. *European Journal of Radiology*, *84*(7), 1269–1276. https://doi.org/10.1016/j.ejrad.2015.04.010

Cruz, I., Van den Brule, A. J., Steenbergen, R. D., Snijders, P. J., Meijer, C. J., Walboomers, J. M., Snow, G. B., & Van der Waal, I. (1997). Prevalence of Epstein-Barr virus in oral squamous cell carcinomas, premalignant lesions and normal mucosa--a study using the polymerase chain reaction. *Oral Oncology*, *33*(3), 182–188. https://doi.org/10.1016/s0964-1955(96)00054-1

De Bondt, R. B. J., Hoeberigs, M. C., Nelemans, P. J., Deserno, W. M. L. L. G., Peutz-Kootstra, C., Kremer, B., & Beets-Tan, R. G. H. (2009). Diagnostic accuracy and additional value of diffusion-weighted imaging for discrimination of malignant cervical lymph nodes in head and neck squamous cell carcinoma. *Neuroradiology*, *51*(3), 183–192. https://doi.org/10.1007/s00234-008-0487-2

de Figueiredo, E. H. M. S. G., Borgonovi, A. F. N. G., & Doring, T. M. (2011). Basic concepts of MR imaging, diffusion MR imaging, and diffusion tensor imaging. *Magnetic Resonance Imaging Clinics of North America*, *19*(1), 1–22. https://doi.org/10.1016/j.mric.2010.10.005

Deeken, J. F., Tjen-A-Looi, A., Rudek, M. A., Okuliar, C., Young, M., Little, R. F., & Dezube, B. J. (2012). The rising challenge of non-AIDS-defining cancers in HIV-infected patients.

Clinical Infectious Diseases : An Official Publication of the Infectious Diseases Society of America, *55*(9), 1228–1235. https://doi.org/10.1093/cid/cis613

Edge, S. B., & Compton, C. C. (2010). The American Joint Committee on Cancer: the 7th Edition of the AJCC Cancer Staging Manual and the Future of TNM. *Annals of Surgical Oncology*, *17*(6), 1471–1474. https://doi.org/10.1245/s10434-010-0985-4

Eis, M., Els, T., & Hoehn-Berlage, M. (1995). High resolution quantitative relaxation and diffusion mri of three different experimental brain tumors in rat. *Magnetic Resonance in Medicine*, *34*(6), 835–844. https://doi.org/10.1002/mrm.1910340608

*European crude and age adjusted incidence by cancer, years of diagnosis 2000 and 2007 Analisys based on 83 population-based cancer registries *.* (2014). http://www.rarecarenet.eu/rarecarenet/images/indicators/Incidence.pdf

Even, A. J. G., De Ruysscher, D., & van Elmpt, W. (2016). The promise of multiparametric imaging in oncology: how do we move forward? *European Journal of Nuclear Medicine and Molecular Imaging*, *43*(7), 1195–1198. https://doi.org/10.1007/s00259-016-3361-1

Fitzmaurice, C., Abate, D., Abbasi, N., Abbastabar, H., Abd-Allah, F., Abdel-Rahman, O., Abdelalim, A., Abdoli, A., Abdollahpour, I., Abdulle, A. S. M., Abebe, N. D., Abraha, H. N., Abu-Raddad, L. J., Abualhasan, A., Adedeji, I. A., Advani, S. M., Afarideh, M., Afshari, M., Aghaali, M., … Murray, C. J. L. (2019). Global, regional, and national cancer incidence, mortality, years of life lost, years lived with disability, and disability-Adjusted life-years for 29 cancer groups, 1990 to 2017: A systematic analysis for the global burden of disease study. *JAMA Oncology*, *5*(12), 1749–1768. https://doi.org/10.1001/jamaoncol.2019.2996

Globocan. (2019). Globocan. *Https://Gco.Iarc.Fr/Today/Data/Factsheets/Populations/348-Hungary-Fact-Sheets.Pdf*, *004*, 2018–2019.

Grulich, A. E., van Leeuwen, M. T., Falster, M. O., & Vajdic, C. M. (2007). Incidence of cancers in people with HIV/AIDS compared with immunosuppressed transplant recipients: a meta-analysis. *Lancet (London, England)*, *370*(9581), 59–67. https://doi.org/10.1016/S0140-6736(07)61050-2

Guha, N., Warnakulasuriya, S., Vlaanderen, J., & Straif, K. (2014). Betel quid chewing and the risk of oral and oropharyngeal cancers: a meta-analysis with implications for cancer control. *International Journal of Cancer*, *135*(6), 1433–1443. https://doi.org/10.1002/ijc.28643

Haerle, S. K., Huber, G. F., Hany, T. F., Ahmad, N., & Schmid, D. T. (2010). Is there a correlation

between 18F-FDG-PET standardized uptake value, T-classification, histological grading and the anatomic subsites in newly diagnosed squamous cell carcinoma of the head and neck? *European Archives of Oto-Rhino-Laryngology*, *267*(10), 1635–1640. https://doi.org/10.1007/s00405-010-1348-2

Hashibe, M., Brennan, P., Chuang, S., Boccia, S., Castellsague, X., Chen, C., Curado, M. P., Maso, L. D., Daudt, A. W., Fernandez, L., Wünsch-filho, V., Franceschi, S., Richard, B., Herrero, R., Kelsey, K., Koifman, S., Vecchia, C. La, Mcclean, M. D., Muscat, J., … Andrew, F. (2011). *NIH Public Access Author Manuscript Cancer Epidemiol Biomarkers Prev. Author manuscript; available in PMC 2011 March 9. Published in final edited form as: Cancer Epidemiol Biomarkers Prev. 2009 February ; 18(2): 541–550. doi: 10.1158/1055-9965.EPI-08-0347*. *33*(0). https://doi.org/10.1158/1055-9965.EPI-08-0347.Interaction

Hashim, D., Sartori, S., Brennan, P., Curado, M. P., Wünsch-Filho, V., Divaris, K., Olshan, A. F., Zevallos, J. P., Winn, D. M., Franceschi, S., Castellsagué, X., Lissowska, J., Rudnai, P., Matsuo, K., Morgenstern, H., Chen, C., Vaughan, T. L., Hofmann, J. N., D'Souza, G., … Boffetta, P. (2016). The role of oral hygiene in head and neck cancer: results from International Head and Neck Cancer Epidemiology (INHANCE) consortium. *Annals of Oncology : Official Journal of the European Society for Medical Oncology*, *27*(8), 1619–1625. https://doi.org/10.1093/annonc/mdw224

Herneth, A. M., Guccione, S., & Bednarski, M. (2003). Apparent diffusion coefficient: A quantitative parameter for in vivo tumor characterization. *European Journal of Radiology*, *45*(3), 208–213. https://doi.org/10.1016/S0720-048X(02)00310-8

Johnson, J. T. (1990). A surgeon looks at cervical lymph nodes. *Radiology*, *175*(3), 607–610. https://doi.org/10.1148/radiology.175.3.2188292

Kanmaz, L., & Karavas, E. (2018). The Role of Diffusion-Weighted Magnetic Resonance Imaging in the Differentiation of Head and Neck Masses. *Journal of Clinical Medicine*, *7*(6), 130. https://doi.org/10.3390/jcm7060130

Kim, Y. Il, Paeng, J. C., Cheon, G. J., Suh, K. S., Lee, D. S., Chung, J. K., & Kang, K. W. (2016). Prediction of posttransplantation recurrence of hepatocellular carcinoma using metabolic and volumetric indices of 18F-FDG PET/CT. *Journal of Nuclear Medicine*, *57*(7), 1045–1051. https://doi.org/10.2967/jnumed.115.170076

King, A. D., Tse, G. M. K., Ahuja, A. T., Yuen, E. H. Y., Vlantis, A. C., To, E. W. H., & van

Hasselt, A. C. (2004). Necrosis in metastatic neck nodes: diagnostic accuracy of CT, MR imaging, and US. *Radiology*, *230*(3), 720–726. https://doi.org/10.1148/radiol.2303030157

Kwee, T. C., Quarles van Ufford, H. M. E., Beek, F. J., Takahara, T., Uiterwaal, C. S., Bierings, M. B., Ludwig, I., Fijnheer, R., & Nievelstein, R. A. J. (2009). Whole-Body MRI, Including Diffusion-Weighted Imaging, for the Initial Staging of Malignant Lymphoma. *Investigative Radiology*, *44*(10), 683–690. https://doi.org/10.1097/RLI.0b013e3181afbb36

Lacko, M., Braakhuis, B. J. M., Sturgis, E. M., Boedeker, C. C., Suárez, C., Rinaldo, A., Ferlito, A., & Takes, R. P. (2014). Genetic susceptibility to head and neck squamous cell carcinoma. *International Journal of Radiation Oncology, Biology, Physics*, *89*(1), 38–48. https://doi.org/10.1016/j.ijrobp.2013.09.034

Larsson, P. A., Edström, S., Westin, T., Nordkvist, A., Hirsch, J. M., & Vahlne, A. (1991). Reactivity against herpes simplex virus in patients with head and neck cancer. *International Journal of Cancer*, *49*(1), 14–18. https://doi.org/10.1002/ijc.2910490104

Le Bihan, D, Breton, E., Lallemand, D., Grenier, P., Cabanis, E., & Laval-Jeantet, M. (1986). MR imaging of intravoxel incoherent motions: application to diffusion and perfusion in neurologic disorders. *Radiology*, *161*(2), 401–407. https://doi.org/10.1148/radiology.161.2.3763909

Le Bihan, Denis, & Iima, M. (2015). Diffusion Magnetic Resonance Imaging: What Water Tells Us about Biological Tissues. *PLOS Biology*, *13*(7), e1002203. https://doi.org/10.1371/journal.pbio.1002203

Lee, M. C., Tsai, H. Y., Chuang, K. S., Liu, C. K., & Chen, M. K. (2013). Prediction of nodal metastasis in head and neck cancer using a 3T MRI ADC MAP. *American Journal of Neuroradiology*, *34*(4), 864–869. https://doi.org/10.3174/ajnr.A3281

Leibfarth, S., Simoncic, U., Mönnich, D., Welz, S., Schmidt, H., Schwenzer, N., Zips, D., & Thorwarth, D. (2016). Analysis of pairwise correlations in multi-parametric PET/MR data for biological tumor characterization and treatment individualization strategies. *European Journal of Nuclear Medicine and Molecular Imaging*, *43*(7), 1199–1208. https://doi.org/10.1007/s00259-016-3307-7

Li, S., Xue, H., Li, J., Sun, F., Jiang, B., Liu, D., Sun, H., & Jin, Z. (2008). Application of whole body diffusion weighted MR imaging for diagnosis and staging of malignant lymphoma. *Chinese Medical Sciences Journal = Chung-Kuo i Hsueh k'o Hsueh Tsa Chih*, *23*(3), 138–

144. https://doi.org/10.1016/S1001-9294(09)60028-6

Lin, C., Luciani, A., Itti, E., El-Gnaoui, T., Vignaud, A., Beaussart, P., Lin, S. J., Belhadj, K., Brugières, P., Evangelista, E., Haioun, C., Meignan, M., & Rahmouni, A. (2010). Whole-body diffusion-weighted magnetic resonance imaging with apparent diffusion coefficient mapping for staging patients with diffuse large B-cell lymphoma. *European Radiology*, *20*(8), 2027–2038. https://doi.org/10.1007/s00330-010-1758-y

Luypaert, R., Boujraf, S., Sourbron, S., & Osteaux, M. (2001). Diffusion and perfusion MRI: Basic physics. *European Journal of Radiology*, *38*(1), 19–27. https://doi.org/10.1016/S0720-048X(01)00286-8

Maeda, M., Kato, H., Sakuma, H., Maier, S. E., & Takeda, K. (2005). Usefulness of the apparent diffusion coefficient in line scan diffusion-weighted imaging for distinguishing between squamous cell carcinomas and malignant lymphomas of the head and neck. *American Journal of Neuroradiology*, *26*(5), 1186–1192. https://doi.org/10.3174/ajnr.a0743

Maeda, M., & Maier, S. E. (2008). Usefulness of diffusion-weighted imaging and the apparent diffusion coefficient in the assessment of head and neck tumors. *Journal of Neuroradiology*, *35*(2), 71–78. https://doi.org/10.1016/j.neurad.2008.01.080

Miccò, M., Vargas, H. A., Burger, I. A., Kollmeier, M. A., Goldman, D. A., Park, K. J., Abu-Rustum, N. R., Hricak, H., & Sala, E. (2014). Combined pre-treatment MRI and 18F-FDG PET/CT parameters as prognostic biomarkers in patients with cervical cancer. *European Journal of Radiology*, *83*(7), 1169–1176. https://doi.org/10.1016/j.ejrad.2014.03.024

Nakajo, M., Nakajo, M., Kajiya, Y., Tani, A., Kamiyama, T., Yonekura, R., Fukukura, Y., Matsuzaki, T., Nishimoto, K., Nomoto, M., & Koriyama, C. (2012). FDG PET/CT and diffusion-weighted imaging of head and neck squamous cell carcinoma: Comparison of prognostic significance between primary tumor standardized uptake value and apparent diffusion coefficient. *Clinical Nuclear Medicine*, *37*(5), 475–480. https://doi.org/10.1097/RLU.0b013e318248524a

OECD, on Health Systems, E. O., & Policies. (2017). *Hungary: Country Health Profile 2017*. https://doi.org/https://doi.org/https://doi.org/10.1787/9789264283411-en

Onal, C., Reyhan, M., Parlak, C., Guler, O. C., & Oymak, E. (2013). Prognostic value of pretreatment 18F-fluorodeoxyglucose uptake in patients with cervical cancer treated with definitive chemoradiotherapy. *International Journal of Gynecological Cancer : Official*

Journal of the International Gynecological Cancer Society, *23*(6), 1104–1110. https://doi.org/10.1097/IGC.0b013e3182989483

Pace L, Nicolai E, Aiello M, Catalano OA, S. M. (2013). Whole-body PET/MRI in oncology: current status and clinical applications. *Transl Imaging.*, *1*(1), 31–44.

Partovi, S., Kohan, A., Vercher-Conejero, J. L., Rubbert, C., Margevicius, S., Schluchter, M. D., Gaeta, C., Faulhaber, P., & Robbin, M. R. (2014). Qualitative and Quantitative Performance of [18] F-FDG-PET/MRI versus [18] F-FDG-PET/CT in Patients with Head and Neck Cancer. *American Journal of Neuroradiology*, *35*(10), 1970–1975. https://doi.org/10.3174/ajnr.A3993

Perrone, A., Guerrisi, P., Izzo, L., D'Angeli, I., Sassi, S., Mele, L. Lo, Marini, M. M., Mazza, D., & Marini, M. M. (2011). Diffusion-weighted MRI in cervical lymph nodes: Differentiation between benign and malignant lesions. *European Journal of Radiology*, *77*(2), 281–286. https://doi.org/10.1016/j.ejrad.2009.07.039

Queiroz, M. A., Hüllner, M., Kuhn, F., Huber, G., Meerwein, C., Kollias, S., von Schulthess, G., & Veit-Haibach, P. (2014). PET/MRI and PET/CT in follow-up of head and neck cancer patients. *European Journal of Nuclear Medicine and Molecular Imaging*, *41*(6), 1066–1075. https://doi.org/10.1007/s00259-014-2707-9

Rasmussen, J. H., Nørgaard, M., Hansen, A. E., Vogelius, I. R., Aznar, M. C., Johannesen, H. H., Costa, J., Engberg, A. M. E., Kjær, A., Specht, L., & Fischer, B. M. (2017). Feasibility of multiparametric imaging with PET/MR in head and neck Squamous cell carcinoma. *Journal of Nuclear Medicine*, *58*(1), 69–74. https://doi.org/10.2967/jnumed.116.180091

Razek, A. A. K. A., Tawfik, A. M., Elsorogy, L. G. A., & Soliman, N. Y. (2014). Perfusion CT of head and neck cancer. *European Journal of Radiology*, *83*(3), 537–544. https://doi.org/10.1016/j.ejrad.2013.12.008

Sale, K. A., Wallace, D. I., Girod, D. A., & Tsue, T. T. (2004). Radiation-induced malignancy of the head and neck. *Otolaryngology--Head and Neck Surgery : Official Journal of American Academy of Otolaryngology-Head and Neck Surgery*, *131*(5), 643–645. https://doi.org/10.1016/j.otohns.2004.05.012

Sankaranarayanan, R., Masuyer, E., Swaminathan, R., Ferlay, J., & Whelan, S. (1998). Head and neck cancer: a global perspective on epidemiology and prognosis. *Anticancer Research*, *18*(6B), 4779–4786.

Sauter, A. W., Spira, D., Schulze, M., Pfannenberg, C., Hetzel, J., Reimold, M., Klotz, E., Claussen, C. D., & Horger, M. S. (2013). Correlation between [18F]FDG PET/CT and volume perfusion CT in primary tumours and mediastinal lymph nodes of non-small-cell lung cancer. *European Journal of Nuclear Medicine and Molecular Imaging*, *40*(5), 677–684. https://doi.org/10.1007/s00259-012-2318-2

Schaarschmidt, B. M., Buchbender, C., Nensa, F., Grueneien, J., Gomez, B., Köhler, J., Reis, H., Ruhlmann, V., Umutlu, L., & Heusch, P. (2015). Correlation of the apparent diffusion coefficient (ADC) with the standardized uptake value (SUV) in lymph node metastases of non-small cell lung cancer (NSCLC) patients using hybrid 8F-FDG PET/MRI. *PLoS ONE*, *10*(1), 1–14. https://doi.org/10.1371/journal.pone.0116277

Schakel, T. (2018). *Diffusion weighted MRI for tumor delineation in head and neck radiotherapy*.

Schakel, Tim, Hoogduin, J. M., Terhaard, C. H. J., & Philippens, M. E. P. (2013). Diffusion weighted MRI in head-and-neck cancer: Geometrical accuracy. *Radiotherapy and Oncology*, *109*(3), 394–397. https://doi.org/https://doi.org/10.1016/j.radonc.2013.10.004

Schakel, Tim, Hoogduin, J. M., Terhaard, C. H. J., & Philippens, M. E. P. (2017). Technical Note: Diffusion-weighted MRI with minimal distortion in head-and-neck radiotherapy using a turbo spin echo acquisition method. *Medical Physics*, *44*(8), 4188–4193. https://doi.org/https://doi.org/10.1002/mp.12363

Society for Medical Oncology, E. (2017). *2017 ESMO Essentials for Clinicians Head and Neck Cancers Chapter 1*. 1–6. http://oncologypro.esmo.org/content/download/113133/1971849/file/2017-ESMO-Essentials-for-Clinicians-Head-Neck-Cancers-Chapter-1.pdf

Stejskal, E. O., & Tanner, J. E. (1965). Spin Diffusion Measurements: Spin Echoes in the Presence of a Time-Dependent Field Gradient. *The Journal of Chemical Physics*, *42*(1), 288–292. https://doi.org/10.1063/1.1695690

Sumi, M., Van Cauteren, M., & Nakamura, T. (2006). MR microimaging of benign and malignant nodes in the neck. *American Journal of Roentgenology*, *186*(3), 749–757. https://doi.org/10.2214/AJR.04.1832

Taha Ali, T. F. (2012). Neck lymph nodes: Characterization with diffusion-weighted MRI. *Egyptian Journal of Radiology and Nuclear Medicine*, *43*(2), 173–181. https://doi.org/10.1016/j.ejrnm.2012.01.008

Tamás, J. (2018). *Molecular examination of the microenvironment of head and neck tumors*. 0–21.

Toth, Z., Lukacs, G., Cselik, Z., Bajzik, G., Egyed, M., Vajda, Z., Borbely, K., Hadjiev, J., Gyarmati, T., Emri, M., Kovacs, A., & Repa, I. (2018). [Hungarian clinical application opportunities of PET/MR imaging and first experiences]. *Orvosi hetilap*, *159*(34), 1375–1384. https://doi.org/10.1556/650.2018.31141

Vandecaveye, V., De Keyzer, F., Dirix, P., Lambrecht, M., Nuyts, S., & Hermans, R. (2010). Applications of diffusion-weighted magnetic resonance imaging in head and neck squamous cell carcinoma. *Neuroradiology*, *52*(9), 773–784. https://doi.org/10.1007/s00234-010-0743-0

Vaughan, T. L., Stewart, P. A., Davis, S., & Thomas, D. B. (1997). Work in dry cleaning and the incidence of cancer of the oral cavity, larynx, and oesophagus. *Occupational and Environmental Medicine*, *54*(9), 692–695. https://doi.org/10.1136/oem.54.9.692

Veit-Haibach, P., Schmid, D., Strobel, K., Soyka, J. D., Schaefer, N. G., Haerle, S. K., Huber, G., Studer, G., Seifert, B., & Hany, T. F. (2013). Combined PET/CT-perfusion in patients with head and neck cancers. *European Radiology*, *23*(1), 163–173. https://doi.org/10.1007/s00330-012-2564-5

Wu, X., Kellokumpu-Lehtinen, P.-L., Pertovaara, H., Korkola, P., Soimakallio, S., Eskola, H., & Dastidar, P. (2011). Diffusion-weighted MRI in early chemotherapy response evaluation of patients with diffuse large B-cell lymphoma--a pilot study: comparison with 2-deoxy-2-fluoro- D-glucose-positron emission tomography/computed tomography. *NMR in Biomedicine*, *24*(10), 1181–1190. https://doi.org/10.1002/nbm.1689

Yamauchi H, S. A. (2014). Diffusion imaging of the head and neck. *Curr Radiol Rep. 2014;2:49*, *2*(49).

Yildirim, I. O., Ekici, K., Doğan, M., Temelli, Ö., Kekilli, E., Saglık, S., Erbay, F., & Comak, A. (2017). Can diffusion weighted magnetic resonance imaging (DW-MRI) be an alternative to18f-FDG PET/CT (18f fluorodeoxyglucose positron emission tomography) in nasopharyngeal cancers? *Biomedical Research (India)*, *28*(9), 4255–4260.

Yousem, D. M., Som, P. M., Hackney, D. B., Schwaibold, F., & Hendrix, R. A. (1992). Central nodal necrosis and extracapsular neoplastic spread in cervical lymph nodes: MR imaging versus CT. *Radiology*, *182*(3), 753–759. https://doi.org/10.1148/radiology.182.3.1535890

5. METHODOLOGY:

5.1. DIFFUSION-WEIGHTED IMAGING (DWI) DERIVED FROM PET/MRI FOR LYMPH NODE ASSESSMENT IN PATIENTS WITH HEAD AND NECK SQUAMOUS CELL CARCINOMA (HNSCC)

A retrospective study was conducted for patients who underwent ^{18}F-FDG PET/MRI (3T) for staging and clinical assessment. From April 2016 to July 2019, 65 patients were recruited with confirmed primary HNSCCs. All 65 patients were confirmed with metastatic lymph nodes due to HNSCC (time between imaging scan and biopsy ranged between 1-3 days), and 25 healthy subjects were randomly chosen from the radiology department available database, one node was selected from the neck region for evaluation. ***Appendix 1.***

5.2. PRE-TREATMENT PET/MRI BASED FDG AND DWI IMAGING PARAMETERS FOR PREDICTING HPV STATUS AND TUMOR RESPONSE TO CHEMORADIOTHERAPY INPRIMARY OROPHARYNGEAL SQUAMOUS CELL CARCINOMA (OPSCC).

A retrospective study was conducted for patients underwent imaging from May 2016 to June 2019, 46 patients with proven OPSCC underwent ^{18}F-FDG PET/MRI for staging and restaging, assessment of the disease, and post-therapy follow-up (5-6 months on average). After the inclusion and exclusion criteria, a total of 33 patients were included in our study. Final confirmation of malignancy was done after biopsy of the primary tumor and metastatic lymph nodes. ***Appendix 2.***

5.3. CORRELATION BETWEEN TISSUE CELLULARITY AND METABOLISM REPRESENTED BY DIFFUSION WEIGHTED IMAGING (DWI) AND 18F-FDG PET/MRI IN HEAD AND NECK CANCER (HNC).

From May 2016 to June 2019, 109 patients with proven HNC underwent ^{18}F-FDG PET/MRI for staging and restaging, assessment of the disease. After the inclusion and exclusion criteria, a total of 71 patients were included in our study. Final confirmation of malignancy was done after

PET/MRI examination of the primary tumor and metastatic lymph nodes combined with biopsy.
Appendix 3.

6. IMAGING PROTOCOL:

6.1. APPENDIX 1:

An integrated PET/MRI (3T magnetic field strength) was performed for the head and neck region by OEM neck coil with 16 channels of the head/neck for both conventional and diffusion-weighted MR to cover lymph nodes extending from the skull base to the thoracic outlet. The sequence included a 3D volumetric interpolated breath-hold T1 weighted sequence on the transverse plane and T2 turbo spin-echo imaging (T2WI TSE) on the transverse plane, axial Dixon FS T1-weighted TSE sequence and a coronal TSE Dixon FS sequence on the coronal plane and T1 weighted FS on the axial and coronal plane.

DWI sequence was performed on the axial plane with b values of 0 and 800mm^2/s. DWI pulse sequences were defined as follows: FoV 315 mm, repetition time (TR) 9900 ms, 5 mm slice thickness, voxel size 2.3 x 2.3 x 5 mm and slice gap 10mm. The attenuation correction technique was used based on the Dixon sequence. Images were corrected and reconstructed with an iterative algorithm (21 subsets, 3 iterations, and a Guassian filter (3D iterative (OP-OSEM)) with a full width at half maximum (4 mm) for scatter correction, 172x172 matrix).

6.2. APPENDIX 2 & 3

The examinations were carried out in a dedicated PET/MRI (3 T) unit (Biograph mMR, Siemens AG, Erlangen, Germany) following PET/CT whole-body examinations. Patients were asked to fast for at least 6 h before receiving the 18F-FDG injection and their blood glucose levels were tested to ensure euglycemia before receiving the tracer injection. 18F-FDG with an adapted bodyweight dosage (4 MBq/kg, range 163–403 MBq) Intravenously injected; acquisition began within 75 min (60 ± 10 min after the uptake period) after the FDG tracer injection. On average (15 ± 5 min),

PET/MRI was performed after PET/CT. Images were collected using Head and Neck coils in the supine position. Included were PET/MRI parameters (ADC, SUV, TLG, and MTV).

MRI sequences were T2-weighted TSE turbo inversion recovery magnitude (TIRM) (TR/TE/TI 3300/37/220 ms, FOV: 240 mm, slice thickness: 3 mm, 224 × 320) coronal plan, T1-weighted turbo spin-echo (TSE) (TR/TE 800/12 ms, FOV: 200 mm, slice thickness: 4 mm, 224 × 320) and T1-weighted TSE Dixon fat suppression (FS) (TR/TE 6500/85 ms, FOV: 200 mm, slice thickness: 4 mm, 256 × 320) transversal and were acquired without an intravenous contrast agent. Magnetic resonance-based attenuation correction (MRAC) series was used for PET attenuation correction for the PET data set, and the wide range bed position PET emission scan with a fixed FOV range (20 cm) and matrix (172x172) without bed movement was acquired for 900 s as well. An iterative ordered subset expectation maximization (3D OP-OSEM) PET image reconstruction algorithm was used with 3 iterations and 21 subsets, and 4 mm Gaussian filtering settings. The PET data were corrected for scattering, random coincidences, and attenuation using the MR data.

Diffusion-weighted Imaging (DWI) was obtained by using an axial echo-planar imaging (EPI) sequence with b-values of 0 and 800 and 1,000 s/mm^2 (FoV 315 mm, repetition time TR/TE: 9900/75 ms, 5 mm slice thickness and voxel size 2.3 × 2.3 × 5 mm and slice gap 10 mm). Furthermore, an axial Dixon FS T1-weighted TSE sequence and a coronal TSE Dixon FS sequence were conducted after injection of contrast material (Gadovist© Bayer Healthcare, Leverkusen, Germany) at 0.1 mmol per kg of bodyweight.

7. CLINICAL EVALUATION:

7.1. APPENDIX 1:

The ADC map generated from the DWI was used for the measurement of the ADC values. In each patient with multiple metastatic lymph nodes, the largest lymph node was selected for evaluation. The nodal ADC values were obtained by drawing a region of interest (ROI) covering as much as possible of the most solid and/or homogenous part (most restriction in DWI image), avoiding necrotic parts if the node was partially necrotic while full necrotic nodes were excluded from the study, and avoiding the outer contour of the node. The measurements were made on a single slice

only. "Avg" was the ADC mean average and "Dev" was the standard deviation which represented the homogeneity of the node tissue.

7.2. APPENDIX 2 & 3:

PET SUVmax, TLG, MTV parameters were measured in each patient using Siemens Syngo Via (20VB) application, which provided an automated delineated volumetric analysis based on the SUV. Using the VOI Sphere tool, the metabolic volumetric contours were segmented. VOIs have been assessed blindly to the histopathological characteristics. SUVmax represented the single voxel activity concentration of a specific tumor with the highest SUV. A fixed 2.5 threshold of SUV was used for MTV and TLG calculations. The volume above the given VOI represents MTV while TLG represents the VOI of the average SUVmean multiplied by the MTV.

The ADC map was automatically generated and analyzed on the implemented eRAD picture archive and communicating system (PACS) software. On the ADC map, DWI images were analyzed by drawing a round or oval region of interest (ROI) manually, covering the largest tumor diameter in the most homogenous part within the center of the tumor, the area which represents the lowest ADC or the highest SUV blindly to the histopathological characteristics after excluding or/and avoiding the necrotic and cystic areas. By summing all voxels ADC values on the drawn ROI for the selected slice, the average ADC values determined by the software automatically were referred to as ADCmean. We used the average ADC of the overall area included in the ROI which is calculated automatically by the software, where "Avg" represents the average ADC values for all voxels within the ROI and "Dev" Represents the standard deviation.

8. STATISTICAL ANALYSIS:

8.1. APPENDIX 1

SPSS version 25.0 (IBM Corporation, USA) was used for the statistical analysis. Continuous variables were compared using the Student's t-test or analysis of variance and were expressed as the mean ± standard deviation for the variables with a normal distribution. The Independent sample t-test was used to compare the ADC mean values of the metastatic and the normal lymph nodes as well as between sub-groups analysis. ROC curve was applied to determine the sensitivity and

specificity, AUC, and the optimal threshold to differentiate between normal and malignant nodes. The selection of the optimal threshold was chosen at the point with the highest Youden index (maximizing both sensitivity and specificity). The one-way analysis of variance (ANOVA) was applied to evaluate the coincidence between primary cancer's grade with the metastatic lymph nodes' ADC values and with the primary tumor localization. Post Hoc analysis (Scheffe) was used to compare the parameters in terms of histopathology in case of significant results.

8.2. APPENDIX 2

Statistical analysis was performed by using SPSS 25 (IBM SPSS Statistics, Armonk, New York, USA). The data collected were evaluated using descriptive statistics (mean ± standard deviation), for variables with normal distribution, median, and interquartile range for variables with non-normal distribution. The normality of the measured FDG and DWI was assessed by Shapiro-Wilks test. We used the Spearman correlation coefficient to assess the correlation between FDG and DWI parameters with T stages, N stages, and graders. Mann Whitney test, Wilcoxon's rank-sum test for group comparison with variables not normally distributed; TLG, and MTV ($P<0.001$). ADCmean and SUVmax due to normally distributed were analyzed with independent sample t test for group comparison (HPV status and post-therapy results) and ANOVA test between ADC values and grades of the primary tumor. A Chi-square test was used to assess the association between categorical variables, (HPV, T stages, N stages, grades and post-therapy results). Variables for which $P<0.1$ in univariate analysis were subjected to multiple linear regression analysis to determine those that were independently associated with the imaging parameters by integrating statistical differences in the univariate analysis into the multivariate linear regression model. ROC curve was used to determine the best cut off value to differentiate between HPV+ and HPV-. A p-value <0.05 was indicated as a statistically significant result.

8.3. APPENDIX 3

Statistical analysis was performed by using SPSS 25 (IBM SPSS Statistics, Armonk, New York, USA). The data collected were evaluated using descriptive statistics (mean ± standard deviation),

for variables with normal distribution and median and interquartile range for variables with non-normal distribution. The Spearman rank correlation (r) was used to estimate the association between 18F-FDG parameters and ADC values and tumor size (continues variable). ANOVA or Kruskal–Wallis test were performed on the clinicopathological features that may affect the 18F-FDG and ADC of the tumor. Variables for which P<0.1 in univariate analysis were subjected to multiple linear regression analysis to determine those that were independently associated with the imaging parameters by integrating statistically significant differences in the univariate analysis into the multivariate linear regression model, we used transforming function to convert variables with non-normal distribution into a normal distribution, then the factors were added one by one (Stepwise). Mann-Whitney test and independent-sample T-test were applied to the imaging parameters after the patients were grouped based on lymph nodes involvement into positive (N+) and negative lymph nodes (N-). A p-value <0.05 was indicated as a statistically significant result.

9. RESULTS:

9.1. APPENDIX 1

We assessed the role of DWI in differentiating benign from malignant tumors in HNSCC'S, we found that ADCmean value of the metastatic lymph nodes in the overall sample ($0.899\pm0.98*10^{-3}mm^2/sec$) was significantly lower than the normal lymph nodes' ADCmean value ($1.267\pm0.88*10^{-3}mm^2/sec$); (P=0.001). The area under the curve (AUC) was 98.3%, sensitivity and specificity were 92.3% and 98.6%, respectively, when using a threshold value of ($1.138\pm0.75*10^{-3}mm^2/sec$) to differentiate between both groups. Significant difference was found between metastatic lymph nodes (short-axis diameter <10mm), ADCmean ($0.898\pm0.72*10^{-3}mm^2/sec$), and the benign lymph nodes ADCmean, (P=0.001). No significant difference was found between ADCmean of the metastatic lymph nodes <10mm and the metastatic lymph nodes >10mm, ADCmean ($0.899\pm0.89*10^{-3}mm^2/sec$), (P=0.967). No significant differences were found between metastatic lymph nodes ADCmean values and different primary tumor grades or different primary tumor localization, (P>0.05).

29

9.2.   APPENDIX 2

We compare the diagnostic efficacy of DWI/MRI and FDG metabolic parameters in OPSCC, we found that ADCmean was significantly lower in patients with HPV+ve than HPV-ev, (P = 0.001), cut off value of (800 ± 0.44*10-3mm2 /s) with 76.9% sensitivity, and 72.2% specificity is able to differentiate between the two groups. No significant differences were found between FDG parameters (SUVmax, TLG, and MTV), and HPV status, (P = 0.873, P = 0.958, and P = 0.817), respectively. Comparison between CR and NCR groups; ADCmean, TLG, and MTV were predictive parameters of treatment response, (P = 0.017, P = 0.013, and P = 0.014), respectively. HPV+ve group shows a higher probability of lymph nodes involvement, (P = 0.006).

9.3.   APPENDIX 3

We studied the correlation between the PET/MRI imaging parameters (DWI and FDG) HNSCC and their diagnostical role in different histopathological characteristics, our results show that there waere no significant correlations were observed between DWI and any ^{18}F-FDG parameters (P>0.05). SUVmax and TLG correlated with N-stages (P=0.023, P=0.033), TLG and MTV correlated with T-stages (P=0.006 and P=0.001), ADC correlated with tumor grades (P=0.05). SUVmax and ADC can differentiate between N+ and N- groups (P=0.004, P=0.012)

10. FUTURE PERSPECTIVES:

This thesis demonstrates the use of combined PET/MRI based treatment imaging modality in HNC. First, diffusion weighted imaging has been demonstrated a high accuracy in differentiating between normal and malignant, however, a challenging task was to assess the ability of DWI to differentiate sub-centimeters lymph nodes wither its helpful for early assessment of the small lymph nodes <10 mm in axial diameter (**Appendix 1**). Another issue was to assess of pre-treatment DWI and FDG imaging parameters to assess their diagnostical role in patients with oropharyngeal squamous cell carcinoma, several studies have demonstrated the clinical ability to predict HPV status, however, no studies have compared between these parameters in the same patient's group (**Appendix 2**). As well as their ability from pre-treatment measurements to predict tumor response

to therapy (**Appendix 2**). Although of the controversial results previously in this topic, we found that DWI might be helpful as a non-invasive technique to predict HPV status. On the other side, we didn't a significant role of FDG parameters to differentiate HPV-related from those with HPV-non-related tumors. Furthermore, we found that DWI, TLG and MTV were able to predict tumor response to therapy, which will give more focus on the treatment plans for patients with OPSCC. We also studied the association between tissue cellularity and tissue metabolism offered by DWI and FDG imaging parameters to investigate their importance during treatment and assessment plan, our results show that both imaging parameters might be complementary to each other, so its highly important to perform both examinations for better understanding tumor behavior (**Appendix 3**).

In the future, more focus should be directed to demonstrate the DWI-ADC to assess small lymph nodes which are difficult to demonstrate by the regular methods, since in our research we found that DWI-ADC is able to differentiate those sub-centimeters lymph nodes earlier to prevent invading surrounding tissue. It's also needed to further studies on DWI-ADC for the purpose of classifying OPSCC into HPV-positive and HPV-negative due to the highly importance for treatment planning since several studies have been demonstrated better survival rates in those patients with HPV-positive as well as to accurately staging the OPSCC since HPV-positive might show overrated aggressive tumors while it has shown better results than HPV-negative tumors, thus, HPV-positive might be estimated as more aggressive tumors while the fact is controversial.

DIFFUSION-WEIGHTED IMAGING (DWI) DERIVED FROM PET/MRI FOR LYMPH NODE ASSESSMENT IN PATIENTS WITH HEAD AND NECK SQUAMOUS CELL CARCINOMA (HNSCC). *doi: 10.1186/s40644-020-00334-x*

Abstract:

***Objectives*:** To determine the usefulness of Diffusion Weighted Imaging (DWI) derived from PET/MRI in discriminating normal from metastatic lymph nodes and the correlation between the metastatic lymph nodes with the grade and the localization of the primary tumor.

Material and Methods: Retrospective study of 90 lymph nodes from 90 subjects; 65 patients who had proven histopathological metastatic lymph nodes from (HNSCC) who had undergone ^{18}F-PET/MRI for clinical staging and assessment and twenty-five lymph nodes were chosen from 25 healthy subjects. Apparent Diffusion Coefficient (ADC) map was generated from DWI with *b* values (0 and 800s/mm^2). ADC values of the metastatic lymph nodes were calculated and compared to the normal lymph nodes ADC values, ROC was used to determine the best cut-off values to differentiate between the two group. Metastatic lymph nodes ADC mean values were compared to primary tumor grade and localization.

Results: ADCmean value of the metastatic lymph nodes in the overall sample ($0.899\pm0.98*10^{-3}$mm^2/sec) was significantly lower than the normal lymph nodes' ADCmean value ($1.267\pm0.88*10^{-3}$mm^2/sec); (P=0.001). The area under the curve (AUC) was 98.3%, sensitivity and specificity were 92.3% and 98.6%, respectively, when using a threshold value of ($1.138\pm0.75*10^{-3}$mm^2/sec) to differentiate between both groups. Significant difference was found between metastatic lymph nodes (short-axis diameter <10mm), ADCmean ($0.898\pm0.72*10^{-3}$mm^2/sec), and the benign lymph nodes ADCmean, (P=0.001). No significant difference was found between ADCmean of the metastatic lymph nodes <10mm and the metastatic lymph nodes >10mm, ADCmean ($0.899\pm0.89*10^{-3}$mm^2/sec), (P=0.967). No significant differences were found between metastatic lymph nodes ADCmean values and different primary tumor grades or different primary tumor localization, (P>0.05).

Conclusion: DWI-ADC is an effective and efficient imaging technique in differentiating between normal and malignant lymph nodes and might be helpful to discriminate sub-centimeters lymph nodes.

Trial registration: the trial is registered in clinical trials under **ID:** NCT04360993, registration date: 17/04/2020.

*Keywords***:** MRI, DWI, ADC, HNSCC, metastasis, benign, lymph nodes.

Introduction:

Worldwide, head and neck cancer is the sixth most common malignancy, accounting for approximately 6% of all cancer cases and an estimated 1%–2% of all cancer deaths. (Siegel et al., 2017) H&N cancers are a heterogeneous group of cancers existing anatomically close to each other, but are different in terms of etiology, histology and diagnostic and treatment approaches. (Grégoire et al., 2010) About 91% of all H&N cancers are squamous cell carcinomas, 2% are sarcomas and the other 7% are adenocarcinomas, melanomas and not well-specified tumors. (*European Crude and Age Adjusted Incidence by Cancer, Years of Diagnosis 2000 and 2007 Analisys Based on 83 Population-Based Cancer Registries **, 2014)

Metastatic lymph nodes in head and neck tumors are malicious prediction factors tending to worsen the prognostics of patients with head and neck neoplasms, the accurate detection and diagnosis will help to optimize the treatment outcomes. (Johnson, 1990) Due to the limitations of the invasive medical interventions (biopsy) which can't always detect heterogeneity of intra-tumor structures from a single attempt, as well as non-rational to perform multiple biopsies for the patient or performing biopsies for all suspected lesions in the individual, (Rasmussen et al., 2017) more realistic diagnostic methods were needed to provide a more inclusive view of tumor texture and biology including internal tumor characteristics. Previous studies have shown that multiparametric imaging can provide precise data for tumor biology and heterogeneity. (Even et al., 2016; Leibfarth et al., 2016) CT and MRI are very useful imaging modalities in the initial assessment and diagnosis of head and neck cancers and it has been widely used for therapy delineation as well as surveillance and post-therapy follow up. (Lee et al., 2013; Razek et al., 2014; Yousem et al., 1992) Morphological characteristics include size, shape, internal biological components and vascularity are important factors associated with the metastatic lymph nodes; although, the accuracy has some

limitations. (Lee et al., 2013; van den Brekel et al., 1994). Hybrid Imaging (PET/CT & PET/MRI), on the other hand, was proposed to provide a more accurate and promising non-invasive alternative. (Balyasnikova et al., 2012; Buchbender et al., 2012; Platzek et al., 2013; Rasmussen et al., 2017).

MRI as single scan or combined with PET scan offers a verity of techniques for tissue assessment and intracellular characteristics in Oncology, this includes PET imaging parameters, MR Spectroscopy (MRS), Intravoxel Incoherent Motion (IVIM), Diffusion Tensor Imaging (DTI), Diffusion Kurtosis Imaging (DKI) as well as DWI represented by Apparent Diffusion Coefficient (ADC). (Abdel Razek, 2018; Abdel Razek & Poptani, 2013) DWI as one of these offered techniques by PET/MRI is a non-invasive examination imaging technique allowing for the characterization of tissues based on the water molecule's displacement motion (Brownian motion), (King et al., 2004; Sumi et al., 2006; Taha Ali, 2012) the range of motion is distinguished by its Apparent Diffusion Coefficient (ADC) values. (Chawla et al., 2009) The signal loss in the diffusion sequences is caused by the water molecule's water motion which causes phase dispersion of the spin, and the ADC map can measure the amount of signal loss within the biologic tissue. (Wu et al., 2011, 2013) Clinically, there is a periodic and crucial question of whether malignant and normal lesions can be distinguished by DWI/ADC. (Kanmaz & Karavas, 2018) In general, it has been shown that benign lymph nodes have higher ADC values than malignant ones. Nevertheless, for daily use, there is a need for sensible threshold values to help physicians to determine whether the node is malignant or benign regardless of the invasive procedures followed to determine the nature of these nodes. DWI/ADC offers this non-invasive medical intervention. For example, a study by Das et al. was reported that $1.791 \times 10^{-3} mm^2/s$ ADC cut off value in Sinonasal lesions was able to differentiate between benign and malignant lesions with 80% sensitivity and 83.3% specificity. (Das et al., 2017) Barchetti et al. in a study of cervical lymph nodes in patients with HNSCC reported a cut off value of $0.965 \times 10^{-3} mm^2/sec$ to differentiate between benign and malignant nodes with a sensitivity of 97%, a specificity of 93%, 92% accuracy, 95% PPV, and 96% NPV of. (Barchetti et al., 2014) Wendl et al. in their study of Oral Squamous Cell Carcinoma (OSCC) reported an ADC value of $0.994 \times 10^{-3} mm^2/sec$ as the best threshold with a sensitivity of 80%, a specificity of 65%, 31% PPV, 93% NPV to discriminate between benign and malignant lymph nodes. (Wendl et al., 2016) Suh et. al. their meta-analysis suggested that the median ADC cutoff value of $0.965 \times 10^{-3} mm^2/s$ can differentiate between benign

and malignant nodes. (C.H. Suh, Y.J. Choi, J.H. Baek, 2018) Most recent meta-analysis indicates that the studies which previously used DWI/ADC for differentiating benign from malignant nodes reported limited role due to small sample studies, a wide range of ADC threshold values. (Surov et al., 2020) The study suggested that it may be only lesions with mean ADC values above 1.75×10^{-3} mm^2/s are probably benign. (Surov et al., 2020)

Our work has been built to distinguish between normal and malignant lymph nodes based on the ADC values and validate the standard ADC threshold value for clinical use. As well as to correlate the lymph nodes' ADC values with the grade and the primary tumor localization.

Material and methods:

Patients:

A retrospective study was approved by the Clinical Center, Regional and Local Research Ethics Committee (CCRLREC), Doctoral School of Health Sciences, University of Pecs, and Somogy Megyei Kaposi Mor Educational Hospital, Pecs, Hungary. Approval number (IG/00686-000/2020). Requirement of the informed consent was waived and confirmed by the (CCRLREC) due to the retrospective nature, and all methods were carried out in accordance with the relevant guidelines and regulations (Declaration of Helsinki). From April 2016 to July 2019, 65 patients were recruited with confirmed primary HNSCCs underwent ^{18}F-FDG PET/MRI (3T) for staging and clinical assessment. All 65 patients were confirmed with metastatic lymph nodes due to HNSCC (time between imaging scan and biopsy ranged between 1-3 days), and 25 healthy subjects were randomly chosen from the radiology department available database, one node was selected from the neck region for evaluation. The inclusion criteria used for the patients in the study were: (1) Confirmed primary HNSCC malignancy by biopsy; (2) Multiparametric MR imaging (DWI); (3) PET/MRI for initial staging prior to primary treatment (Surgery or/and radio-chemotherapy); (4) Histopathological results were available for comparison; (5) No previous neck surgery, chemotherapy or (chemo)-radiotherpay. The criteria used for choosing healthy subjects were: (1) Free history of malignancy; (2) No previous neck surgery; (3) No previous treatment by chemo-radiotherapy; and (4) No head and neck lesions, inflammation or abscess or any abnormalities

The criteria used for considering lymph nodes as metastatic was confirmed after (1) Biopsy (gold standard); (2) High FDG accumulation was considered as indication for malignancy in the <10mm group (biopsy/FNA were taken). Metastatic lymph nodes with short-axis diameter <10mm (n =

17) and short-axis diameter >10mm (n = 48). The criteria used for considering lymph nodes as normal were: (1) Free history of malignancy; (2) Ovoid or smooth in shape; and (3) Short-axis diameter <10mm. Figure (1)
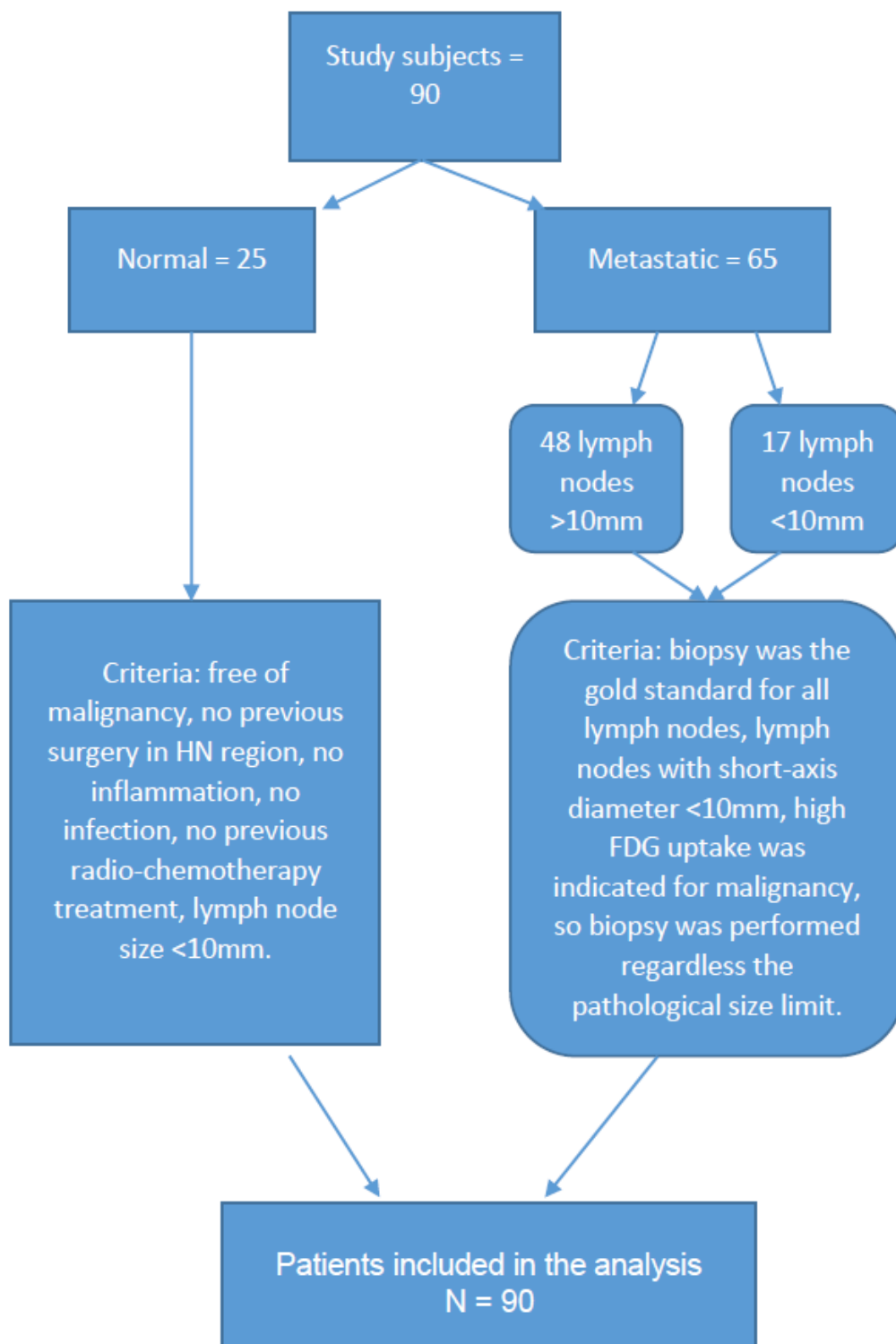
Figure (1). flowchart of the included subjects and the criteria used (Freihat et al., 2020).

Sample demographics were as follow: 65 patients with proven primary HNSCC and 25 healthy subjects. The histological grade of the primary tumor distribution over the primary tumor localization was as follow; well differentiated (G1) (n=10) was in Oropharyngeal (n=1), Hypopharyngeal (n=1), Oral (n=6), Sinus (n=2); moderately differentiated (G2) (n=35) was in Oropharyngeal (n=7), Hypopharyngeal (n=4), Oral (n=11), and Laryngeal (n=11); poorly differentiated (G3) (n= 25) was in Oropharyngeal (n=4), Hypopharyngeal (n=5), Oral (n=7), and Laryngeal (n=7). Patients demographics description in *(Table 1)*.

Table 1. subjects' demographics

Characteristics	Value
Number of lymph nodes	**90**
Metastatic lymph nodes	65 (72.2%)
Benign lymph nodes	25 (27.7%)
Mean age (year)	
Baseline (healthy subjects)	53.4±4.1 (37-64)
Metastatic disease patients	62.3±8.3 (41-82)
Sex (overall)	
Male	59 (65.6 %)
Female	31 (34.4 %)
Primary HNSCC characteristics	
Baseline	25 (27.7%)
Pharyngeal SCC	22 (24.4%)
Oropharyngeal SCC	12 (13.3%)

Hypopharyngeal SCC	10 (11.1%)
Laryngeal SCC	18 (20.0 %)
Oral carcinoma	23 (25.6%)
Sinus carcinoma	2 (2.2%)
Pharyngeal SCC	27 (29.3%)
Tumor grade	
Baseline	25 (27.7%)
Well differentiated	9 (10.0%)
Moderately differentiated	34 (37.8%)
Poorly differentiated	22 (24.4%)
T category	
Baseline	25 (27.7%)
T1	8 (8.7%)
T2	27 (30.0%)
T3	30 (33.3%)
T4	25 (27.8%)
N category	
Baseline	25 (27.7%)
N1	14 (15.6%)
N2	43 (46.7%)
N3	8 (8.9%)

M category	
Baseline	25 (27.7%)
M0	56 (62.3%)
M1	9 (10.0%)

Imaging protocols:

An integrated PET/MRI (3T magnetic field strength) was performed for the head and neck region by OEM neck coil with 16 channels of the head/neck for both conventional and diffusion-weighted MR to cover lymph nodes extending from the skull base to the thoracic outlet. The sequence included a 3D volumetric interpolated breath-hold T1 weighted sequence on the transverse plane and T2 turbo spin-echo imaging (T2WI TSE) on the transverse plane, axial Dixon FS T1-weighted TSE sequence and a coronal TSE Dixon FS sequence on the coronal plane and T1 weighted FS on the axial and coronal plane.

DWI sequence was performed on the axial plane with *b* values of 0 and 800mm^2/s. (Barchetti et al., 2014; Lee et al., 2013; Lombardi et al., 2017) We have chosen two b values because different multiple b values didn't affect the diagnostic performance. (Pereira et al., 2009; Peters et al., 2010) and 800mm^2/s was the best choice to prevent loss of signal and avoiding image distortion which is usually observed at higher b values (Bhatia et al., 2010; Si et al., 2014), most of the previous studies used a range between 0-1000mm^2/s. (Driessen et al., 2014) DWI pulse sequences were defined as follows: FoV 315 mm, repetition time (TR) 9900 ms, 5 mm slice thickness, voxel size 2.3 x 2.3 x 5 mm and slice gap 10mm. The attenuation correction technique was used based on the Dixon sequence. Images were corrected and reconstructed with an iterative algorithm (21 subsets, 3 iterations, and a Guassian filter (3D iterative (OP-OSEM)) with a full width at half maximum (4 mm) for scatter correction, 172x172 matrix).

Image analysis and data interpretation

The PET/MRI examinations were transferred to the main workstation and the patients were assessed by the physicians of the Oncoradiology team at the Baka Jozsef Oncoradiology center. The ADC map generated from the DWI was used for the measurement of the ADC values. In each

patient with multiple metastatic lymph nodes, the largest lymph node was selected for evaluation. The nodal ADC values were obtained by drawing a region of interest (ROI) covering as much as possible of the most solid and/or homogenous part (most restriction in DWI image), (Abdel Razek & Kamal, 2013) avoiding necrotic parts if the node was partially necrotic while full necrotic nodes were excluded from the study, and avoiding the outer contour of the node. The measurements were made on a single slice only. (Lombardi et al., 2017; Wendl et al., 2016) This method was used due its feasibility in the daily use, less time consuming and the results did not differ significantly when compared to other approaches (whole tumor approach for example). (Ahlawat et al., 2016; Han et al., 2017). "Avg" was the ADC mean average and "Dev" was the standard deviation which represented the homogeneity of the node tissue.

Statistical analysis:

SPSS version 25.0 (IBM Corporation, USA) was used for the statistical analysis. Continuous variables were compared using the Student's t-test or analysis of variance and were expressed as the mean ± standard deviation for the variables with a normal distribution. The Independent sample t-test was used to compare the ADC mean values of the metastatic and the normal lymph nodes as well as between sub-groups analysis. ROC curve was applied to determine the sensitivity and specificity, AUC, and the optimal threshold to differentiate between normal and malignant nodes. The selection of the optimal threshold was chosen at the point with the highest Youden index (maximizing both sensitivity and specificity). The one-way analysis of variance (ANOVA) was applied to evaluate the coincidence between primary cancer's grade with the metastatic lymph nodes' ADC values and with the primary tumor localization. Post Hoc analysis (Scheffe) was used to compare the parameters in terms of histopathology in case of significant results.

Results:

Overall, 90 lymph nodes were studied, 65 metastatic lymph nodes: minimum short-axis diameter size (6-44mm) and maximum short-axis diameter size (7-85mm), Figure (2) & Figure (3), were assessed and compared to 25 normal lymph nodes, minimum short-axis diameter size range (4-9mm), and maximum short-axis diameter size range (6-13 mm), Figure (4).
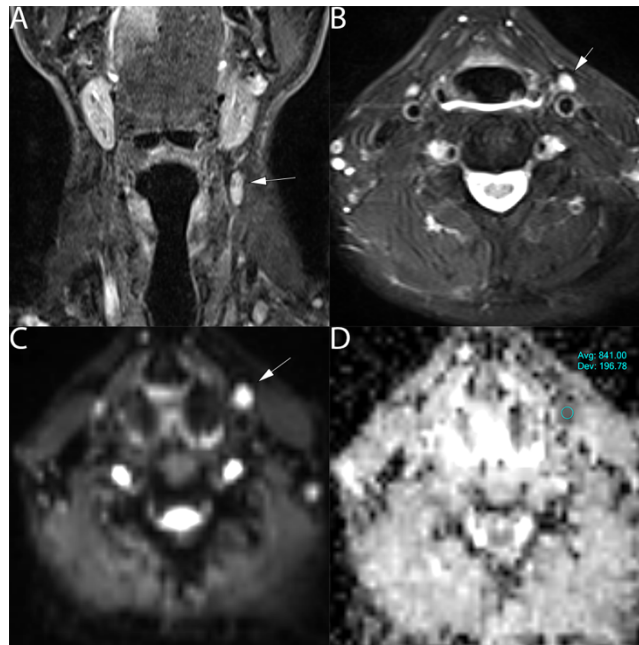

Figure (2). 65 years old male with para-pharyngeal sub-centimeters lymph node positive malignancy from laryngeal SCC on the left side of the neck. (A) T2 coronal show the lymph node, (arrow). (B) T2 axial show the axial extension of the lymph node (6x8mm), (arrow) (C) DWI show hyperintense area at b value 800mm^2/s (arrow) and (D) ADC map on the targeted lymph node show hypointense signal, an ADC value of (0.841±0.19*10^{-3}mm^2/s). (Freihat et al., 2020)
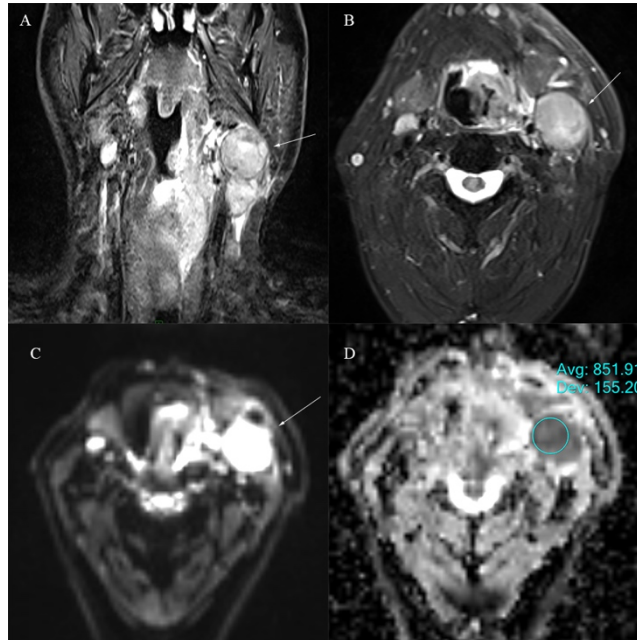
Figure (3). 71 years old male with left positive para-pharyngeal enlarged lymph node from oropharyngeal SCC on the left side of the neck. (A) T2 coronal show enlarged lymph node axial dimensions, (34x35mm) (arrow). (B) T2 axial show the axial extension of the lymph node. (C) DWI show high signal at b value 800mm^2/s and (D) the ADC map on the targeted lymph node show an ADC value of (0.851±0.16*10^{-3}mm^2/s). (Freihat et al., 2020)
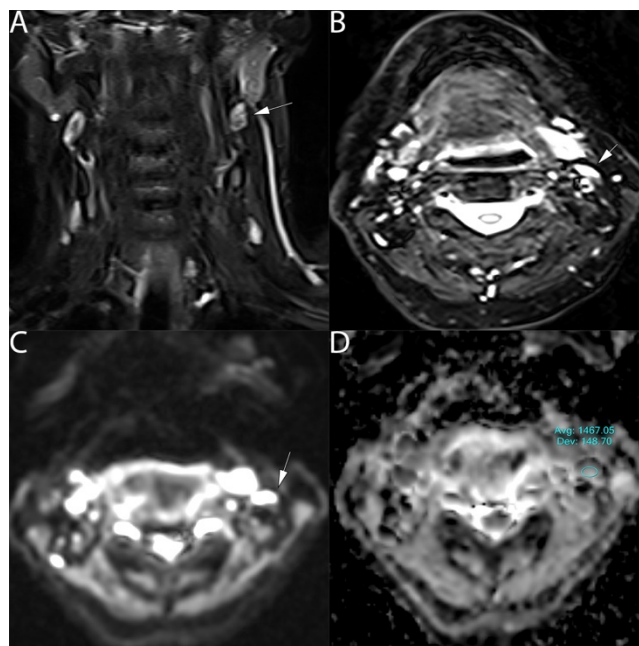
Figure (4). 61 years old healthy male with normal lymph node in the left side of the neck. (A) T2 coronal show normal lymph nodes (arrow). (B) T2 axial view shows the axial extension of the left lymph node, (5x7mm), (arrow). (C) DWI show high signal at b value 800mm^2/s (arrow) and (D) the ADC map on the targeted lymph node show an ADC value of (1.467±0.15*10^{-3}mm^2/s) (arrow).

The ADC values of normal and metastatic lymph nodes:

Biopsy was the gold standard for all metastatic lymph nodes confirmation, sub-centimeters lymph nodes <10mm were first assessed by PET/MRI, lymph nodes that show high FDG uptake were considered for biopsy regardless the pathological size limit, malignancy confirmed lymph nodes by biopsy then considered in the study. According to the statistical analysis after comparing ADC values of the metastatic lymph nodes with ADC values of the normal lymph nodes, the ADCmean value of metastatic lymph nodes (0.899±0.98) was significantly lower than the ADCmean value of normal lymph nodes (1.267± 0.88), (P=0.001), Figure (5A).

To obtain the optimal ADC value to differentiate between metastatic and normal nodes, we applied the ROC curve. The result shows that when using (1.138±0.75) as an optimal threshold value to differentiate between metastatic and normal nodes, the AUC was 98.3%, sensitivity and specificity were 92.3% and 98.6%, respectively. Figure (5B).
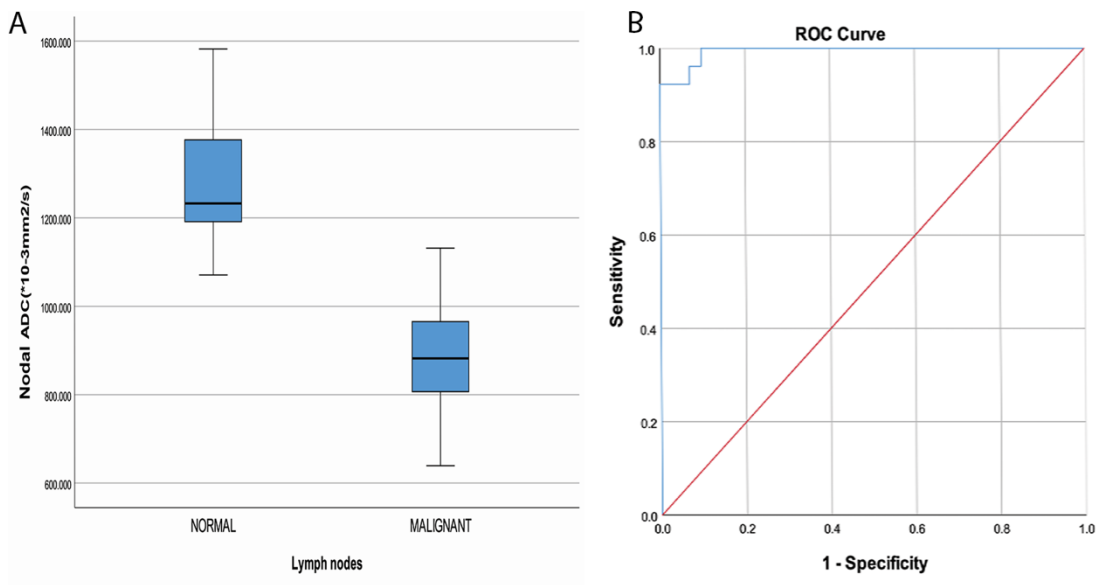
Figure *(5).* (A) Box-and-whisker plots of the normal and metastatic lymph nodes ADC values; significant difference was reported. P<0.05. (B) ROC curve for the ADC value for differentiating between metastatic and normal.

Furthermore, to assess the ability of DWI to discriminate small metastatic lymph, we divided the patients with metastatic lymph nodes into short-axis diameter <10mm (n = 17), and lymph nodes with short-axis diameter >10mm (n = 48) and compared to the ADCmean values with those for the control group (n = 25). The results show that ADCmean values of the metastatic lymph nodes short-axis diameter <10mm (0.898±0.72) was significantly lower than ADCmean values of the normal lymph nodes, (P=0.001). No significant difference found between ADCmean of the metastatic lymph nodes with size <10mm and the metastatic lymph nodes with size >10mm (0.899±0.89), (P=0.967). Figure (6).
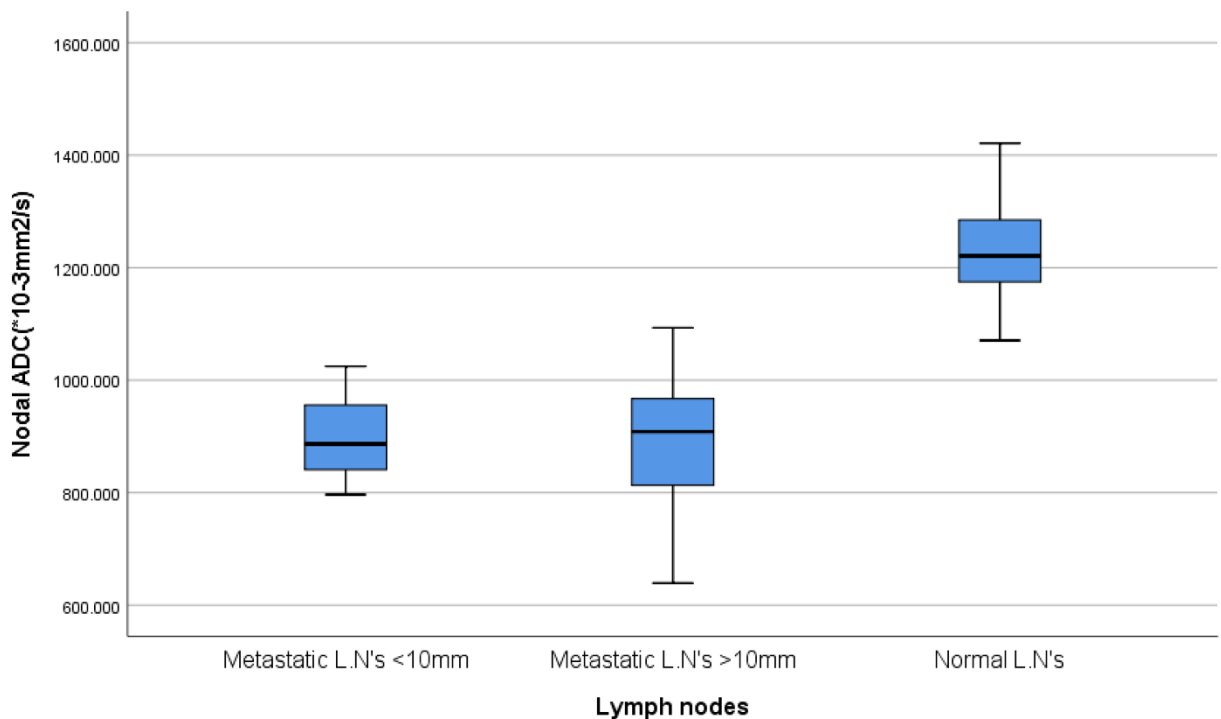

Figure *(6).* Box-and-whisker plots of the mean ADC values of the metastatic lymph nodes sub-grouped into (short-axis diameter <10mm and short-axis diameter >10mm) were significantly lower than normal lymph nodes ADC values (P=0.001), no significant difference between metastatic lymph nodes with short-axis diameter <10mm and metastatic lymph nodes with short-axis diameter >10mm, (P=0.967)

Correlation between the primary HNSCC grade and metastatic lymph nodes' ADC values:

Our results show that metastatic lymph nodes' ADCmean values from poorly differentiated primary HNSCC was (0.863±0.59) and the ADCmean values were (0.916±0.84, 0.936±0.11) for the metastatic lymph nodes from well and moderately differentiated, respectively. Although there was a trend toward decreasing ADC with increasing degree of differentiation, but significant result was not found, (P=0.076). Table (2). Figure (7).
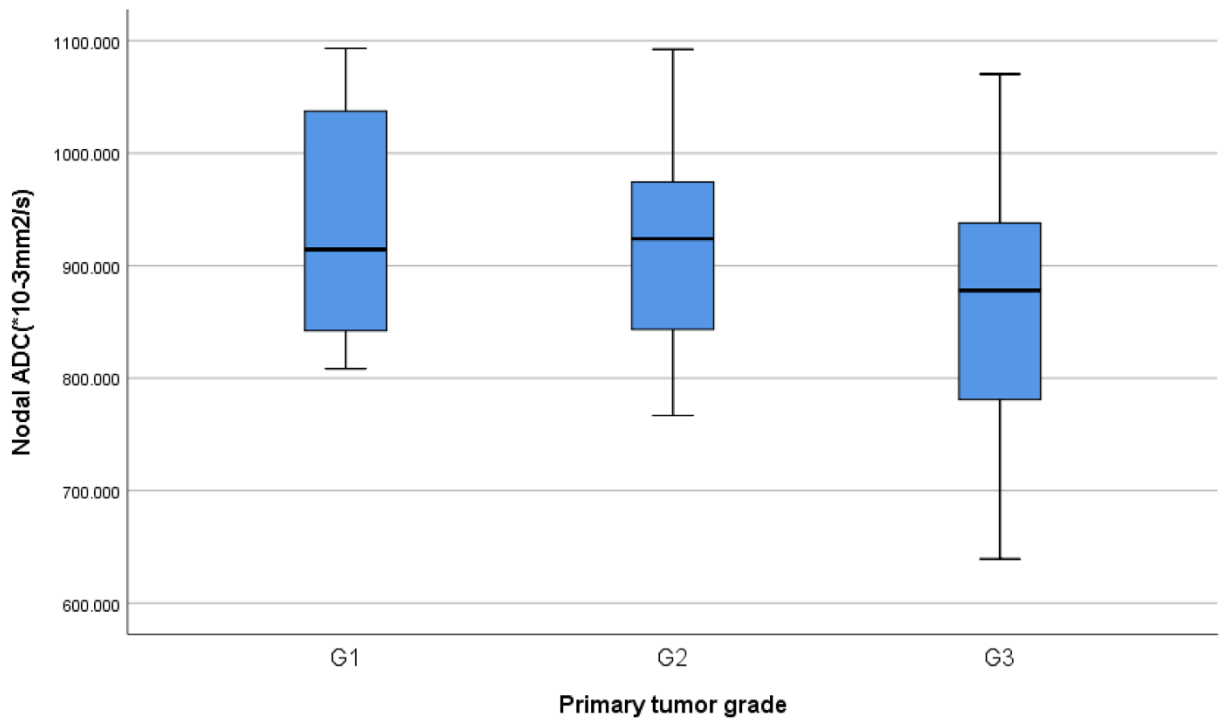

**Figure *(*7). ** (A) Box-and-whisker plots of the lymph nodes ADC according to the primary tumor grades (G1-G3). No significant difference was found between the three grades, P>0.05.

The ADC values of lymph nodes and the correlation with the primary HNSCC tumor localization:

ADCmean values of the metastatic lymph nodes from OPSCC, HPSCC, LSCC, Sinus carcinoma and Oral cavity carcinoma were calculated and assessed, Table (2). ANOVA test was used to compare the groups' mean value differences; ADCmean values were (0.866±0.93, 0.936±0.18, 0.898±0.15, 0.879±0.54, and 0.903±0.95), respectively. No significant difference was found (P=0.431). Table (2). Figure (8).
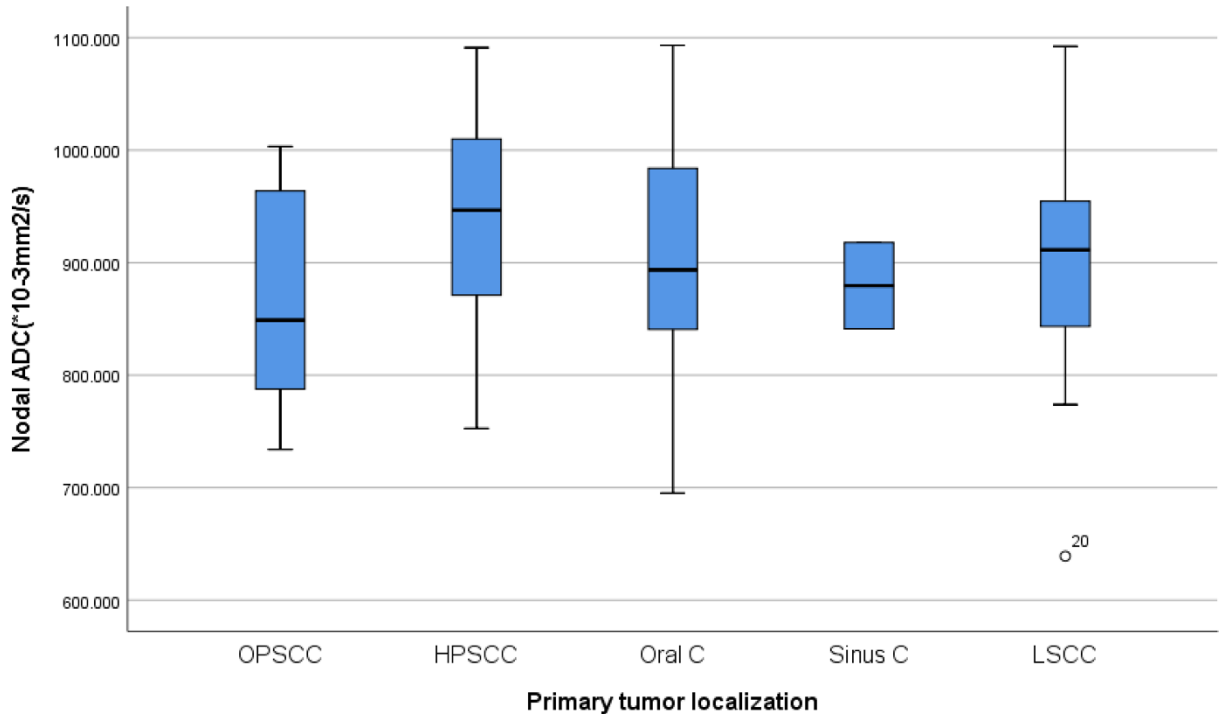
Figure (8). Box-and-whisker plots of the lymph nodes ADC according to the primary tumor localization. No significant differences were reported, P>0.05.

Discussion

In our study, we found a statistically significant difference between metastatic and normal lymph nodes' ADC values (P=0.001); the result was in agreement with previous authors. (Goldsmid & Willis, 2016; Kwee et al., 2011; Perrone et al., 2011; Srinivasan et al., 2012; Taha Ali, 2012) Moreover, our study proposes that the best threshold to differentiate between normal and malignant nodes was ($1.138+0.75*10^{-3}mm^2$/sec), with (92.3%) sensitivity and (98.6%) specificity. Our study shows that DWI might be helpful to discriminate sub-centimeters metastatic lymph nodes.

The characteristics of the malignant tumors in comparison to the benign lesions were the tendency of the malignant tumors to have high cellularity, large nucleus to cytoplasmic ratio, less intercellular space, and a larger number of intercellular organelles than the benign lesions. (Driessen, n.d.) In general, malignant cancers are hyperchromatic, associated with nuclei, and show hypercellularity. (Anderson JR. Tumours, 1985) These features explain why the water molecules are more likely to be restricted in malignant tumors in comparison to benign lesions. (Driessen, n.d.) Moreover, accurate differentiation can prevent patients with non-cancerous lymph

nodes from unnecessary procedures. (Chawla et al., 2013) In addition, the differentiation between the metastatic and benign lymph nodes remain challenging when taking into account that none of the morphological characteristics, such as lymph node size, shape or availability of necrosis is definitely reliable. (Sumi et al., 2003).

Our result was similar to other authors, for example; Vandecaveye et al reported that the best threshold to differentiate between benign and malignant lymph nodes was $0.94*10^{-3}mm^2/sec$. (Vandecaveye et al., 2009) de Bondt et al. found that the best threshold to differentiate between benign and malignant lymph nodes was $1.0*10^{-3}mm^2/sec$. (De Bondt et al., 2009) Perrone et al. were found that a cut-off value of $1.03*10^{-3}mm^2/s$ was the best to differentiate between benign and malignant tumors in their study of the cervical lymph nodes in HNSCC. (Perrone et al., 2011) It's also questionable whether DWI can provide valuable information when measuring sub-centimeters lymph nodes (<10mm), in our study we found that DWI might be useful for discriminating small lymph. According to Barchetti et al. DWI was efficient to differentiate small metastatic lymph nodes in HNSCC, (94.6%) of the measured lymph nodes were <10mm in size, a threshold of $0.965 10^{-3}mm^2/sec$ was used as best cut-off value.(Barchetti et al., 2014) De Bondt et al. found a similar result, DWI was able to differentiate metastatic from benign lesion in HNSCC (95.4% of the measured lymph nodes were <10mm) using an optimal ADC threshold of 1.0×10^{-3} mm^2/s. (De Bondt et al., 2009) Although, other authors found that DWI does not allow to differentiate small metastatic lymph nodes in HNSCC. (Lim et al., 2014)

It has been suggested that the cellularity of the metastatic lymph nodes might be similar to those of the primary tumor, therefore, it was proposed that the ADC values from metastatic lymph nodes from highly and moderately differentiated carcinomas may exhibit higher ADC values than those from poorly differentiated carcinomas. (Sumi et al., 2003) Thus, poorly differentiated (G3) malignancies which are characterized by high mitotic activity will result in a high nucleus cytoplasmic ratio, be comparatively smaller in size, and have higher cellularity of the cells compared to well-moderately differentiated ones (G1, G2). (Bhatt et al., 2017) Therefore, high-grade malignancies tend to have more restricted diffusion than low-grade malignancies. (Bhatt et al., 2017) These clinical suggestions have been studied and proven after having been tested and documented as reliable findings. (Srinivasan et al., 2008)

The results from our study of comparing the metastatic lymph nodes' ADC values with the primary tumor grade showed that the ADC values of the lymph nodes from different primary HNSCC

tumor grades were not significantly different when compared to the lymph nodes from the G1 and G2 primary HNSCCs. This was in agreement with *King et al.* when reported that there was no significant correlation between the ADC values of the metastatic lymph nodes with the grade of the primary tumor. (King et al., 2007) *Nakamatsu et al.* also found no statistical differences in the ADC values of enlarged lymph nodes from the three histological grades of the primary tumors. (Nakamatsu et al., 2012) On the other hand, some studies reported that metastatic lymph nodes ADC values were significantly different when compared to the primary tumor grades. (Abdel Razek et al., 2006; Sumi et al., 2003) Which means that metastatic lymph nodes from higher tumor grade (G3) shows lower ADC values. (Abdel Razek et al., 2006; Sumi et al., 2003) However, our result was controversial to these reports.

We have assessed the metastatic lymph nodes to determine the accuracy of DWI in discriminating lymph nodes from different primary tumor localization. Although the ADC values showed variations, no significant differences were found.

The study's limitations include First, the heterogeneity of the sample, which means multiple primary tumor localization. Second, the result may not be valid for all health centers due to the variation of MRI technologies and b-value strengths (the accuracy and quality of the magnetic field depend on the vendor). Third, only one slice measurements were applied, which may represent weakness in the study, although, we applied this method because it easier to perform, less time consuming and does not differ significantly from other approaches. (Ahlawat et al., 2016; Han et al., 2017) Fourth, retrospective design of the study.

Conclusion:

Our study confirms the feasibility of DWI in differentiating between normal and metastatic lymph nodes. It's also might be useful to differentiate sub-centimeters lymph node.

Bibliography:

Abdel Razek, A. A. K. (2018). Routine and Advanced Diffusion Imaging Modules of the Salivary Glands. *Neuroimaging Clinics of North America*, *28*(2), 245–254. https://doi.org/10.1016/j.nic.2018.01.010

Abdel Razek, A. A. K., & Kamal, E. (2013). Nasopharyngeal carcinoma: Correlation of apparent diffusion coefficient value with prognostic parameters. *Radiologia Medica*, *118*(4), 534–539. https://doi.org/10.1007/s11547-012-0890-x

Abdel Razek, A. A. K., & Poptani, H. (2013). MR spectrsocopy of head and neck cancer. *European Journal of Radiology*, *82*(6), 982–989. https://doi.org/10.1016/j.ejrad.2013.01.025

Abdel Razek, A. A. K., Soliman, N. Y., Elkhamary, S., Alsharaway, M. K., & Tawfik, A. (2006). Role of diffusion-weighted MR imaging in cervical lymphadenopathy. *European Radiology*, *16*(7), 1468–1477. https://doi.org/10.1007/s00330-005-0133-x

Ahlawat, S., Khandheria, P., Del Grande, F., Morelli, J., Subhawong, T. K., Demehri, S., & Fayad, L. M. (2016). Interobserver variability of selective region-of-interest measurement protocols for quantitative diffusion weighted imaging in soft tissue masses: Comparison with whole tumor volume measurements. *Journal of Magnetic Resonance Imaging : JMRI*, *43*(2), 446–454. https://doi.org/10.1002/jmri.24994

Anderson JR. Tumours. (1985). *Anderson JR, ed. Muir's textbook of pathology. 20th ed.*

Balyasnikova, S., Löfgren, J., de Nijs, R., Zamogilnaya, Y., Højgaard, L., & Fischer, B. M. (2012). PET/MR in oncology: an introduction with focus on MR and future perspectives for hybrid imaging. *American Journal of Nuclear Medicine and Molecular Imaging*, *2*(4), 458–474. http://www.ncbi.nlm.nih.gov/pubmed/23145362%0Ahttp://www.pubmedcentral.nih.gov/articlerender.fcgi?artid=PMC3484424

Barchetti, F., Pranno, N., Giraldi, G., Sartori, A., Gigli, S., Barchetti, G., Lo Mele, L., & Marsella, L. T. (2014). The role of 3 Tesla diffusion-weighted imaging in the differential diagnosis of benign versus malignant cervical lymph nodes in patients with head and neck squamous cell carcinoma. *BioMed Research International*, *2014*. https://doi.org/10.1155/2014/532095

Bhatia, K. S. S., King, A. D., Yeung, D. K. W., Mo, F., Vlantis, A. C., Yu, K. H., Wong, J. K. T.,

& Ahuja, A. T. (2010). Can diffusion-weighted imaging distinguish between normal and squamous cell carcinoma of the palatine tonsil? *British Journal of Radiology*, *83*(993), 753–758. https://doi.org/10.1259/bjr/58331222

Bhatt, N., Gupta, N., Soni, N., Hooda, K., Sapire, J. M., & Kumar, Y. (2017). Role of diffusion-weighted imaging in head and neck lesions: Pictorial review. *Neuroradiology Journal*, *30*(4), 356–369. https://doi.org/10.1177/1971400917708582

Buchbender, C., Heusner, T. A., Lauenstein, T. C., Bockisch, A., & Antoch, G. (2012). Oncologic PET/MRI, Part 1: Tumors of the Brain, Head and Neck, Chest, Abdomen, and Pelvis. *Journal of Nuclear Medicine*, *53*(6), 928–938. https://doi.org/10.2967/jnumed.112.105338

C.H. Suh, Y.J. Choi, J.H. Baek, and J. H. L. (2018). The Diagnostic Value of Diffusion-Weighted Imaging in Differentiating Metastatic Lymph Nodes of Head and Neck. *American Journal of Neuroradiology*, *39*, 188–1895.

Chawla, S., Kim, S., Dougherty, L., Wang, S., Loevner, L. A., Quon, H., & Poptani, H. (2013). Pretreatment diffusion-weighted and dynamic contrast-enhanced MRI for prediction of local treatment response in squamous cell carcinomas of the head and neck. *American Journal of Roentgenology*, *200*(1), 35–43. https://doi.org/10.2214/AJR.12.9432

Chawla, S., Kim, S., Wang, S., & Poptani, H. (2009). Diffusion-weighted imaging in head and neck cancers. *Future Oncology*, *5*(7), 959–975. https://doi.org/10.2217/fon.09.77

Das, A., Bhalla, A. S., Sharma, R., Kumar, A., Thakar, A., Vishnubhatla Sreenivas, M., Sharma, M. C., & Sharma, S. C. (2017). Can diffusion weighted imaging aid in differentiating benign from malignant sinonasal masses?: A useful adjunct. *Polish Journal of Radiology*, *82*, 345–355. https://doi.org/10.12659/PJR.900633

De Bondt, R. B. J., Hoeberigs, M. C., Nelemans, P. J., Deserno, W. M. L. L. G., Peutz-Kootstra, C., Kremer, B., & Beets-Tan, R. G. H. (2009). Diagnostic accuracy and additional value of diffusion-weighted imaging for discrimination of malignant cervical lymph nodes in head and neck squamous cell carcinoma. *Neuroradiology*, *51*(3), 183–192. https://doi.org/10.1007/s00234-008-0487-2

Driessen, J. P. (n.d.). *Diffusion-weighted MRI in Head and Neck Squamous Cell Carcinomas*.

Driessen, J. P., Kempen, P. M. W. van, Heijden, G. J. van der, Philippens, M. E. P., Pameijer, F. A., Stegeman, I., Terhaard, C. H. J., Janssen, L. M., & Grolman, W. (2014). Diffusion-

weighted imaging in head and neck squamous cell carcinomas: A systematic review. *Head & Neck*, *36*(10), 1391. https://doi.org/10.1002/HED

*European crude and age adjusted incidence by cancer, years of diagnosis 2000 and 2007 Analisys based on 83 population-based cancer registries *. (2014). http://www.rarecarenet.eu/rarecarenet/images/indicators/Incidence.pdf

Even, A. J. G., De Ruysscher, D., & van Elmpt, W. (2016). The promise of multiparametric imaging in oncology: how do we move forward? *European Journal of Nuclear Medicine and Molecular Imaging*, *43*(7), 1195–1198. https://doi.org/10.1007/s00259-016-3361-1

Freihat, O., Pinter, T., Kedves, A., Sipos, D., Cselik, Z., Repa, I., & Kovács, Á. (2020). Diffusion-Weighted Imaging (DWI) derived from PET/MRI for lymph node assessment in patients with Head and Neck Squamous Cell Carcinoma (HNSCC). *Cancer Imaging*, *20*(1), 1–12. https://doi.org/10.1186/s40644-020-00334-x

Goldsmid, S., & Willis, M. (2016). Methamphetamine use and acquisitve crime: Evidence of a relatonship. *Trends and Issues in Crime and Criminal Justice*, *516*, 1–14. https://doi.org/10.1002/hed

Grégoire, V., Lefebvre, J. L., Licitra, L., & Felip, E. (2010). Squamous cell carcinoma of the head and neck: EHNS-ESMO-ESTRO clinical practice guidelines for diagnosis, treatment and follow-up. *Annals of Oncology*, *21*(SUPPL. 5), 184–186. https://doi.org/10.1093/annonc/mdq185

Han, X., Suo, S., Sun, Y., Zu, J., Qu, J., Zhou, Y., Chen, Z., & Xu, J. (2017). Apparent diffusion coefficient measurement in glioma: Influence of region-of-interest determination methods on apparent diffusion coefficient values, interobserver variability, time efficiency, and diagnostic ability. *Journal of Magnetic Resonance Imaging*, *45*(3), 722–730. https://doi.org/10.1002/jmri.25405

Johnson, J. T. (1990). A surgeon looks at cervical lymph nodes. *Radiology*, *175*(3), 607–610. https://doi.org/10.1148/radiology.175.3.2188292

Kanmaz, L., & Karavas, E. (2018). The Role of Diffusion-Weighted Magnetic Resonance Imaging in the Differentiation of Head and Neck Masses. *Journal of Clinical Medicine*, *7*(6), 130. https://doi.org/10.3390/jcm7060130

King, A. D., Ahuja, A. T., Yeung, D. K. W., Fong, D. K. Y., Lee, Y. Y. P., Lei, K. I. K., & Tse, G. M. K. (2007). Malignant Cervical Lymphadenopathy : Diagnostic Accuracy of

Diffusion-weighted MR Imaging. *Radiology*, *245*(3).

King, A. D., Tse, G. M. K., Ahuja, A. T., Yuen, E. H. Y., Vlantis, A. C., To, E. W. H., & van
Hasselt, A. C. (2004). Necrosis in metastatic neck nodes: diagnostic accuracy of CT, MR
imaging, and US. *Radiology*, *230*(3), 720–726. https://doi.org/10.1148/radiol.2303030157

Kwee, T. C., Ludwig, I., Uiterwaal, C. S., Van Ufford, H. M. E. Q., Vermoolen, M. A., Fijnheer,
R., Bierings, M. B., & Nievelstein, R. A. J. (2011). ADC measurements in the evaluation of
lymph nodes in patients with non-Hodgkin lymphoma: Feasibility study. *Magnetic
Resonance Materials in Physics, Biology and Medicine*, *24*(1), 1–8.
https://doi.org/10.1007/s10334-010-0226-7

Lee, M. C., Tsai, H. Y., Chuang, K. S., Liu, C. K., & Chen, M. K. (2013). Prediction of nodal
metastasis in head and neck cancer using a 3T MRI ADC MAP. *American Journal of
Neuroradiology*, *34*(4), 864–869. https://doi.org/10.3174/ajnr.A3281

Leibfarth, S., Simoncic, U., Mönnich, D., Welz, S., Schmidt, H., Schwenzer, N., Zips, D., &
Thorwarth, D. (2016). Analysis of pairwise correlations in multi-parametric PET/MR data
for biological tumor characterization and treatment individualization strategies. *European
Journal of Nuclear Medicine and Molecular Imaging*, *43*(7), 1199–1208.
https://doi.org/10.1007/s00259-016-3307-7

Lim, H. K., Lee, J. H., Baek, H. J., Kim, N., Lee, H., Park, J. W., Kim, S. Y., Cho, K. J., & Baek,
J. H. (2014). Is diffusion-weighted mri useful for differentiation of small non-necrotic
cervical lymph nodes in patients with head and neck malignancies? *Korean Journal of
Radiology*, *15*(6), 810–816. https://doi.org/10.3348/kjr.2014.15.6.810

Lombardi, M., Cascone, T., Guenzi, E., Stecco, A., Buemi, F., Krengli, M., & Carriero, A.
(2017). Predictive value of pre-treatment apparent diffusion coefficient (ADC) in radio-
chemiotherapy treated head and neck squamous cell carcinoma. *Radiologia Medica*, *122*(5),
345–352. https://doi.org/10.1007/s11547-017-0733-y

Nakamatsu, S., Matsusue, E., Miyoshi, H., Kakite, S., Kaminou, T., & Ogawa, T. (2012).
Correlation of apparent diffusion coefficients measured by diffusion-weighted MR imaging
and standardized uptake values from FDG PET/CT in metastatic neck lymph nodes of head
and neck squamous cell carcinomas. *Clinical Imaging*, *36*(2), 90–97.
https://doi.org/10.1016/j.clinimag.2011.05.002

Pereira, F. P. A., Martins, G., Figueiredo, E., Domingues, M. N. A., Domingues, R. C., Da

Fonseca, L. M. B., & Gasparetto, E. L. (2009). Assessment of breast lesions with diffusion-weighted MRI: Comparing the use of different b values. *American Journal of Roentgenology*, *193*(4), 1030–1035. https://doi.org/10.2214/AJR.09.2522

Perrone, A., Guerrisi, P., Izzo, L., D'Angeli, I., Sassi, S., Mele, L. Lo, Marini, M. M., Mazza, D., & Marini, M. M. (2011). Diffusion-weighted MRI in cervical lymph nodes: Differentiation between benign and malignant lesions. *European Journal of Radiology*, *77*(2), 281–286. https://doi.org/10.1016/j.ejrad.2009.07.039

Peters, N. H. G. M., Vincken, K. L., Van Den Bosch, M. A. A. J., Luijten, P. R., Mali, W. P. T. M., & Bartels, L. W. (2010). Quantitative diffusion weighted imaging for differentiation of benign and malignant breast lesions: The influence of the choice of b-values. *Journal of Magnetic Resonance Imaging*, *31*(5), 1100–1105. https://doi.org/10.1002/jmri.22152

Platzek, I., Beuthien-Baumann, B., Schneider, M., Gudziol, V., Langner, J., Schramm, G., Laniado, M., Kotzerke, J., & Van Den Hoff, J. (2013). PET/MRI in head and neck cancer: Initial experience. *European Journal of Nuclear Medicine and Molecular Imaging*, *40*(1), 6–11. https://doi.org/10.1007/s00259-012-2248-z

Rasmussen, J. H., Nørgaard, M., Hansen, A. E., Vogelius, I. R., Aznar, M. C., Johannesen, H. H., Costa, J., Engberg, A. M. E., Kjær, A., Specht, L., & Fischer, B. M. (2017). Feasibility of multiparametric imaging with PET/MR in head and neck Squamous cell carcinoma. *Journal of Nuclear Medicine*, *58*(1), 69–74. https://doi.org/10.2967/jnumed.116.180091

Razek, A. A. K. A., Tawfik, A. M., Elsorogy, L. G. A., & Soliman, N. Y. (2014). Perfusion CT of head and neck cancer. *European Journal of Radiology*, *83*(3), 537–544. https://doi.org/10.1016/j.ejrad.2013.12.008

Si, J., Huang, S., Shi, H., Liu, Z., Hu, Q., Wang, G., Shen, G., & Zhang, D. (2014). Usefulness of 3T diffusion-weighted MRI for discrimination of reactive and metastatic cervical lymph nodes in patients with oral squamous cell carcinoma: A pilot study. *Dentomaxillofacial Radiology*, *43*(3), 1–9. https://doi.org/10.1259/dmfr.20130202

Siegel, R., Miller, K. D., & Ahmedin, J. (2017). Cancer Statistics. *Ca Cancer Journal*, *67*(1), 7–30. https://doi.org/10.3322/caac.21387.

Srinivasan, A., Chenevert, T. L., Dwamena, B. A., Eisbruch, A., Watcharotone, K., Myles, J. D., & Mukherji, S. K. (2012). Utility of pretreatment mean apparent diffusion coefficient and apparent diffusion coefficient histograms in prediction of outcome to chemoradiation in

head and neck squamous cell carcinoma. *Journal of Computer Assisted Tomography*, *36*(1), 131–137. https://doi.org/10.1097/RCT.0b013e3182405435

Srinivasan, A., Dvorak, R., Perni, K., Rohrer, S., & Mukherji, S. K. (2008). Differentiation of benign and malignant pathology in the head and neck using 3T apparent diffusion coefficient values: Early experience. *American Journal of Neuroradiology*, *29*(1), 40–44. https://doi.org/10.3174/ajnr.A0743

Sumi, M., Sakihama, N., Sumi, T., Morikawa, M., Uetani, M., Kabasawa, H., Shigeno, K., Hayashi, K., Takahashi, H., & Nakamura, T. (2003). Discrimination of metastatic cervical lymph nodes with diffusion-weighted MR imaging in patients with head and neck cancer. *American Journal of Neuroradiology*, *24*(8), 1627–1634.

Sumi, M., Van Cauteren, M., & Nakamura, T. (2006). MR microimaging of benign and malignant nodes in the neck. *American Journal of Roentgenology*, *186*(3), 749–757. https://doi.org/10.2214/AJR.04.1832

Surov, A., Meyer, H. J., & Wienke, A. (2020). Apparent Diffusion Coefficient for Distinguishing Between Malignant and Benign Lesions in the Head and Neck Region: A Systematic Review and Meta-Analysis. *Frontiers in Oncology*, *9*(January), 1–8. https://doi.org/10.3389/fonc.2019.01362

Taha Ali, T. F. (2012). Neck lymph nodes: Characterization with diffusion-weighted MRI. *Egyptian Journal of Radiology and Nuclear Medicine*, *43*(2), 173–181. https://doi.org/10.1016/j.ejrnm.2012.01.008

van den Brekel, M. W., Castelijns, J. A., & Snow, G. B. (1994). Detection of lymph node metastases in the neck: radiologic criteria. *Radiology*, *192*(3), 617–618. https://doi.org/10.1148/radiology.192.3.8058923

Vandecaveye, V., Keyzer, F. De, Poorten, V. Vander, Dirix, P., Verbeken, E., Nuyts, S., & Hermans, R. (2009). Head and Neck Squamous Cell Carcinoma : Value of Diffusion-weighted MR Imaging for Nodal STAGING. *Radiology*, *251*(1), 134–146.

Wendl, C. M., Müller, S., Eiglsperger, J., Fellner, C., Jung, E. M., & Meier, J. K. (2016). Diffusion-weighted imaging in oral squamous cell carcinoma using 3 Tesla MRI: Is there a chance for preoperative discrimination between benign and malignant lymph nodes in daily clinical routine? *Acta Radiologica*, *57*(8), 939–946. https://doi.org/10.1177/0284185115609365

Wu, X., Kellokumpu-Lehtinen, P.-L., Pertovaara, H., Korkola, P., Soimakallio, S., Eskola, H., & Dastidar, P. (2011). Diffusion-weighted MRI in early chemotherapy response evaluation of patients with diffuse large B-cell lymphoma--a pilot study: comparison with 2-deoxy-2-fluoro- D-glucose-positron emission tomography/computed tomography. *NMR in Biomedicine*, *24*(10), 1181–1190. https://doi.org/10.1002/nbm.1689

Wu, X., Pertovaara, H., Dastidar, P., Vornanen, M., Paavolainen, L., Marjomäki, V., Järvenpää, R., Eskola, H., & Kellokumpu-Lehtinen, P. L. (2013). ADC measurements in diffuse large B-cell lymphoma and follicular lymphoma: A DWI and cellularity study. *European Journal of Radiology*, *82*(4), e158–e164. https://doi.org/10.1016/j.ejrad.2012.11.021

Yousem, D. M., Som, P. M., Hackney, D. B., Schwaibold, F., & Hendrix, R. A. (1992). Central nodal necrosis and extracapsular neoplastic spread in cervical lymph nodes: MR imaging versus CT. *Radiology*, *182*(3), 753–759. https://doi.org/10.1148/radiology.182.3.1535890

Abstract:

Objectives: To determine the feasibility of pre-treatment primary tumor FDG-PET and DWI-MR imaging parameters in predicting HPV status and the second aim was to assess the feasibility of those imaging parameters to predict response to therapy.

Material and Methods: We retrospectively analyzed primary tumors in 33 patients with proven OPSCC. PET/MRI was performed before and 6 months after chemo-radiotherapy for assessing treatment response. PET Standardized uptake value (SUVmax), total lesion glycolysis (TLG), metabolic tumor volume (MTV), and apparent diffusion coefficient (ADC) from pre-treatment measurements were assessed and compared to the clinicopathological characteristics (T stages, N stages, tumor grades, HPV and post-treatment follow up). HPV was correlated to the clinicopathological characteristics.

Results: ADCmean was significantly lower in patients with HPV+ve than HPV-ev, $(P = 0.001)$, cut off value of $(800 \pm 0.44*10\text{-}3mm2\ /s)$ with 76.9% sensitivity, and 72.2% specificity is able to differentiate between the two groups. No significant differences were found between FDG parameters (SUVmax, TLG, and MTV), and HPV status, $(P = 0.873, P = 0.958,$ and $P = 0.817)$, respectively. Comparison between CR and NCR groups; ADCmean, TLG, and MTV were predictive parameters of treatment response, $(P = 0.017, P = 0.013,$ and $P = 0.014)$, respectively. HPV+ve group shows a higher probability of lymph nodes involvement, $(P = 0.006)$.

Conclusion: Our study found that pretreatment ADC of the primary tumor can predict HPV status and treatment response. On the other hand, metabolic PET parameters (TLG, and MTV) were able to predict primary tumor response to therapy.

Keywords: Diffusion-Weighted Imaging; Head and Neck Squamous Cell Carcinoma, PET/MRI, HPV, Therapy response, primary tumor.

Abbreviations: *PET/MRI: Positron Emission Tomography/Magnetic Resonance Imaging *SUV: Standardized Uptake Value *MTV: Metabolic Tumor Volume *TLG: Total Lesion Glycolysis *CRT: Chemo-Radiotherapy *HCC: Head and Neck Cancer *FDG: Fluorodeoxyglucose *AJCC: American Joint Committee on Cancer. *OPSCC: oropharyngeal squamous cell carcinoma. *EORTC: European Organization for Research and Treatment of Cancer

Introduction:

There is an increasing incidence worldwide for reporting aggressive OPSCC. (Marur et al., 2010) Alcohol and tobacco are the most etiological factors of developing OPCCS. (Ang et al., 2010; Gillison et al., 2012) It has been also found that high-risk sexual behavior is a growing factor for increasing HPV-positive especially among young people. (Benson E, Li R, 2014) There are several biological, clinical, and epidemiological to distinguish HPV-positive from HPV-negative entities. (Glastonbury et al., 2017) Previous studies have demonstrated that patients with positive HPV have been shown better response to therapy and better survival compared to negative HPV. (Huang et al., 2013; Leemans et al., 2011; O'Sullivan et al., 2013)

DWI-MRI as a non-invasive technique is a widely used technology to assess the motion of water molecules (Brownian motion) as a noninvasive diagnosis technology of tissue biology, (Yamauchi H, 2014) by taking apart the texture of a biologic tissue based on the water molecules motion at a microscopic level.(Queiroz et al., 2014) Several studies have reported the feasibility of DWI represented as apparent diffusion coefficient (ADC) in clinical uses ranging from interpretation microstructures of the tumors to the assessment of treatment response to therapy. (Jansen et al., 2010; Vandecaveye et al., 2012) Moreover, DWI weighted imaging has been shown promising results for the assessment of HPV in patients with OPSCC. (Nakahira et al., 2014; Payabvash et al., 2019; Ravanelli et al., 2018).

The combined PET/MRI imaging modality used nowadays, offers wider imaging parameters to assess tissue microstructure. In addition to DWI, it provides information from the metabolic parameters which assess the tumor metabolism, as such, maximum standardized uptake value (SUVmax) which represents maximum FDG uptake in the tumor has been found to provide prognostic information in HNSCC, although, the information gathered was controversial. (Kim et

al., 2015; Mena et al., 2017; Romesser et al., 2012) Volumetric FDG parameters such as total lesion glycolysis (TLG) and metabolic tumor volume (MTV) have been also widely studied. (Kyoungjune Pak et al., 2014) TLG and MTV derived from F-18FDG-PET have been shown to have prognostic significance in HNSCC, including HPV-associated OPSCCs. (Alluri et al., 2014; Lim et al., 2012; Schwartz et al., 2016; Tahari et al., 2014a) As well as several studies have demonstrated the ability of MTV and TLG to predict treatment outcomes in OPSCC. (Kikuchi et al., 2015; Kim et al., 2015; Martens, Noij, Ali, et al., 2019; Mena et al., 2017; Pollom et al., 2016) The purpose of our study was to assess and compare the prognostic value of the FDG PET (SUVmax, TLG, and MTV) and DWI imaging parameters in predicting HPV status and prognostic value after 6 months of treatment.

Materials and methods:

A retrospective study was approved by the Clinical Center, Regional and Local Research Ethics Committee (CCRLREC), Doctoral School of Health Sciences, University of Pecs, and Somogy County Mór Kaposi Teaching Hospital, Kaposvar, Hungary. The requirement of the informed consent was waived and confirmed by the (CCRLREC) due to the retrospective nature, and all methods were carried out following the relevant guidelines and regulations (Declaration of Helsinki). From May 2016 to June 2019, 46 patients with proven OPSCC underwent ^{18}F-FDG PET/MRI for staging and restaging, assessment of the disease, and post-therapy follow-up (5-6 months on average). The inclusion criteria were (1) proved non-treated primary OPSCC, (2) patients underwent PET/MRI including DWI sequence (3) HPV test was performed. Exclusion criteria were: (1) patients who had non-measurable ADC (2) patients with motion artifact or suboptimal image quality including motion artifacts, and patients who did not underwent post-therapy follow up. Finally, a total of 33 patients were included in our study. *Table (1)*. Final confirmation of malignancy was done after biopsy of the primary tumor and metastatic lymph nodes.

Table1: patients demographics

Number of patients	*33*
Mean Age (y)	*(61.4±0.7)*

Men	*23 (69.7%)*
Women	*10 (30.3%)*
Histologic Grade	
Well-differentiated	*4 (12.1%)*
Moderately differentiated	*14 (42.4%)*
Poorly- differentiated	*15 (45.5%)*
Primary tumor	
Palatine tonsil	*7 (21.2%)*
Tongue root	*15 (45.5%)*
Soft palate	*2 (64.1%)*
Pharyngeal wall	*9 (27.3%)*
T category	
T1	*2 (6.1%)*
T2	*13 (39.3%)*
T3	*12 (36.4%)*
T4	*6 (18.2%)*
N category	
N0	*3 (9.1%)*
N1	*6 (18.2%)*
N2	*16 (48.5%)*

N3	*8 (24.2%)*
M Category	
M0	*32 (97.0%)*
M1	*1 (3.0%)*
HPV STATUS	
HPV+	*17 (51.5%)*
HPV -	*16 (48.5%)*
Treatment response	
CR	*21 (63.6%)*
NCR	*12(36.4%)*

PET/MRI imaging:

The examinations were carried out in a dedicated PET/MRI (3 T) unit (Biograph mMR, Siemens AG, Erlangen, Germany) following PET/CT whole-body examinations. Patients were asked to fast for at least 6 h before receiving the 18F-FDG injection and their blood glucose levels were tested to ensure euglycemia before receiving the tracer injection. 18F-FDG with an adapted bodyweight dosage (4 MBq/kg, range 163–403 MBq) Intravenously injected; acquisition began within 75 min (60 ± 10 min after the uptake period) after the FDG tracer injection (Kedves et al., 2020). On average (15 ± 5 min), PET/MRI was performed after PET/CT. Images were collected using Head and Neck coils in the supine position. Included were PET/MRI parameters (ADC, SUV, TLG, and MTV) (Kedves et al., 2020).

MRI sequences were T2-weighted TSE turbo inversion recovery magnitude (TIRM) (TR/TE/TI 3300/37/220 ms, FOV: 240 mm, slice thickness: 3 mm, 224×320) coronal plan, T1-weighted turbo spin-echo (TSE) (TR/TE 800/12 ms, FOV: 200 mm, slice thickness: 4 mm, 224×320) and T1-weighted TSE Dixon fat suppression (FS) (TR/TE 6500/85 ms, FOV: 200 mm, slice thickness: 4 mm, 256×320) transversal and were acquired without an intravenous contrast agent. Magnetic resonance-based attenuation correction (MRAC) series was used for PET attenuation correction for the PET data set, and the wide range bed position PET emission scan with a fixed FOV range (20 cm) and matrix (172x172) without bed movement was acquired for 900 s as well. An iterative ordered subset expectation maximization (3D OP-OSEM) PET image reconstruction algorithm was used with 3 iterations and 21 subsets, and 4 mm Gaussian filtering settings. The PET data were corrected for scattering, random coincidences, and attenuation using the MR data (Kedves et al., 2020).

Diffusion-weighted Imaging (DWI) was obtained by using an axial echo-planar imaging (EPI) sequence with b-values of 0 and 800 and 1,000 s/mm^2 (FoV 315 mm, repetition time TR/TE: 9900/75 ms, 5 mm slice thickness and voxel size $2.3 \times 2.3 \times 5$ mm and slice gap 10 mm). Furthermore, an axial Dixon FS T1-weighted TSE sequence and a coronal TSE Dixon FS sequence were conducted after injection of contrast material (Gadovist© Bayer Healthcare, Leverkusen, Germany) at 0.1 mmol per kg of bodyweight (Freihat et al., 2020; Kedves et al., 2020).

Image analysis:

PET SUVmax, TLG, MTV parameters were measured in each patient using Siemens Syngo Via (20VB) application, which provided an automated delineated volumetric analysis based on the SUV. Using the VOI Sphere tool, the metabolic volumetric contours were segmented. VOIs have been assessed blindly to the histopathological characteristics. SUVmax represented the single voxel activity concentration of a specific tumor with the highest SUV (Kedves et al., 2020). A fixed 2.5 threshold of SUV was used for MTV and TLG calculations proposed by Pak et al (Kyoungjune Pak et al., 2014) The volume above the given VOI represents MTV while TLG represents the VOI of the average SUVmean multiplied by the MTV (Kedves et al., 2020)

The ADC map was automatically generated and analyzed on the implemented eRAD picture archive and communicating system (PACS) software. On the ADC map, DWI images were analyzed by drawing a round or oval region of interest (ROI) manually, covering the largest tumor diameter (Miccò et al., 2014), on a single DWI slice (Fruehwald-Pallamar et al., 2011) in the most homogenous part within the center of the tumor, the area which represents the lowest ADC or the highest SUV blindly to the histopathological characteristics after excluding or/and avoiding the necrotic and cystic areas. We didn't use the whole tumor volume technique for calculating ADC value while this method is more reproducible than those obtained from the measurements of a single slice or small ROI, the explanation is that there was no significant difference between the tumor ADCs obtained using whole-volume measurements and the single-slice approach (Lambregts et al., 2011). Thus, we chose the single-slice approach because it's simpler, quicker, and as a result, more favored in clinical practice than the whole volume ROIs protocol which is time-consuming and more complicated. By summing all voxels ADC values on the drawn ROI for the selected slice, the average ADC values determined by the software automatically were referred to as ADCmean. We evaluated ADCmean values only, which was previously proposed as a more reliable indicator of tumor cellularity since the entire lesion is taken into account (Jeong et al., 2016) Besides, ADCmean minimizes the effect of tumor heterogeneity and its higher reliability to distinguish different entities in the same image (Sakane et al., 2015). We used the average ADC of the overall area included in the ROI which is calculated automatically by the software, where "Avg" represents the average ADC values for all voxels within the ROI and "Dev" Represents the standard deviation.

Clinical evaluation:

To evaluate the treatment results of the primary tumor based on pre and post-therapy PET/CT and PET/MRI data, we used the European Organization for Research and Treatment of Cancer (EORTC) system. (Young et al., 1999) To evaluate the predictive value of the pre-treatment imaging parameters we created two patient's groups based on the PET/MRI therapeutic response and clinical follow-up. The two groups were representing complete remission (CR) which includes only patients with complete remission and non-complete remission (NCR) which includes patients with partial response, stable disease, and progressive disease patients.

Analysis of the HPV status:

Immunohistochemistry of p16 protein overexpression from tumor blocks (Ventana Medical System – p16 protocol, Roche p16 cintec histology assay antibody 1: 5 dilution) was performed by the pathology department of Csolnoky Ferenc hospital from the primary tumor to detect the presence of high-risk HPV infection. We identified cases as positive, in which we observed so-called "block positivity", meani g both the nucleus and the plasma show strong staining in the tumor cells. Additional staining patterns (e.g., cytoplasmic only) were assessed as negative.

Statistical analysis:

Statistical analysis was performed by using SPSS 25 (IBM SPSS Statistics, Armonk, New York, USA). The data collected were evaluated using descriptive statistics (mean ± standard deviation), for variables with normal distribution, median, and interquartile range for variables with non-normal distribution. The normality of the measured FDG and DWI was assessed by Shapiro-Wilks test. We used the Spearman correlation coefficient to assess the correlation between FDG and DWI parameters with T stages, N stages, and graders. Mann Whitney test, Wilcoxon's rank-sum test for group comparison with variables not normally distributed; TLG, and MTV ($P<0.001$). ADCmean and SUVmax due to normally distributed were analyzed with independent sample t test for group comparison (HPV status and post-therapy results) and ANOVA test between ADC values and grades of the primary tumor. A Chi-square test was used to assess the association between categorical variables, (HPV, T stages, N stages, grades and post-therapy results). Variables for which $P<0.1$ in univariate analysis were subjected to multiple linear regression analysis to determine those that were independently associated with the imaging parameters by integrating statistical differences in the univariate analysis into the multivariate linear regression model. ROC

curve was used to determine the best cut off value to differentiate between HPV+ and HPV-. A p-value <0.05 was indicated as a statistically significant result.

Results:

A total of 33 patients were enrolled in the study. The SUVmax, TLG, MTV and ADCmean measured from the primary tumors were 12.61±0.5 (range, 3.4-23.5); 139±0.87 (range, 5.79-883.46), 15±0.14 (range, 1.91-88.83) and 0.820±1.12*10^{-3}mm^2/s (range, 0.610-1.050±1.12*10^{-3}mm^2/s), respectively.

Correlation between HPV with FDG and DWI parameters:

Based on the baseline measurements, 16 patients were positive and 17 were negative for HPV. Independent sample t-test indicates that the ADCmean values of HPV$^+$ (0.758±0.70*10^{-3}mm^2/s) were significantly lower than HPV$^-$ (0.905±0.74*10^{-3}mm^2/s), (P=0.001), (Table 2), (Figure 1). Additionally, Spearman correlation coefficient indicates a significant inverse correlation between ADC and primary tumor grades (well, moderately and poorly differentiated tumors), (r = - 0.378, P = 0.030), (Table 2). On the other hand, no significant differences were found between SUVmax, TLG, and MTV with HPV status, (P=0.873, P=0.958, and P=0.817), respectively, (Table 2), (Figure 1). Moreover, SUVmax was significantly higher in patients with higher N stage (r = 0.0366, P=0.036). Higher TLG and MTV were observed with a higher T stage, (r = 0.0361, P=0.039 and r = 0.368, P=0.035), respectively. (Table 2).
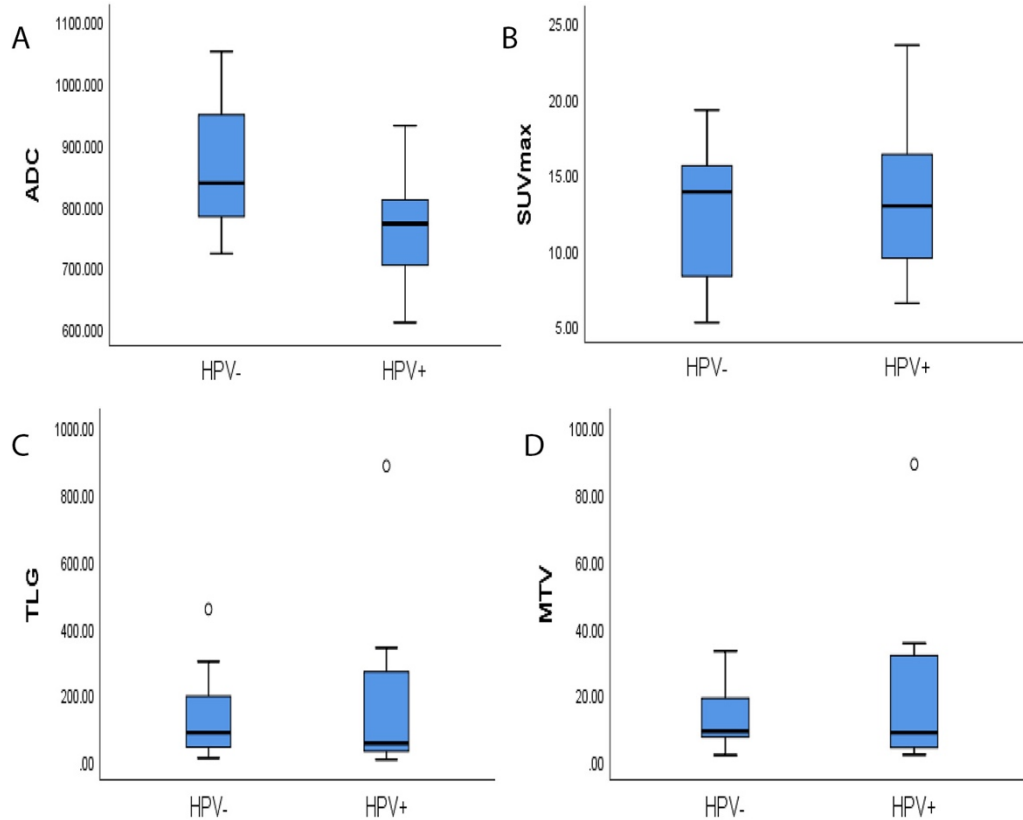
Figure (1): Boxplots displaying the distribution of ADC, TLG, MTV, and SUVmax (A, B, C, and D) according to HPV status. (A) ADCmean values of HPV+ev tumors were significantly lower than those of HPV-ev tumors (P=0.001). (B) SUVmax shows no significant difference, (P=0.873). (C) TLG shows no significant difference, (P=0.958), and finally, (D) MTV shows no significant difference, (P=0.817).

Table 2: Clinicopathological comparison with FDG and DWI imaging parameters

Grouping	SUVmax	TLG	MTV	ADC
T stages *	r = 0.51	*r = 0.361*	*r = 0.368*	r = 0.171
	P=0.780	*P=0.039*	*P=0.035*	P=0.341
N stages *	*r = 0.366*	r = 0.132	r = 0.127	r = - 0.276
	P=0.036	P=0.466	P=0.485	P=0.101

Grades *	r =0.081	r = 0.000	r = - 0.007	*r = - 0.378*
	P=0.656	P=1.000	P=1.000	*P=0.030*
HPV status	P=0.873	P=0.958	P=0.817	*P=0.001*

* spearman rho test was used to assess the correlation between ADC, SUVmax, TLG and MTV imaging parameters with T stages, N stages and Grades of the primary tumor. Mann-Whitney test for two categorical variables (M stages, HPV) with TLG and MTV parameters, Independent sample t test with ADC, and SUVmax values. A significant result at a level of p<0.05 was highlighted in Bold

To investigate which factors were independently influencing change in the ADC of the primary tumor (due to the significant results with HPV and primary tumor degree of differentiation), a multiple regression model was applied on HPV status and grade of the primary tumor, the results show that only HPV was an independent factor influencing change in ADC, (P=0.001), while the effect of the degree of differentiation was not significant, (P=0.138).

ROC curve was used to calculate the best cut-off value of ADC to differentiate between HPV+ and HPV- groups. The result shows that at a value of ($800 \pm 0.44*10^{-3}mm^2/s$), the area under the curve (AUC) was 69.7% with 76.9% sensitivity and 73.3% specificity. Figure (2).
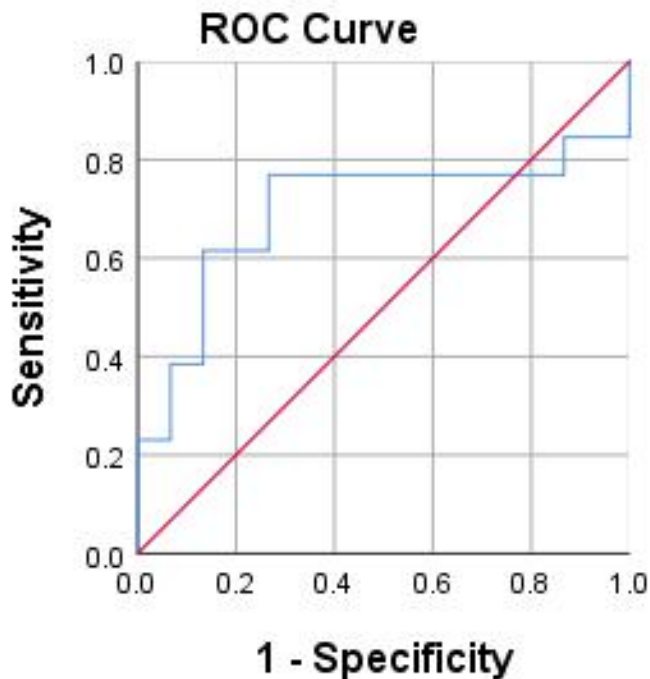
Figure (2): Receiver operating characteristic (ROC) curve analysis of HPV according to primary tumor ADC, (ROC) curve with AUC (69.7%), 95% confidence interval was ranged between 0.478 and 0.917, best cut off value was (800±0.00*10^{-3}mm^2/s) to distinguish between HPV+ from HPV- with a sensitivity of 76.9% and specificity of 73.3%.

Correlation between HPV and histopathological characteristics:

Chi-square test used to assess the association between the categorical variables. Details of the TNM staging summarized in (supplementary 1). No significant correlations were found between HPV groups and T stages; HPV+ (T1 = 2, T2 = 7, T3 = 4, and T4 = 3), HPV- (T1 = 0, T2 = 6, T3 = 8, and T4 = 3), (P = 0.336), no significant association between HPV status and N stages, HPV+ (N0 = 1, N1 = 1, N2 = 8 and N3 = 6), HPV- (N0 = 2, N1 = 5, N2 = 8 and N3 = 3), (P = 0.174)., or with primary tumor degree of differentiation; HPV+ (well differentiated = 0, moderately differentiated = 7, and poorly differentiated = 9), HPV- (well differentiated = 4, moderately differentiated = 7, and poorly differentiated = 6), (P = 0.102).

Predicting treatment response:

According to the independent sample t test, a statistically significant difference was found between CR (n = 21) vs NCR (n = 12) with pre-treatment ADC values (0.801 vs 0.893*10^{-3}mm^2/s, P=0.017), respectively. Wilcoxon rank test demonstrates a significant difference between CR and

NCR with pre-treatment TLG (76.77 vs 224.80, P=0.013) and MTV (9.088 vs 23.27, P=0.014), (Figure 3). CR and NCR were illustrated in (Figure 4) and (Figure 5), respectively. No statistically significant difference was found between the two groups and SUVmax, (P=0.664). (Figure 3). Moreover, according to Chi-square test, HPV+ (CR = 14, NCR = 2) and HPV- (CR = 7, NCR = 10) were significantly associated, (P=0.006) between CR and NCR patients.
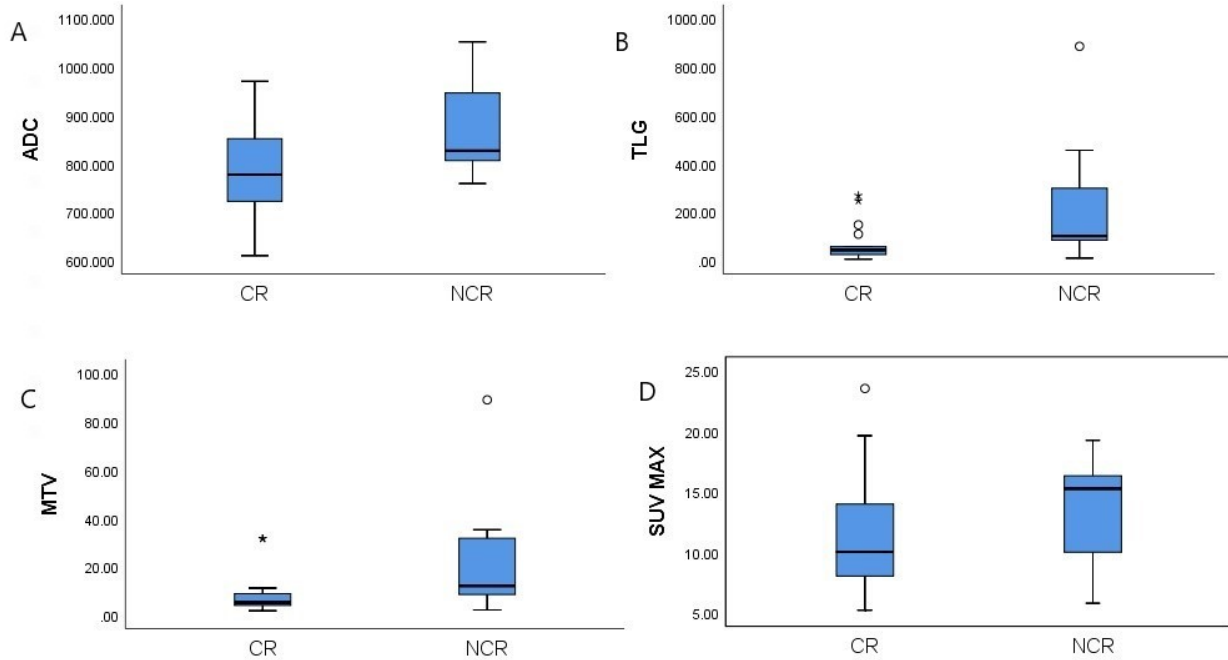

Figure (3): Boxplots displaying the distribution of ADC, TLG, MTV, and SUVmax (A, B, C, and D) according to treatment results. (A) pretreatment ADC values of CR tumors were statistically significant lower than those of NCR tumors (P=0.017). (B) pre-treatment TLG shows a statistically significant higher in NCR than CR tumors, (P=0.013). (C) pre-treatment MTV shows a statistically significant higher in NCR than CR tumors, (P=0.014), and (D) pre-treatment SUVmax didn't differ significantly between both groups, (P=0.664).

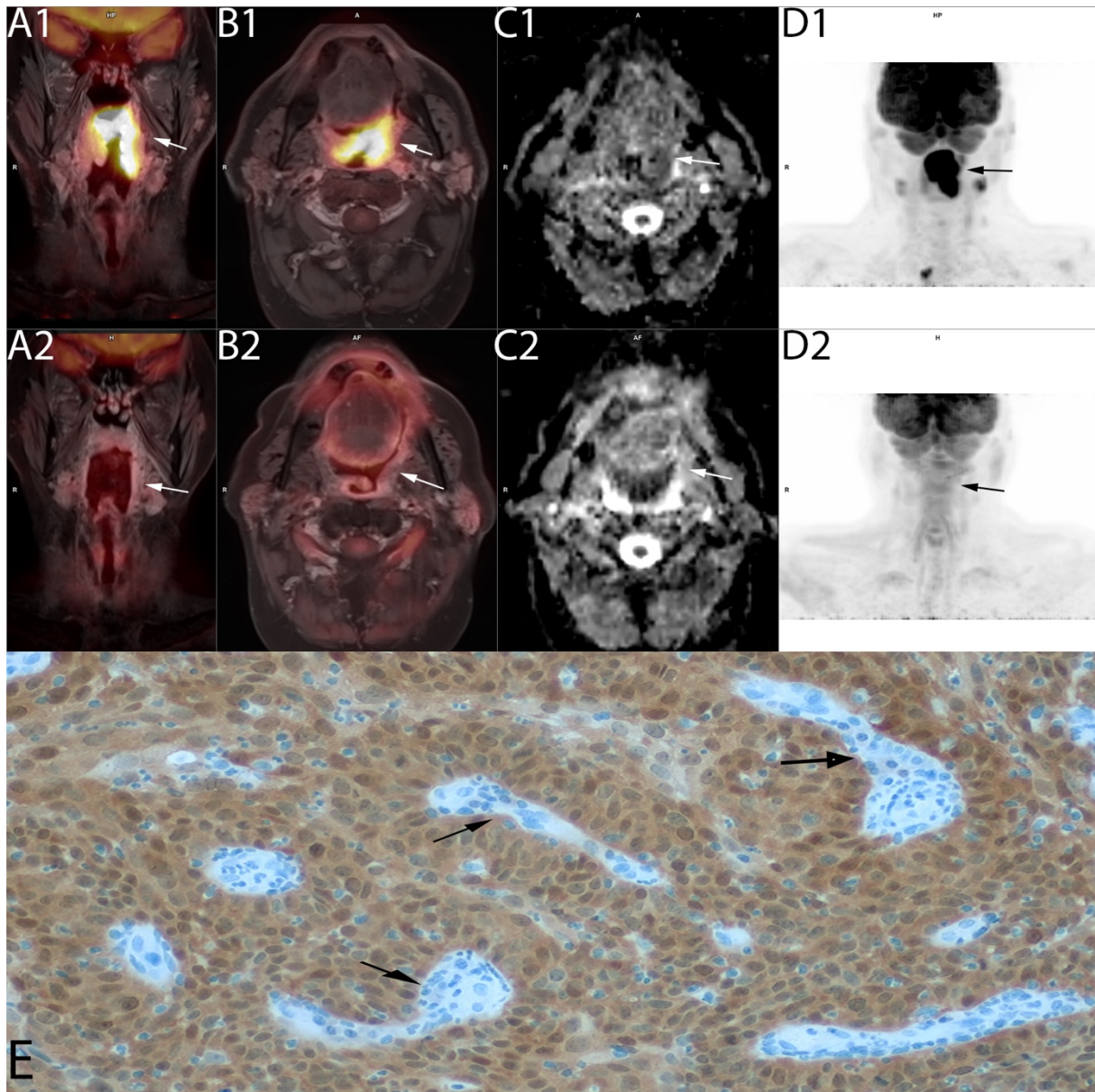**Figure (4):** complete remission (CR) for HPV+ patient: pre-treatment coronal **(A₁)**, axial **(B₁)** **PET/MRI images**, axial **(C₁)** MR-diffusion weighted imaging (DWI) apparent diffusion coefficient (ADC) map of the tumor, and **(D₁)** PET imaging show oropharyngeal tumor spread over the soft palate, palatine tonsil and posterior wall of the pharynx, pretreatment maximum standardized uptake value (SUV_{max}): 19.61, total lesion glycolysis (TLG): 147.81, metabolic tumor volume (MTV): 11.28 cm^3, mean ADC (ADC_{mean}): $0.610\pm0.52\times10^{-6}$s/mm^2. Post-treatment coronal PET **(A₂)**, axial **(B₂)** PET/MR, axial DWI ADC **(C₂), (D₂)** images show complete remission (CR); without any pathologic FDG accumulation, and diffusion restriction on the

observed volume, and **I** Representative immunohistochemical staining showing examples of P16 expression levels in HPV+
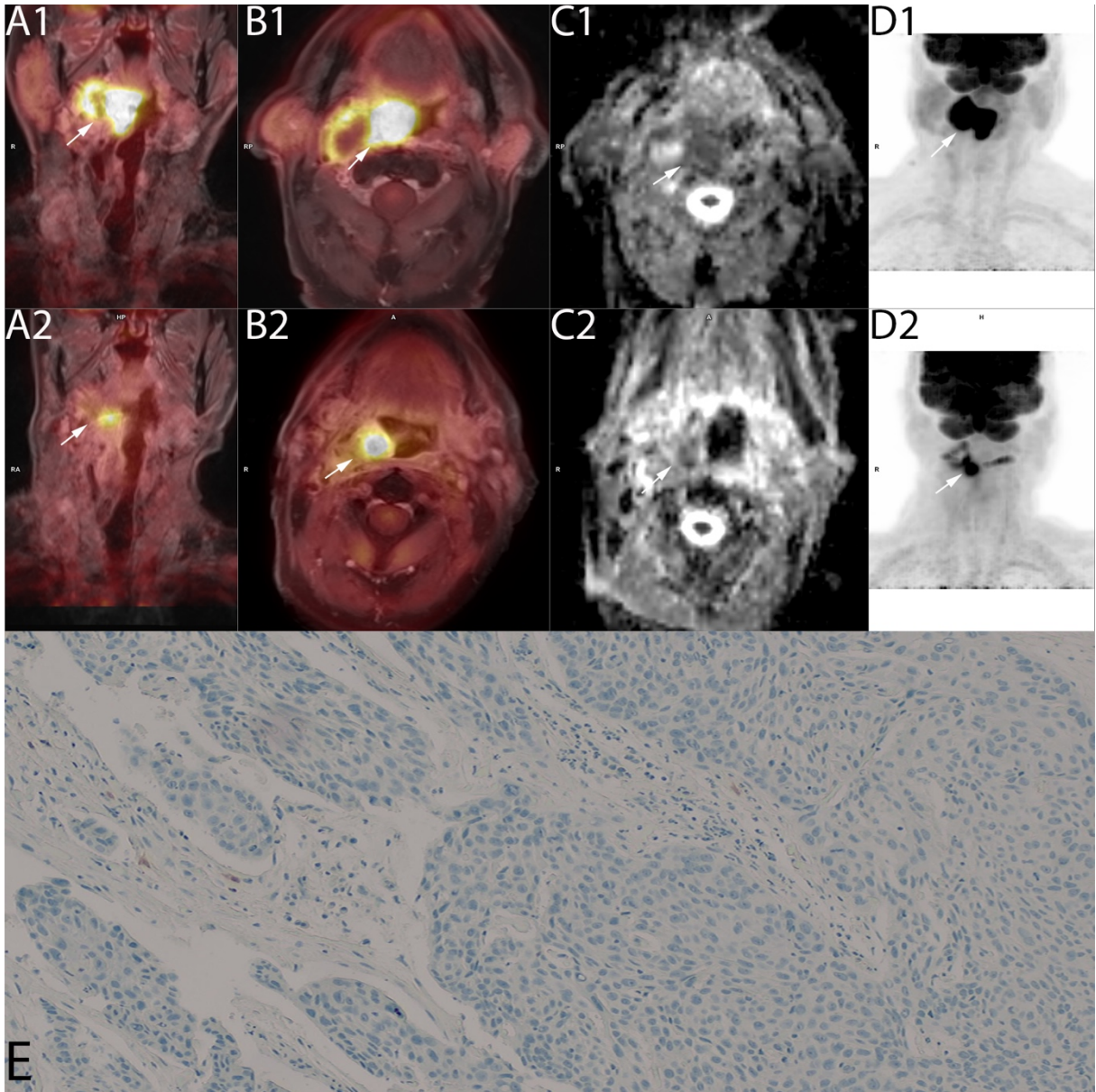

Figure (5): non-complete remission (NCR) for HPV- patient: coronal **(A₁)**, axial **(B₁)** **PET/MRI images**, axial **(C₁)** MR-diffusion weighted imaging (DWI) apparent diffusion coefficient (ADC) map of the tumor, and **(D₁)** PET imaging show right palatine tonsil tumor spreading into tongue root, pretreatment maximum standardized uptake value (SUV$_{max}$): 15.24, total lesion glycolysis (TLG): 99.72, metabolic tumor volume (MTV): 9.16 cm^3, mean ADC (ADC$_{mean}$):

1.050±0.680×10^{-6}s/mm^2. Post-treatment coronal PET **(A₂)**, axial **(B₂)** PET/MR, axial DWI ADC **(C₂), (D₂)** PET image show non-complete remission (CR); with pathologic FDG accumulation, and diffusion restriction on the observed volume, and I Representative immunohistochemical staining showing examples of P16 expression levels in HPV-. (Freihat et al., 2021)

Discussion:

We analyzed the efficacy of combined PET/MRI imaging parameters to predict HPV status and local response of OPSCC treated by CRT with curative intent. We found that HPV+ lesions are associated with lower ADC values than HPV- lesions, which might be useful as a non-invasive technique to evaluate HPV status. With a value of ($809±0.37*10^{-3}$mm^2/s), the area under the curve (AUC) was 80.0% with 73.7% sensitivity, and 73.3% specificity was able to differentiate between HPV groups. In contrast, FDG parameters did not show any statistical significance between HPV groups, which means that FDG might be not useful for predicting HPV status. Our study has also shown that DWI, FDG volumetric metabolism parameters (TLG and MTV) are useful predictor biomarkers to assess the response before treatment in OPSCC, while SUVmax may not. Besides, the HPV+ patient's group have shown better response to therapy than HPV- patients.

In head and neck squamous cell carcinoma (HNSCC), OPSCCs are the most associated HPV-related tumors; they tend to respond well to therapy and carry a favorable prognosis. (Lawrence et al., 2015) HPV status has been previously studied and investigated in OPSCC based on morphology (El-Mofty & Patil, 2006; Mendelsohn et al., 2010) or molecular biology (Jordan et al., 2012; Rainsbury et al., 2013; Smeets et al., 2007). Imaging parameters have been also used to predict HPV infection as a non-invasive technique, DWI was proposed to have the ability to differentiate between HPV-positive and HPV-negative. Several studies found that HPV+ has lower ADC than HPV- OPSCC's. (Driessen et al., 2016; Martens, Noij, Koopman, et al., 2019a; Nakahira et al., 2014; Payabvash et al., 2019; Ravanelli et al., 2018) This might be attributed to the positive correlation between ADC and total percentage area of stroma, and an inverse correlation with the cell density in tumors. (Driessen et al., 2014) Our result was similar to previous reports, which suppose the hypothesis of the association between ADC and HPV infection. A value of ($809±0.37*10^{-3}$mm^2/s) was able to differentiate between the two groups, which was parallel with previous studies.(Nakahira et al., 2014; Ravanelli et al., 2018) The significance of this result

is due to the fact that tumors with low pretreatment ADC values respond better to chemo/radiotherapy than tumors with low ADC values. (Nakahira et al., 2014)

The diagnosis of primary and metastatic (HNSCC) has been increasingly studied by FDG-PET, which due to its accuracy and sensitivity has been recognized as a standard of reference nowadays, as well as being used for post-treatment surveillance. Some studies have investigated the role of FDG PET imaging parameters in predicting HPV infection. However, previous studies show a controversial result, some reports found that the FDG parameter (SUVmax) is helpful to differentiate between HPV+ and HPV-, (Kendi et al., 2015; Martens, Noij, Koopman, et al., 2019b; Sharma et al., 2017; Tahari et al., 2014b) while others didn't. (Cheng et al., 2012; Fleming et al., 2019; Sharma et al., 2017; Vidiri et al., 2020). It has also been proposed that volumetric metabolism parameters (TLG, MTV) could provide more details for tumor metabolism. Previous studies have demonstrated that TLG and MTV have superior prognostic values than SUVmax since they reported that larger tumor volume correlates with the overall survival and inferior local control (Romesser et al., 2012; Schwartz et al., 2016; Tahari et al., 2014a), this, in turn, might be reflected on patients with HPV+ since it shows a higher percentage of loco-regional response and longer free survival. However, our study found no significant difference between FDG imaging parameters and HPV infection, which in turn, might limit the prospective use of these imaging parameters in clinical use. Similar results were reported by other authors. (Cheng et al., 2012; Sharma et al., 2017; Vidiri et al., 2020) The reason of our results might be attributed to the lack of a significant correlation between T stages and HPV status, since previous reports were found that HPV- tumors have higher T stages than HPV+, which as a results affect the tumor metabolism, since higher FDG uptake was observed in higher T stages, this might explain why HPV- tumors have higher FDG values (SUVmax, TLG, and MTV), in our study there was no significant difference between HPV+ and HPV- because there was no difference in T stages between the two groups. (Baschnagel et al., 2015; Tahari et al., 2014a) Thus, we suppose that the significant correlation between HPV status and FDG parameters, if reported, is attributed to the size difference between HPV+ and HPV-. (Baschnagel et al., 2015) However, most of the previous studies have heterogeneous primary tumor localization (oral, laryngeal, nasopharyngeal, pharyngeal), as a result, the concluded results might have limited accuracy. Thus, to investigate more efficient results of PET parameters role in OPSCC, this should be investigated separately

New hybrid imaging modalities such as PET/CT or PET/MRI have emerged as useful technologies to assess HNSCC tumors in terms of prognosis and follow up. Overall, HNC's as proposed previously, have a possibility of locoregional recurrence in the first two years after therapy up to 50-60% of the patients. (Denaro et al., 2016) Several imaging parameters have been used for the Propose of predicting response to therapy, DWI represented by ADC, and metabolic parameters (SUVmax, TLG, and MTV), different results have been reported, while some studies found some of them are feasible while other didn't. There is a need in clinical practice to assess accurately the tumor response to therapy, this is due to the high mortality in patients with HNSCC'S, therefor, all available tools to assess cancer should be combined to allow the physicians to select the most appropriate treatment protocols, especially to assess the prognosis of the patient, so it's highly important to identify potential predictive biomarkers to have better treatment strategies.

In this study, we found that DWI and metabolic imaging parameters TLG and MTV can provide more accurate information for treatment prediction since we found that higher TLG and MTV before therapy lead to a higher probability of recurrence and lower rates of response, (Paidpally et al., 2014; K Pak et al., 2014) these findings do not eliminate the role of the basic FDG parameter (SUVmax) for prediction, although, in our study, we found no significant correlation between SUVmax and response. Overall, in OPSCC, it has been reported that TLG and MTV have better results in the prediction of overall survival and disease-free survival. (Moan et al., 2019) In regards to ADC, our results revealed that ADC might be useful for predicting response after therapy, although we have lost data for 5 patients in post-treatment examinations. According to Sae et al. there is a trend that DWI can predict tumor response to therapy in HNSCC, several studies have reported higher ADC after therapy, but still of the major limitations of the previous studies is the heterogeneity of the tumors, as well as the number of studies, are small. (Chung et al., 2019) PET imaging parameters also provide very important information regarding tumor microstructures. Our study compared to the previous published in HNS has more homogenous primary tumor localization (OPSCC), it also one of the fewest papers which compare the role of the combined biomarkers derived from PET/MRI combined technique. However, since we didn't find a significant correlation between PET parameters and HPV status, PET parameters seem to be less important to add a significant diagnostic role during OPSCC related HPV lesions assessment. (Moan et al., 2019) Finally, our study emphasize that HPV+ tumors tend to have better response to therapy than HPV- tumors. (Koshkareva et al., 2014)

As a limitation of the current study; small sample size, retrospective design, single institute approach, and using the conventional FDG and DWI parameters which do not include texture analysis should be noted. Although moderate sample size, we only included OPSCC patients from the HNC group to ensure a homogeneous population that may increase the reliability of our results.

In conclusion, this study found that pre-treatment ADC was a predictor of HPV status and post-therapy results. On the other side, FDG parameters were able to predict tumor response to therapy, but they don't show a feasible role in predicting HPV status. Based on the reported results, both DWI and FDG parameters are important to assess patients with OPSCC and their role might be complementary to each other.

Bibliography:

Alluri, K. C., Tahari, A. K., Wahl, R. L., Koch, W., Chung, C. H., & Subramaniam, R. M. (2014). Prognostic value of FDG PET metabolic tumor volume in human papillomavirus-positive stage III and IV oropharyngeal squamous cell carcinoma. *American Journal of Roentgenology*, *203*(4), 897–903. https://doi.org/10.2214/AJR.14.12497

Ang, K. K., Harris, J., Wheeler, R., Weber, R., Rosenthal, D. I., Nguyen-Tân, P. F., Westra, W. H., Chung, C. H., Jordan, R. C., Lu, C., Kim, H., Axelrod, R., Silverman, C. C., Redmond, K. P., & Gillison, M. L. (2010). Human papillomavirus and survival of patients with oropharyngeal cancer. *New England Journal of Medicine*, *363*(1), 24–35. https://doi.org/10.1056/NEJMoa0912217

Baschnagel, A. M., Wobb, J. L., Dilworth, J. T., Williams, L., Eskandari, M., Wu, D., Pruetz, B. L., & Wilson, G. D. (2015). The association of 18F-FDG PET and glucose metabolism biomarkers GLUT1 and HK2 in p16 positive and negative head and neck squamous cell carcinomas. *Radiotherapy and Oncology*, *117*(1), 118–124. https://doi.org/10.1016/j.radonc.2015.08.025

Benson E, Li R, E. D. et al. (2014). The clinical impact ofHPV tumor status upon head and neck squamous cell carcin- omas. *Oral Oncol*, *50*, 565–574.

Cheng, N. M., Chang, J. T. C., Huang, C. G., Tsan, D. L., Ng, S. H., Wang, H. M., Liao, C. T., Lin, C. Y., Hsu, C. L., & Yen, T. C. (2012). Prognostic value of pretreatment 18F-FDG

PET/CT and human papillomavirus type 16 testing in locally advanced oropharyngeal squamous cell carcinoma. *European Journal of Nuclear Medicine and Molecular Imaging*, *39*(11), 1673–1684. https://doi.org/10.1007/s00259-012-2186-9

Chung, S. R., Choi, Y. J., Suh, C. H., Lee, J. H., & Baek, J. H. (2019). Diffusion-weighted Magnetic Resonance Imaging for Predicting Response to Chemoradiation Therapy for Head and Neck Squamous Cell Carcinoma: A Systematic Review. *Korean Journal of Radiology*, *20*(4), 649. https://doi.org/10.3348/kjr.2018.0446

Denaro, N., Merlano, M. C., & Russi, E. G. (2016). Follow-up in Head and Neck Cancer: Do More Does It Mean Do Better? A Systematic Review and Our Proposal Based on Our Experience. *Clinical and Experimental Otorhinolaryngology*, *9*(4), 287–297. https://doi.org/10.21053/ceo.2015.00976

Driessen, J. P., Caldas-Magalhaes, J., Janssen, L. M., Pameijer, F. A., Kooij, N., Terhaard, C. H. J., Grolman, W., & Philippens, M. E. P. (2014). Diffusion-weighted MR Imaging in Laryngeal and Hypopharyngeal Carcinoma: Association between Apparent Diffusion Coefficient and Histologic Findings. *Radiology*, *272*(2), 456–463. https://doi.org/10.1148/radiol.14131173

Driessen, J. P., van Bemmel, A. J. M., van Kempen, P. M. W., Janssen, L. M., Terhaard, C. H. J., Pameijer, F. A., Willems, S. M., Stegeman, I., Grolman, W., & Philippens, M. E. P. (2016). Correlation of human papillomavirus status with apparent diffusion coefficient of diffusion-weighted MRI in head and neck squamous cell carcinomas. *Head & Neck*, *38*(S1), E613–E618. https://doi.org/10.1002/hed.24051

El-Mofty, S. K., & Patil, S. (2006). Human papillomavirus (HPV)-related oropharyngeal nonkeratinizing squamous cell carcinoma: characterization of a distinct phenotype. *Oral Surgery, Oral Medicine, Oral Pathology, Oral Radiology, and Endodontics*, *101*(3), 339–345. https://doi.org/10.1016/j.tripleo.2005.08.001

Fleming, J. C., Woo, J., Moutasim, K., Mellone, M., Frampton, S. J., Mead, A., Ahmed, W., Wood, O., Robinson, H., Ward, M., Woelk, C. H., Ottensmeier, C. H., King, E., Kim, D., Blaydes, J. P., & Thomas, G. J. (2019). HPV, tumour metabolism and novel target identification in head and neck squamous cell carcinoma. *British Journal of Cancer*, *120*(3), 356–367. https://doi.org/10.1038/s41416-018-0364-7

Freihat, O., Pinter, T., Kedves, A., Sipos, D., Cselik, Z., Repa, I., & Kovács, Á. (2020).

Diffusion-Weighted Imaging (DWI) derived from PET/MRI for lymph node assessment in patients with Head and Neck Squamous Cell Carcinoma (HNSCC). *Cancer Imaging*, *20*(1), 1–12. https://doi.org/10.1186/s40644-020-00334-x

Fruehwald-Pallamar, J., Czerny, C., Mayerhoefer, M. E., Halpern, B. S., Eder-Czembirek, C., Brunner, M., Schuetz, M., Weber, M., Fruehwald, L., & Herneth, A. M. (2011). Functional imaging in head and neck squamous cell carcinoma: Correlation of PET/CT and diffusion-weighted imaging at 3 Tesla. *European Journal of Nuclear Medicine and Molecular Imaging*, *38*(6), 1009–1019. https://doi.org/10.1007/s00259-010-1718-4

Gillison, M. L., Zhang, Q., Jordan, R., Xiao, W., Westra, W. H., Trotti, A., Spencer, S., Harris, J., Chung, C. H., & Ang, K. K. (2012). Tobacco smoking and increased risk of death and progression for patients with p16-positive and p16-negative oropharyngeal cancer. *Journal of Clinical Oncology*, *30*(17), 2102–2111. https://doi.org/10.1200/JCO.2011.38.4099

Glastonbury, C. M., Mukherji, S. K., O'Sullivan, B., & Lydiatt, W. M. (2017). Setting the Stage for 2018: How the Changes in the American Joint Committee on Cancer/Union for International Cancer Control Cancer Staging Manual Eighth Edition Impact Radiologists. *AJNR. American Journal of Neuroradiology*, *38*(12), 2231–2237. https://doi.org/10.3174/ajnr.A5409

Huang, S. H., Perez-Ordonez, B., Weinreb, I., Hope, A., Massey, C., Waldron, J. N., Kim, J., Bayley, A. J., Cummings, B., Cho, B. C. J., Ringash, J., Dawson, L. A., Siu, L. L., Chen, E., Irish, J., Gullane, P., Hui, A., Liu, F.-F., Shen, X., … O'Sullivan, B. (2013). Natural course of distant metastases following radiotherapy or chemoradiotherapy in HPV-related oropharyngeal cancer. *Oral Oncology*, *49*(1), 79–85. https://doi.org/10.1016/j.oraloncology.2012.07.015

Jansen, J. F. A., Koutcher, J. A., & Shukla-Dave, A. (2010). Non-invasive imaging of angiogenesis in head and neck squamous cell carcinoma. *Angiogenesis*, *13*(2), 149–160. https://doi.org/10.1007/s10456-010-9167-z

Jeong, J. H., Cho, I. H., Chun, K. A., Kong, E. J., Kwon, S. D., & Kim, J. H. (2016). Correlation Between Apparent Diffusion Coefficients and Standardized Uptake Values in Hybrid 18F-FDG PET/MR: Preliminary Results in Rectal Cancer. *Nuclear Medicine and Molecular Imaging*, *50*(2), 150–156. https://doi.org/10.1007/s13139-015-0390-9

Jordan, R. C., Lingen, M. W., Perez-Ordonez, B., He, X., Pickard, R., Koluder, M., Jiang, B.,

Wakely, P., Xiao, W., & Gillison, M. L. (2012). Validation of methods for oropharyngeal cancer HPV status determination in US cooperative group trials. *The American Journal of Surgical Pathology*, *36*(7), 945–954. https://doi.org/10.1097/PAS.0b013e318253a2d1

Kedves, A., Tóth, Z., Emri, M., Fábián, K., Sipos, D., Freihat, O., Tollár, J., Cselik, Z., Lakosi, F., Bajzik, G., Repa, I., & Kovács, Á. (2020). Predictive Value of Diffusion, Glucose Metabolism Parameters of PET/MR in Patients With Head and Neck Squamous Cell Carcinoma Treated With Chemoradiotherapy. *Frontiers in Oncology*, *10*(September). https://doi.org/10.3389/fonc.2020.01484

Kendi, A. T. K., Magliocca, K., Corey, A., Nickleach, D. C., Galt, J., Higgins, K., Beitler, J. J., El-Deiry, M. W., Wadsworth, J. T., Hudgins, P. A., Saba, N. F., & Schuster, D. M. (2015). Do 18F-FDG PET/CT parameters in oropharyngeal and oral cavity squamous cell carcinomas indicate HPV status? *Clinical Nuclear Medicine*, *40*(3), e196–e200. https://doi.org/10.1097/RLU.0000000000000691

Kikuchi, M., Koyasu, S., Shinohara, S., Usami, Y., Imai, Y., Hino, M., Itoh, K., Tona, R., Kanazawa, Y., Kishimoto, I., Harada, H., & Naito, Y. (2015). Prognostic value of pretreatment 18F-fluorodeoxyglucose positron emission tomography/CT volume-based parameters in patients with oropharyngeal squamous cell carcinoma with known p16 and p53 status. *Head & Neck*, *37*(10), 1524–1531. https://doi.org/10.1002/hed.23784

Kim, J. W., Oh, J. S., Roh, J.-L., Kim, J. S., Choi, S.-H., Nam, S. Y., & Kim, S. Y. (2015). Prognostic significance of standardized uptake value and metabolic tumour volume on 18F-FDG PET/CT in oropharyngeal squamous cell carcinoma. *European Journal of Nuclear Medicine and Molecular Imaging*, *42*(9), 1353–1361. https://doi.org/10.1007/s00259-015-3051-4

Koshkareva, Y., Branstetter IV, B. F., Gaughan, J. P., & Ferris, R. L. (2014). Predictive accuracy of first post-treatment PET/CT in HPV-related oropharyngeal squamous cell carcinoma. *Laryngoscope*, *124*(8), 1843–1847. https://doi.org/10.1002/lary.24617

Lambregts, D. M. J., Beets, G. L., Maas, M., Curvo-Semedo, L., Kessels, A. G. H., Thywissen, T., & Beets-Tan, R. G. H. (2011). Tumour ADC measurements in rectal cancer: effect of ROI methods on ADC values and interobserver variability. *European Radiology*, *21*(12), 2567–2574. https://doi.org/10.1007/s00330-011-2220-5

Lawrence, M. S., Sougnez, C., Lichtenstein, L., Cibulskis, K., Lander, E., Gabriel, S. B., Getz,

G., Ally, A., Balasundaram, M., Birol, I., Bowlby, R., Brooks, D., Butterfield, Y. S. N., Carlsen, R., Cheng, D., Chu, A., Dhalla, N., Guin, R., Holt, R. A., … Consortium, I. G. (2015). Comprehensive genomic characterization of head and neck squamous cell carcinomas. *Nature*, *517*(7536), 576–582. https://doi.org/10.1038/nature14129

Leemans, C. R., Braakhuis, B. J. M., & Brakenhoff, R. H. (2011). The molecular biology of head and neck cancer. *Nature Reviews Cancer*, *11*(1), 9–22. https://doi.org/10.1038/nrc2982

Lim, R., Eaton, A., Lee, N. Y., Setton, J., Ohri, N., Rao, S., Wong, R., Fury, M., & Schöder, H. (2012). 18F-FDG PET/CT metabolic tumor volume and total lesion glycolysis predict outcome in oropharyngeal squamous cell carcinoma. *Journal of Nuclear Medicine*, *53*(10), 1506–1513. https://doi.org/10.2967/jnumed.111.101402

Martens, R. M., Noij, D. P., Ali, M., Koopman, T., Marcus, J. T., Vergeer, M. R., de Vet, H., de Jong, M. C., Leemans, C. R., Hoekstra, O. S., de Bree, R., de Graaf, P., Boellaard, R., & Castelijns, J. A. (2019). Functional imaging early during (chemo)radiotherapy for response prediction in head and neck squamous cell carcinoma; a systematic review. *Oral Oncology*, *88*(September 2018), 75–83. https://doi.org/10.1016/j.oraloncology.2018.11.005

Martens, R. M., Noij, D. P., Koopman, T., Zwezerijnen, B., Heymans, M., de Jong, M. C., Hoekstra, O. S., Vergeer, M. R., de Bree, R., Leemans, C. R., de Graaf, P., Boellaard, R., & Castelijns, J. A. (2019a). Predictive value of quantitative diffusion-weighted imaging and 18-F-FDG-PET in head and neck squamous cell carcinoma treated by (chemo)radiotherapy. *European Journal of Radiology*, *113*(August 2018), 39–50. https://doi.org/10.1016/j.ejrad.2019.01.031

Martens, R. M., Noij, D. P., Koopman, T., Zwezerijnen, B., Heymans, M., de Jong, M. C., Hoekstra, O. S., Vergeer, M. R., de Bree, R., Leemans, C. R., de Graaf, P., Boellaard, R., & Castelijns, J. A. (2019b). Predictive value of quantitative diffusion-weighted imaging and 18-F-FDG-PET in head and neck squamous cell carcinoma treated by (chemo)radiotherapy. *European Journal of Radiology*, *113*(January), 39–50. https://doi.org/10.1016/j.ejrad.2019.01.031

Marur, S., D'Souza, G., Westra, W. H., & Forastiere, A. A. (2010). HPV-associated head and neck cancer: A virus-related cancer epidemic. *The Lancet Oncology*, *11*(8), 781–789. https://doi.org/10.1016/S1470-2045(10)70017-6

Mena, E., Taghipour, M., Sheikhbahaei, S., Jha, A. K., Rahmim, A., Solnes, L., & Subramaniam,

R. M. (2017). Value of Intratumoral Metabolic Heterogeneity and Quantitative 18F-FDG PET/CT Parameters to Predict Prognosis in Patients with HPV-Positive Primary Oropharyngeal Squamous Cell Carcinoma. *Clinical Nuclear Medicine*, *42*(5), e227–e234. https://doi.org/10.1097/RLU.0000000000001578

Mendelsohn, A. H., Lai, C. K., Shintaku, I. P., Elashoff, D. A., Dubinett, S. M., Abemayor, E., & St John, M. A. (2010). Histopathologic findings of HPV and p16 positive HNSCC. *The Laryngoscope*, *120*(9), 1788–1794. https://doi.org/10.1002/lary.21044

Miccò, M., Vargas, H. A., Burger, I. A., Kollmeier, M. A., Goldman, D. A., Park, K. J., Abu-Rustum, N. R., Hricak, H., & Sala, E. (2014). Combined pre-treatment MRI and 18F-FDG PET/CT parameters as prognostic biomarkers in patients with cervical cancer. *European Journal of Radiology*, *83*(7), 1169–1176. https://doi.org/10.1016/j.ejrad.2014.03.024

Moan, J. M., Amdal, C. D., Malinen, E., Svestad, J. G., Bogsrud, T. V., & Dale, E. (2019). The prognostic role of 18F-fluorodeoxyglucose PET in head and neck cancer depends on HPV status. *Radiotherapy and Oncology*, *140*, 54–61. https://doi.org/10.1016/j.radonc.2019.05.019

Nakahira, M., Saito, N., Yamaguchi, H., Kuba, K., & Sugasawa, M. (2014). Use of quantitative diffusion-weighted magnetic resonance imaging to predict human papilloma virus status in patients with oropharyngeal squamous cell carcinoma. *European Archives of Oto-Rhino-Laryngology*, *271*(5), 1219–1225. https://doi.org/10.1007/s00405-013-2641-7

O'Sullivan, B., Huang, S. H., Siu, L. L., Waldron, J., Zhao, H., Perez-Ordonez, B., Weinreb, I., Kim, J., Ringash, J., Bayley, A., Dawson, L. A., Hope, A., Cho, J., Irish, J., Gilbert, R., Gullane, P., Hui, A., Liu, F.-F., Chen, E., & Xu, W. (2013). Deintensification candidate subgroups in human papillomavirus-related oropharyngeal cancer according to minimal risk of distant metastasis. *Journal of Clinical Oncology : Official Journal of the American Society of Clinical Oncology*, *31*(5), 543–550. https://doi.org/10.1200/JCO.2012.44.0164

Paidpally, V., Chirindel, A., Chung, C. H., Richmon, J., Koch, W., Quon, H., & Subramaniam, R. M. (2014). FDG volumetric parameters and survival outcomes after definitive chemoradiotherapy in patients with recurrent head and neck squamous cell carcinoma. *American Journal of Roentgenology*, *203*(2), 139–145. https://doi.org/10.2214/AJR.13.11654

Pak, K, Cheon, G., Nam, H., Kim, S., Med, K. K.-J. N., & 2014, U. (2014). Prognostic value of

metabolic tumor volume and total lesion glycolysis in head and neck cancer: a systematic review and meta-analysis. *THE JOURNAL OF NUCLEAR MEDICINE*, *55*(6), 1–7. http://www.academia.edu/download/46307953/Prognostic_Value_of_Metabolic_Tumor_V olu20160607-17979-obn7np.pdf

Pak, Kyoungjune, Cheon, G. J., Nam, H. Y., Kim, S. J., Kang, K. W., Chung, J. K., Kim, E. E., & Lee, D. S. (2014). Prognostic value of metabolic tumor volume and total lesion glycolysis in head and neck cancer: A systematic review and meta-analysis. *Journal of Nuclear Medicine*, *55*(6), 884–890. https://doi.org/10.2967/jnumed.113.133801

Payabvash, S., Chan, A., Jabehdar Maralani, P., & Malhotra, A. (2019). Quantitative diffusion magnetic resonance imaging for prediction of human papillomavirus status in head and neck squamous-cell carcinoma: A systematic review and meta-analysis. *Neuroradiology Journal*, *32*(4), 232–240. https://doi.org/10.1177/1971400919849808

Pollom, E. L., Song, J., Durkee, B. Y., Aggarwal, S., Bui, T., von Eyben, R., Li, R., Brizel, D. M., Loo, B. W., Le, Q.-T., & Hara, W. Y. (2016). Prognostic value of midtreatment FDG-PET in oropharyngeal cancer. *Head & Neck*, *38*(10), 1472–1478. https://doi.org/10.1002/hed.24454

Queiroz, M. A., Hüllner, M., Kuhn, F., Huber, G., Meerwein, C., Kollias, S., von Schulthess, G., & Veit-Haibach, P. (2014). Use of diffusion-weighted imaging (DWI) in PET/MRI for head and neck cancer evaluation. *European Journal of Nuclear Medicine and Molecular Imaging*, *41*(12), 2212–2221. https://doi.org/10.1007/s00259-014-2867-7

Rainsbury, J. W., Ahmed, W., Williams, H. K., Roberts, S., Paleri, V., & Mehanna, H. (2013). Prognostic biomarkers of survival in oropharyngeal squamous cell carcinoma: systematic review and meta-analysis. *Head & Neck*, *35*(7), 1048–1055. https://doi.org/10.1002/hed.22950

Ravanelli, M., Grammatica, A., Tononcelli, E., Morello, R., Leali, M., Battocchio, S., Agazzi, G. M., Buglione Di Monale E Bastia, M., Maroldi, R., Nicolai, P., & Farina, D. (2018). Correlation between human papillomavirus status and quantitative MR imaging parameters including diffusion-weighted imaging and texture features in oropharyngeal carcinoma. *American Journal of Neuroradiology*, *39*(10), 1878–1883. https://doi.org/10.3174/ajnr.A5792

Romesser, P. B., Qureshi, M. M., Shah, B. A., Chatburn, L. T., Jalisi, S., Devaiah, A. K.,

Subramaniam, R. M., & Truong, M. T. (2012). Superior prognostic utility of gross and metabolic tumor volume compared to standardized uptake value using PET/CT in head and neck squamous cell carcinoma patients treated with intensity-modulated radiotherapy. *Annals of Nuclear Medicine*, *26*(7), 527–534. https://doi.org/10.1007/s12149-012-0604-5

Sakane, M., Tatsumi, M., Kim, T., Hori, M., Onishi, H., Nakamoto, A., Eguchi, H., Nagano, H., Wakasa, K., Hatazawa, J., & Tomiyama, N. (2015). Correlation between apparent diffusion coefficients on diffusion-weighted MRI and standardized uptake value on FDGPET/ CT in pancreatic adenocarcinoma. *Acta Radiologica*, *56*(9), 1034–1041. https://doi.org/10.1177/0284185114549825

Schwartz, D. L., Harris, J., Yao, M., Rosenthal, D. I., Opanowski, A., Levering, A., Ang, K. K., Trotti, A. M., Garden, A. S., Jones, C. U., Harari, P., Foote, R., Zhang, Q., Le, Q., Office, S., Group, M., Clinic, M., Health, O., & Alto, P. (2016). Metabolic Tumor Volume as a Prognostic Imaging-Based Biomarker for Head and Neck Cancer—Pilot Results from RTOG 0522. *Int J Radiat Oncol Biol Phys.*, *91*(4), 721–729. https://doi.org/10.1016/j.ijrobp.2014.12.023.Metabolic

Sharma, S. J., Wittekindt, C., Knuth, J., Steiner, D., Wuerdemann, N., Laur, M., Kroll, T., Wagner, S., & Klussmann, J. P. (2017). Intraindividual homogeneity of 18F-FDG PET/CT parameters in HPV-positive OPSCC. *Oral Oncology*, *73*(August), 166–171. https://doi.org/10.1016/j.oraloncology.2017.08.019

Smeets, S. J., Hesselink, A. T., Speel, E.-J. M., Haesevoets, A., Snijders, P. J. F., Pawlita, M., Meijer, C. J. L. M., Braakhuis, B. J. M., Leemans, C. R., & Brakenhoff, R. H. (2007). A novel algorithm for reliable detection of human papillomavirus in paraffin embedded head and neck cancer specimen. *International Journal of Cancer*, *121*(11), 2465–2472. https://doi.org/10.1002/ijc.22980

Tahari, A. K., Alluri, K. C., Quon, H., Koch, W., Wahl, R. L., & Subramaniam, R. M. (2014a). FDG PET/CT imaging of oropharyngeal squamous cell carcinoma: Characteristics of human papillomavirus-positive and -negative tumors. *Clinical Nuclear Medicine*, *39*(3), 225–231. https://doi.org/10.1097/RLU.0000000000000255

Tahari, A. K., Alluri, K. C., Quon, H., Koch, W., Wahl, R. L., & Subramaniam, R. M. (2014b). FDG PET/CT Imaging of Oropharyngeal Squamous Cell Carcinoma. *Clinical Nuclear Medicine*, *39*(3), 225–231. https://doi.org/10.1097/rlu.0000000000000255

Vandecaveye, V., Dirix, P., De Keyzer, F., Op De Beeck, K., Vander Poorten, V., Hauben, E., Lambrecht, M., Nuyts, S., & Hermans, R. (2012). Diffusion-weighted magnetic resonance imaging early after chemoradiotherapy to monitor treatment response in head-and-neck squamous cell carcinoma. *International Journal of Radiation Oncology Biology Physics*, *82*(3), 1098–1107. https://doi.org/10.1016/j.ijrobp.2011.02.044

Vidiri, A., Gangemi, E., Ruberto, E., Pasqualoni, R., Sciuto, R., Sanguineti, G., Farneti, A., Benevolo, M., Rollo, F., Sperati, F., Spasiano, F., Pellini, R., & Marzi, S. (2020). Correlation between histogram-based DCE-MRI parameters and 18F-FDG PET values in oropharyngeal squamous cell carcinoma: Evaluation in primary tumors and metastatic nodes. *PLOS ONE*, *15*(3), e0229611. https://doi.org/10.1371/journal.pone.0229611

Yamauchi H, S. A. (2014). Diffusion imaging of the head and neck. *Curr Radiol Rep. 2014;2:49*, *2*(49).

Young, H., Baum, R., & Cremerius, U. (1999). Position paper. Measurement of clinical and subclinical tumour response using -fluorodeoxyglucose and positron emission tomography: review and 1999. *Eur J ...*, *35*(13). http://www.vailworkshop.org/files/2010/LibraryResources/Villalona References/Young H, Measurement of Clinical and Subclinical Tumour Response.pdf

Appendix 3:

CORRELATION BETWEEN TISSUE CELLULARITY AND METABOLISM REPRESENTED BY DIFFUSION WEIGHTED IMAGING (DWI) AND 18F-FDG PET/MRI IN HEAD AND NECK CANCER (HNC).

Abstract

Background: Hybrid PET/MRI is an emerging imaging technology proved to be useful for better understanding of the tumor metabolism and cellularity, it also plays a very important in staging, assessment and post-therapy follow up. PET/MRI can be used to better understand how tumors act, especially prior to therapy. This study aimed to assess the association of ^{18}F-Fluorodeoxyglucose positron-emission-tomography (18F-FDG/PET) and DWI imaging parameters from the primary tumor and their correlations with clinicopathological factors.

Methods:

We retrospectively analyzed primary tumor in 71 patients with proven HNC. Primary tumor radiological parameters DWI and FDG as well as pathological characteristics were analyzed. Spearman correlation coefficient was used to assess the correlation between DWI and FDG parameters, ANOVA or Kruskal–Wallis, independent sample t test, Mann-Whitney test and multiple regression were performed on the clinicopathological features that may affect the 18F-FDG and ADC of the tumor.

Results: No significant correlations were observed between DWI and any ^{18}F-FDG parameters (P>0.05). SUVmax and TLG correlated with N-stages (P=0.023, P=0.033), TLG and MTV correlated with T-stages (P=0.006 and P=0.001), ADC correlated with tumor grades (P=0.05). SUVmax and ADC can differentiate between N+ and N- groups (P=0.004, P=0.012).

Conclusions: Our results revealed a non-significant correlation between the FDG-PET and ADC-MR parameters. The FDGPET-based glucose metabolic and DWI-MR-derived cellularity data may represent different biological aspects of HNC.

Trial registration: The trial is registered in clinical trials registry under **ID:**NCT04360993, registration date: 24/04/2020. Retrospectively registered. URL: https://clinicaltrials.gov/ct2/show/NCT04360993

Keywords: Diffusion-Weighted Imaging; Apparent Diffusion Coefficient; Head and Neck Squamous Cell Carcinoma, PET/MRI, glucose metabolism, primary tumor.

Introduction:

Worldwide; Head and neck cancer is the sixth most common malignancy; approximately 6% of all cancer cases, accountable for an estimated 1%–2% of all cancer deaths.(Siegel et al., 2017) H&N cancers are a heterogeneous group of cancers that existed anatomically close to each other, but different in terms of etiology, histology, diagnostic, and treatment approaches.(Grégoire et al., 2010) About 91% of all H&N cancer are squamous cell carcinomas, 2% are sarcomas and the other 7% are adenocarcinomas, melanomas, and not well-specified tumors.(*European Crude and Age Adjusted Incidence by Cancer, Years of Diagnosis 2000 and 2007 Analisys Based on 83 Population-Based Cancer Registries *, 2014)

Recently, ^{18}F-fluorodeoxyglucose (FDG) positron emission tomography (PET)/magnetic resonance imaging (MRI) has emerged as an effective and accurate imaging modality in oncology.(Pace L, Nicolai E, Aiello M, Catalano OA, 2013) The PET/MRI is expected to be more valuable than PET or CT alone or combined because the PET/MRI involves better contrast in soft tissues and a lower radiation dose from the MRI system. (Pace L, Nicolai E, Aiello M, Catalano OA, 2013) The advantage of clinical PET/MR is rather to replace PET/CT + MR, and reduce the radiation dose in comparison with PET/CT. PET/MRI also offers DWI which is a widely used technology to assess the motion of water molecules (Brownian motion) as a noninvasive diagnosis technology of tissue biology, (Yamauchi H, 2014) by taking apart the texture of a biologic tissue based on the water molecules motion at a microscopic level. (Queiroz et al., 2014) ADC represents DWI in determining the tumor's cellularity. (Becker & Zaidi, 2014; Surov et al., 2017) The higher cellular tumor resulted in more restriction to water molecule motion which, as a result, gives lower ADC values and vice versa. (Abdel Razek AA, 2013) This means that the water molecule's motion is reflecting the signal loss on DWI due to different water permeability through the structures. (Herneth et al., 2003; Queiroz et al., 2014) Previous studies have proved the inversely proportional correlation between ADC and tumor cellularity. (Hayashida et al., 2006; Jeh et al., 2011) ADC also was found to be effective in primary tumor assessment, differentiating between benign and

malignant neoplasms, staging, and monitoring post-treatment follow-up. (Srinivasan et al., 2008; Zhang et al., 2016) Moreover, ADC was found to be useful for predicting treatment response in HNSCC. (King & Thoeny, 2016)

The FDG uptake values measured from PET imaging has an important role in head and neck imaging due to its ability to measure the glucose metabolism in the tumors, (Miccò et al., 2014; Toth et al., 2018; Yildirim et al., 2017) which may also reflect the tumor's aggressiveness and the risk of the metastasis to spread to the adjacent structures. (Haerle et al., 2010; Nakajo et al., 2012) SUV is the most common parameter used to estimate glucose metabolism, and it has shown promising results in predicting the presence of lymph nodes metastatic during the primary assessment as well as a predictor of survival and recurrence. (Onal et al., 2013) Metabolic parameters, TLG and MTV have emerged as new parameters that can measure the glucose metabolism activity of tumors and have been founded to be more effective than SUV because tumor contour is considered when using MTV and TLG. (Kim et al., 2016) Since SUVmax doesn't reflect the metabolic activity of the entire lesion but it measures the highest glucose metabolism in the target ROI. (Sridhar P, Mercier G, Tan J, 2014) While MTV represents the volume of the ^{18}F-FDG activity in the lesion and TLG represents the sum of the SUV within the lesion. Furthermore, glucose metabolic activity is positively correlated to the tumor cellularity. (Bos et al., 2002; Ito et al., 1996)

Therefore, our study was aimed to investigate the correlation between FDG parameters and ADC values, which has focused, in-depth, on finding out if there is a correlation between tumor metabolic activity and cellularity represented by ADC and SUVmax, TLG and MTV, as well as assessing the ability of these imaging parameters to determine tumor aggressiveness by predicting lymph nodes involvement.

Materials and methods:

Patients and demographics:

A retrospective study was approved by the Clinical Center, Regional and Local Research Ethics Committee (CCRLREC), Doctoral School of Health Sciences, University of Pecs, and Somogy Megyei Kaposi Mor Educational Hospital, Pecs, Hungary (Approval Number: IG/04866.000/2020). The requirement of the informed consent was waived and confirmed by the

(CCRLREC) due to the retrospective nature, and all methods were carried out following the relevant guidelines and regulations (Declaration of Helsinki). From May 2016 to June 2019, 109 patients with proven HNC underwent ^{18}F-FDG PET/MRI for staging and restaging, assessment of the disease. The inclusion criteria were (1) proved non-treated primary HNC, (2) patients underwent PET/CT and PET/MRI including DWI sequence (3) single tracer injection session. Exclusion criteria (1) patients who had non-measurable ADC, or FDG parameters (2) patients with motion artifact or bad image quality. Finally, a total of 71 patients were included in our study. *Table (1)*. Final confirmation of malignancy was done after PET/MRI examination of the primary tumor and metastatic lymph nodes combined with biopsy.

Table1: patients demographics

Number of patients	*71*
Mean Age (y)	*(61.6±0.8)*
Men	*49 (69.0%)*
Women	*22 (31.0%)*
Histologic Grade	
Grade 1	*12 (16.9%)*
Grade 2	*41 (57.7%)*
Grade 3	*18 (20.4%)*
Localization	
Pharyngeal	*32 (45.1%)*
Laryngeal	*15 (21.1%)*
Oral	*22 (33.8%)*
T category	

T1	4 (5.6%)
T2	19 (26.8%)
T3	26 (36.6%)
T4	22 (31.0%)
N category	
N0	10 (14.1%)
N1	9 (12.7%)
N2	45(63.4%)
N3	7 (9.9%)
M Category	
M0	63 (88.7%)
M1	8 (11.3%)
N groups	
N+	61(85.9%)
N -	10 (14.1%)

PET/MRI imaging:

Examinations were performed in a dedicated PET/MRI (3T) unit (Biograph mMR, Siemens AG, Erlangen, Germany) after PET/CT examinations (single tracer injection). Patients were requested to fast for at least 6 hours before ^{18}F-FDG injection and their Blood glucose levels were checked before they received the tracer injection to ensure euglycemia. Intravenous ^{18}F-FDG with a bodyweight adapted dose (4 MBq/kg, range 163-403 MBq) was intravenously injected; after the FDG tracer injection, the acquisition was started within (60±30) minutes for PET/CT and (15±5) minutes after PET/CT, the PET/MRI was done. Images were obtained in the supine position using Head and Neck coils. MRI sequences were T2-weighted TSE turbo inversion recovery magnitude (TIRM) (TR/TE/TI 3300/37/220ms, FOV: 240 mm, slice thickness: 3 mm,

224 x 320) coronal plan, T1-weighted turbo spin-echo (TSE) (TR/TE 800/12ms, FOV: 200 mm, slice thickness: 4 mm, 224 x 320) and T1-weighted TSE Dixon fat suppression (FS) (TR/TE 6500/85ms, FOV: 200 mm, slice thickness: 4 mm, 256 x 320) transversal and were acquired without an intravenous contrast agent. For the PET data collection, a magnetic resonance-based attenuation correction (MRAC) sequence was used for PET attenuation correction, and the wide range bed position PET Emission scan was acquired for 900 seconds with a fixed FOV range (20 cm) and matrix (172x172) without bed movement as well. An iterative ordered subset expectation maximization (3D OP-OSEM) PET image reconstruction algorithm was used with 3 iterations and 21 subsets, and 4mm Gaussian filtering settings. The PET data were corrected for scattering, random coincidences, and attenuation using the MR data. The DWI was obtained by using an axial echo-planar imaging (EPI) sequence with b-values of 0 and 800 s/mm^2 (FoV 315 mm, repetition time TR/TE: 9900/75 ms, 5 mm slice thickness and voxel size 2.3 x 2.3 x 5 mm and slice gap 10mm). Furthermore, an axial Dixon FS T1-weighted TSE sequence and a coronal TSE Dixon FS sequence were conducted after injection of contrast material (Gadovist$^©$ Bayer Healthcare, Leverkusen, Germany) at 0.1 mmol per kg of bodyweight.

Image analysis:

In each patient, the SUVmax, TLG, MTV were measured from the PET imaging; Siemens (Syngo Via 10VB) was used, which provided an automatized delineated SUV-based volumetric analysis. The metabolic volumetric contours were segmented by using the Syngo Via (VOI) Sphere tool. The single voxel activity concentration of a particular tumor with the highest SUV was represented by SUVmax. A fixed 2.5 threshold of SUV was used for tumor SUVmax for both MTV and TLG proposed by *Pak et al.*(Pak et al., 2014) The volume above the given VOI was represented the MTV while the TLG represented the VOI of the average SUVmean or SULmean multiplied by the MTV. The ADC map was automatically generated and analyzed on the implemented eRAD software. DWI images were analyzed by drawing round or oval region of interest (ROI) manually on the ADC map covering the largest tumor diameter, (Miccò et al., 2014) on a single DWI slice (Fruehwald-Pallamar et al., 2011) within the center of the lesion in the most homogenous part which aswas the lowest ADC or the highest SUV reported after excluding or/and avoiding the necrotic and cystic areas. We did not use the whole tumor volumes ADC measurements approach although it is more reproducible than those obtained from a single slice or small ROI's

measurements. However, there was no significant difference between the tumor ADCs obtained using whole-volume measurements and the single-slice approach.(Lambregts et al., 2011) Thus, we have chosen the single-slice method because it's easier, faster and as a result more preferred in clinical practice than the whole volume ROIs protocol which is time-consuming and more complicated. Average ADC values calculated by the software automatically was referred to as ADCmean by summing all voxels ADC values on the drawn ROI for the chosen slice. We assessed only ADCmean values, which as previously proposed as a more reliable indicator of tumor cellularity since the entire lesion is taken into account.(Jeong et al., 2016) ADCmin, on the other hand, was suggested to reflect the most proliferative portion of a tumor or highest tumor cell density, due to the effects of lesion heterogeneity or artifacts the use of ADCmin is likely to result in more errors.(Er et al., 2014) Besides, ADCmean minimizes the effect of tumor heterogeneity and its higher reliability to distinguish different entities in the same image. (Sakane et al., 2015) We used the average ADC of the overall area included in the ROI which is calculated automatically by the software (Hounsfield unit). *Figure 1 (D),* where "Avg" represents the average ADC values for all voxels within the ROI and "Dev" Represents the standard deviation. *Figure (1).*
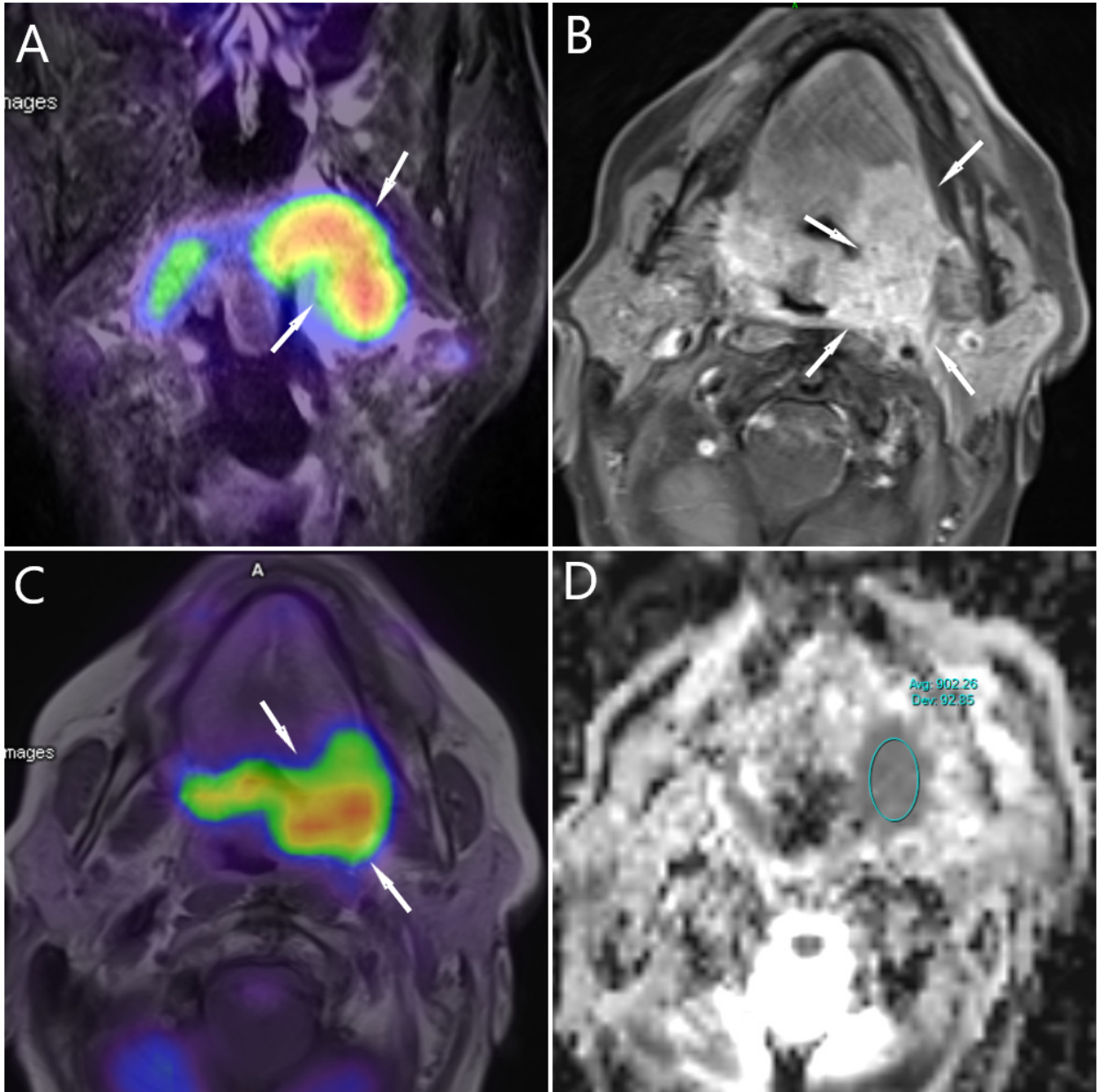
Figure (1): *ADC and ^{18}F-FDG measurements of 67 male patient with Oropharyngeal carcinoma. (A) T2-PET_tirm coronal MRI show the intensive FDG accumulation (arrow). (B) T1-tse-sagittal show the extent of the tumor, lateral pharyngeal wall into tongue root to the left tongue body (arrows). (C) T1-PET fused image show the ROI within the tumor (arrows), and (D) DWI/ADC map showing the average and standard deviation of ADC value.*

Statistical analysis:

Statistical analysis was performed by using SPSS 25 (IBM SPSS Statistics, Armonk, New York, USA). The data collected were evaluated using descriptive statistics (mean ± standard deviation),

for variables with normal distribution and median and interquartile range for variables with non-normal distribution. The Spearman rank correlation (r) was used to estimate the association between 18F-FDG parameters and ADC values and tumor size (continues variable). ANOVA or Kruskal–Wallis test were performed on the clinicopathological features that may affect the 18F-FDG and ADC of the tumor. Variables for which P<0.1 in univariate analysis were subjected to multiple linear regression analysis to determine those that were independently associated with the imaging parameters by integrating statistically significant differences in the univariate analysis into the multivariate linear regression model, we used transforming function to convert variables with non-normal distribution into a normal distribution, then the factors were added one by one (Stepwise). Mann-Whitney test and independent-sample T-test were applied to the imaging parameters after the patients were grouped based on lymph nodes involvement into positive (N+) and negative lymph nodes (N-). A p-value <0.05 was indicated as a statistically significant result.

Results:

A summary of the measurements in supplementary 1. Spearman's correlation coefficient was applied on ^{18}F-FDG parameters and ADC values; the results show that ^{18}F-FDG parameters (SUVmax, TLG and, MTV) were not correlated with ADC values (r = -0.184, P=0.125, r = -0.182, P=0.248, and r = -0.037, P=0.756), respectively. A summary of correlations is shown in *Table (2)*. *Figure 2 (A, B, and C).*
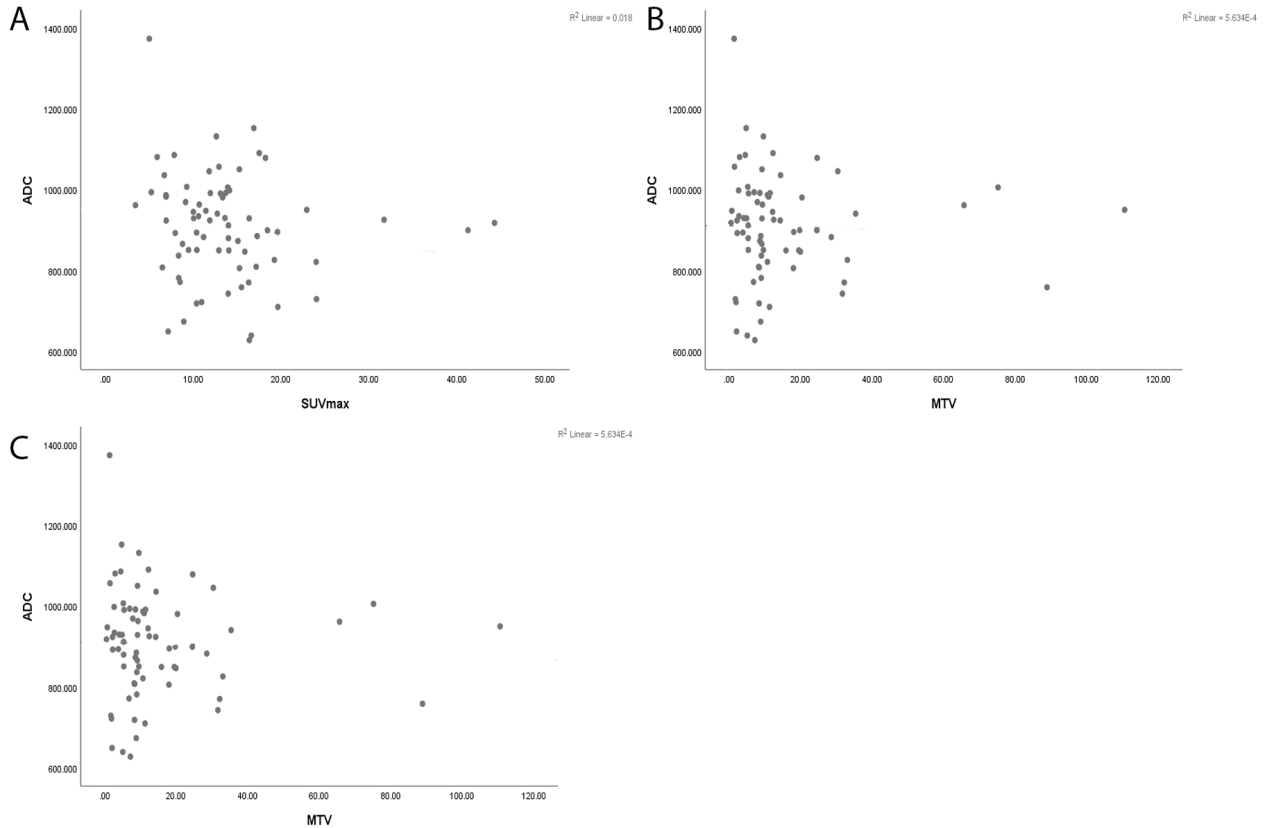
Figure (2): Scatter diagram showing the correlation between the ADCmean and (A) SUVmax, (B) TLG and (C) MTV. No significant linear correlation observed between ADCmean and any of 18F-FDG parameters, P>0.05.

Moreover, the Spearman correlation coefficient was used to assess the correlation between 18F-FDG and tumor size (Tumor size was measured as the maximum diameter of the tumor in pathologic results, mean size was 49.8±2.5 mm). The results show that 18F-FDG parameters (SUVmax, TLG and MTV) were significantly and positively correlated with tumor size (r =0.456, P=0.001; r =0.794, P=0.001 and r =0.739, P=0.001), respectively. ADC, on the other side, show no significant correlation with tumor size (r = -0.088, P=0.464). *Table (2). Figure 3 (A, B, C, and D).*

Table 2: summary of correlations between FDG and DWI imaging parameters

Parameter		ADC	SUVmax	TLG	MTV	Tumor size
ADC	Spearman (rho)		-.184	-.182	-.037	-.088
	Sig. (2-tailed)		.125	.129	.756	.464
SUVmax	Spearman (rho)					.456**
	Sig. (2-tailed)					.000
TLG	Spearman (rho)					.794**
	Sig. (2-tailed)					.000
MTV	Spearman (rho)					.739**
	Sig. (2-tailed)					.000

*significant at level of 0.05
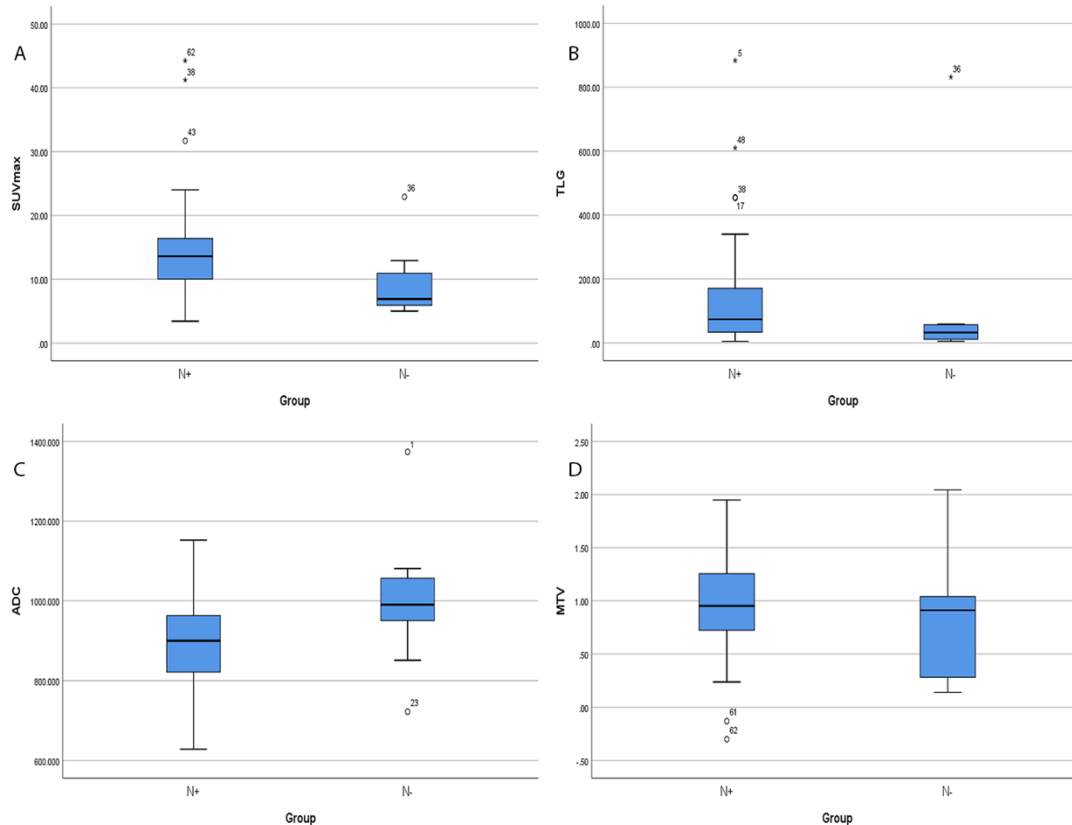
** significant at level of 0.01

Figure (3): Scatter diagram showing the correlation between the tumor size and each of 18F-FDG and DWI/ADC imaging parameters. The relationship between tumor size and (A) SUVmax is linear (r = 0.456, P=0.000). (B) TLG is linear (r =0.794, P=0.000) and (C) MTV is linear (r =0.739, P=0.000). Finally, (D) there was no linear correlation between tumor size and ADC (r = -0.088, P=0.464).

For clinicopathological comparison, we compared primary tumor FDG (SUVmax, MTV, and TLG) and ADC parameters with sex, T stages, N stages, M stages (7th Edition American Joint Committee on Cancer pathological staging criteria), (Edge & Compton, 2010) localization, and the degree of differentiation (grades). The results show that N stages were correlated with higher SUVmax, (P=0.023). T stages and N stages were correlated with higher TLG values (P=0.006 and P=0.033), respectively. T stages were correlated with higher MTV values (P=0.001). Lower ADC, on the other side, was found to be correlated with the degree of differentiation (P=0.05), a tendency for ADC to correlate with N stages increase, decreasing in the ADC as the number of lymph nodes

increase, (P=0.092). No other significant correlations were observed, (P>0.05) for all parameters. *Table (3)*.

Table 3: Clinicopathological comparison with FDG and DWI imaging parameters

Grouping	SUVmax	TLG	MTV	ADC
SEX	P=0.314	P=0.522	P=0.784	P=0.897
T stages	P=0.267	***P=0.006***	***P=0.001***	P=0.880
N stages	***P=0.023***	***P=0.033***	P=0.605	P=0.092
M stages	P=0.283	P=0.785	P=0.913	P=0.347
Grades	P=0.233	P=0.310	P=0.713	***P=0.050***
Localization	P=0.389	P=0.128	P=0.367	P=0.270

. Kruskal-Wallis for multi-categorical variables (T stages, N stages, Localization and tumor grades) and Mann-Whitney test for two category variables (sex, M stages) were used with (SUVmax, TLG and MTV). ANOVA and Independent Sample T test was used with ADC values.

. Significant result was highlighted in Bold

Multiple regression was recruited for factors that shown a statistically significant correlation in univariate analysis to investigate the factor that influences the change in (SUVmax, TLG, MTV, and ADC). The results showed that tumor size and N stage were independent factors influencing SUVmax, (P=0.001 and P=0.008), respectively. Tumor size was an independent factor influencing TLG and MTV (P=0.001 and P=0.001), respectively. Tumor grade was found to be independent influencing factor of ADC (P=0.05). *Table (4)*.

Table 4: Multiple Regression Analysis Showing the Effects of Prognostic Factors on 18f-FDG parameters

Prognostic factors	B	T	P value
SUVmax			
Tumor size	.409	3.333	**.001***
T stages	N/A	N/A	N/A
N stages	.227	1.995	**.022***
TLG			
Tumor size	.767	8.988	**.000***
T stages	-.050	-.598	.552
N stages	.119	1.500	.138
MTV			
Tumor size	.662	6.857	**.000***
T stages	.140	1.473	.146
N stages	N/A	N/A	N/A
ADC			
N stages	.043	2.042	*.069*
Tumor grades	-.021	-1.846	***.045****

*Significant result

N/A: Not assessed

When removing the effect of the tumor size, SUVmax was correlated with N stages (P=0.011), but not with T stages (P=0.838), TLG was significantly correlated with both T stage and N stages (P=0.018 and P=0.034), and MTV was correlated to T stages (P=0.001).

To investigate the ability of FDG and ADC parameters to predict lymph nodes involvement, we classified the patients based on lymph nodes involvement into negative and positive groups (N- and N+) and compared them with these parameters. Our results show that SUVmax, TLG and

ADC revealed statistically significant differences (P=0.004, P=0.048, and P=0.012), respectively. TLG and MTV did not (P>0.05).

Discussion:

The present study demonstrated that PET/MR provides valuable imaging data for HNC patients. Various pathological factors were associated with PET/MR results and may serve a role in the evaluation of the prognosis of patients with HNC. As for promising technology, PET/MRI offers different imaging data to study tumor microstructure environment, we started our study by correlating these imaging parameters to each other. Previous data demonstrated an inverse correlation between ADC value, derived from DWI, with cellularity.(Abdel Razek AA, 2013; Becker & Zaidi, 2014; Hayashida et al., 2006; Surov et al., 2017) FDG imaging parameters, on the other hand, were found to be positively correlated with cellularity.(Bos et al., 2002; Ito et al., 1996; Vandecaveye et al., 2009) Although glucose metabolism and cellularity of tissue are two different biological biomarkers of a tumor, an inverse correlation between 18F-FDG and DWI parameters has been suggested.(S. et al., 2017) this hypothesis was proposed because both 18F-FDG and ADC were correlated with tumor cellularity.(Jeong et al., 2016) Our results showed that FDG uptake parameters (SUVmax, TLG, and MTV) were not significantly correlated with the ADCmean value. Similar results were observed; *Min et al.,* in their study of HNSCC, reported that there was no significant correlation between ADCmean with SUVmax and SUVmean, also no significant correlation was found between ADCmean and both MTV and TLG.(Min et al., 2016) *Surov et al.,* in a recent study, reported no significant correlation between ADCmean and SUVmax or SUVmean (r = -0.255, P=0.450 and r = -0.318, P=0.340), respectively.(Surov et al., 2016) Other authors reported similar findings.(Fraum et al., 2016; Fruehwald-Pallamar et al., 2011; Rasmussen et al., 2017; Varoquaux et al., 2013)

Controversially to our results, *Nunez et al.* observed, in their study of HNSCC, an inverse significant correlation between the mean SUV and the mean ADC (r = -0.67, P=0.01).(Núñez et al., 2017) *Nakajo et al.* also observed that the SUVmax was correlated inversely with the ADCmean (r = -0.566, P=0.005).(Nakajo et al., 2012) *Nakamatsu et al.,* in their study of metastasis in lymph nodes from HNSCC, found strong negative correlations between SUVmax and ADCmean values (P>0.001), their results showed that the metabolic activity was influenced

strongly by the tumor cellularity.(Nakamatsu et al., 2012) *Han et al.* reported, in their study of HNSCC, that there was a slightly significant inverse correlation between SUV and ADC (r = -0.333, P=0.054). They also found a negative significant correlation between ADC and TLG (r = -0.347, P=0.044).(Han et al., 2015)

Our explanation for the lack of correlation is the fact that both imaging parameters explain different tissue microstructures characteristics, DWI assess the water molecule motion in the tissue and affected by the cellularity, proliferation rate and cell counts which in clinical use affected by ROI size placement and interobserver variability.(Lambregts et al., 2011) While metabolic activity was independent of tumor size and shape because tumor is segmented by adaptive thresholding.(Jeong et al., 2016)

The present study correlated FDG and DWI imaging parameters with T stages, N stages, and tumor size to explore their effect on the imaging parameters values. Our results reveal that FDG metabolic parameters have reported different correlations; it has shown that primary tumor SUVmax and TLG were significantly correlated with the N stages; the higher N stage resulted in a higher value of SUVmax and TLG, while MTV did not show correlation with N stages. According to *Zheng et al.,* there was a positive significant correlation between lymph nodes status and SUVmax, higher SUVmax, resulted in more lymph nodes metastasis, which means that SUVmax has a promising predictive role in lymph node diagnosis.(Zheng et al., 2019) *Micco et al* reported a significant correlation between lymph node occurrence with SUVmax and TLG.(Miccò et al., 2014) *Morand et al.* have observed similar results, higher lymph node involvement was found in patients with higher primary tumor SUVmax.(Morand et al., 2018) In the same study, the authors reported that TLG did not correlate with lymph node status (Morand et al., 2018). Furthermore, in our study, no significant correlation was observed between MTV and the lymph node status. A similar result reported by *Morand et al.* (Morand et al., 2018) and Chan et al. (Chan et al., 2010) In contrast to *Micco et al.* who reported a significant association between MTV and lymph node occurrence.(Miccò et al., 2014) After excluding the confounding factor to investigate which clinical factor influencing the increase in FDG uptake values, we found that N stages and tumor size were independent factors influencing SUVmax. Tumor size and

tumor T stages but not N stages were independent factors influencing TLG and MTV. Thus, SUVmax might be a promising imaging biomarker to predict tumor aggressiveness.

 ADC, on the other hand, shows a significant correlation with tumor grades, which reflect the degree of water motion within the tumor cells, this is from the fact that higher-grade tumors (G3) show more restriction to water molecules motion (lower cellularity) which as result affect ADC. On the other side, ADC did not show significant correlations with T stages, N stages, or Tumor size although there was a slightly negative correlation with N stages (P=0.092). In other words, as the ADC tend to be lower (poorly differentiated tumors), the lymph nodes involvement increase, but this result was not statistically significant, thus, the ADC was not a reliable prognostic imaging biomarker to predict tumor aggressiveness. *Nakajo et al*. have reported in their study of primary HNSCC similar results, there was no significant difference in the ADC between N-positive and N-negative groups (p=0.74).(Nakajo et al., 2012) Previous studies have explored this correlation; similar results were reported.(Choi et al., 2012; Karan et al., 2016) On the other hand, *Abdel Razek et al.* in their study of Nasopharyngeal carcinoma have reported a statistically significant difference between primary tumor ADC and nodal involvement, (P=0.003), (Abdel Razek & Kamal, 2013) this mean that patients without lymph nodes involvement showed higher ADC value than those patients who have confirmed lymph nodes enlargement. The explanation of their result was attributed that those patients with poorly or undifferentiated malignancy are usually reporting metastatic lymph nodes.(Abdel Razek & Kamal, 2013) In our study, a controversial result was reported, our explanation is due to the heterogeneity of the patient's sample which contains multiple primary tumor localization, thus different anatomical and histological components were involved.

Although there are several studies that have investigated the 18F-FDG and ADC diagnostical role to determine tumor aggressiveness in different cancers.(Gong et al., 2019; Kato et al., 2019; Nerad et al., 2019; Xu et al., 2020; Yang et al., 2019; Yu et al., 2019; Zheng et al., 2019) None of the studies have compared the efficacy of PET/MRI system different imaging biomarkers in HNC tumor aggressiveness prediction. Thus, to our knowledge, this is the first study to compare PET/MRI system derived imaging parameters in lymph nodes involvement in HNC. Our results show that SUVmax, TLG, and ADC were found to have the ability to differentiate between the

two lymph node groups (N+ and N-) based on the primary tumor measurements, which as a result might help to predict tumor development and prognosis. Our study shows that SUVmax had higher diagnostic performance, higher sensitivity, and better specificity than ADC, as well as the presence of significant correlation with N stages which has not been found in ADC. Nevertheless, ADC can predict tumor aggressiveness and lymph node involvement prediction but with limited efficacy. The importance of successful prediction of tumor aggressiveness and lymph node involvement might help in practice to increase the aggressiveness of the therapy.

Based on our study results and findings, there were several correlations between PET/MRI imaging parameters and clinical tumor characteristics, we suggest that glucose metabolism assessed by 18F-FDG and cellularity assessed by ADC have different roles in cancer evaluation, so we recommend PET/MRI as a combined examination rather than PET or MRI alone.

As for this study's limitations, First, the heterogeneity of the tumor localization. Second, our study focused on the search of a correlation between 18F-FDG, ADC, and histopathological features only in HNC. Third, associations with other functional tumor parameters, such as apoptosis factors and were not analyzed. Fourth, the design of the study was retrospective.

Conclusion:

Our results revealed no linear correlation between the FDG PET and ADC MR parameters. The FDG PET-based glucose metabolic and DWI MR derived cellularity data may represent different biological aspects of HNC tumors and simultaneous PET/MR imaging could provide complementary diagnostic information. SUVmax, have shown higher accuracy in predicting tumor aggressiveness than DWI.

Bibliography:

Abdel Razek, A. A. K., & Kamal, E. (2013). Nasopharyngeal carcinoma: Correlation of apparent diffusion coefficient value with prognostic parameters. *Radiologia Medica*, *118*(4), 534–539. https://doi.org/10.1007/s11547-012-0890-x

Abdel Razek AA, K. E. (2013). Nadopharyngeal carcinoma: correlation of apparent diffusion coeffecient value with prognostic parameters. *La Radiologia Medicine*, *118*(4), 534–539.

Becker, M., & Zaidi, H. (2014). Imaging in head and neck squamous cell carcinoma: the potential role of PET/MRI. *The British Journal of Radiology*, *87*(1036), 20130677. https://doi.org/10.1259/bjr.20130677

Bos, R., van der Hoeven, J. J. M., van der Wall, E., van der Groep, P., van Diest, P. J., Comans, E. F. I., Joshi, U., Semenza, G. L., Hoekstra, O. S., Lammertsma, A. A., & Molthoff, C. F. M. (2002). Biologic Correlates of 18Fluorodeoxyglucose Uptake in Human Breast Cancer Measured by Positron Emission Tomography. *Journal of Clinical Oncology*, *20*(2), 379–387. https://doi.org/10.1200/JCO.2002.20.2.379

Chan, W. K. S., Mak, H. K. F., Huang, B., Yeung, D. W. C., Kwong, D. L. W., & Khong, P. L. (2010). Nasopharyngeal carcinoma: Relationship between 18F-FDG PET-CT maximum standardized uptake value, metabolic tumour volume and total lesion glycolysis and TNM classification. *Nuclear Medicine Communications*, *31*(3), 206–210. https://doi.org/10.1097/MNM.0b013e328333e3ef

Choi, B. B., Kim, S. H., Kang, B. J., Lee, J. H., Song, B. J., Jeong, S. H., & Yim, H. W. (2012). Diffusion-weighted imaging and FDG PET/CT: predicting the prognoses with apparent diffusion coefficient values and maximum standardized uptake values in patients with invasive ductal carcinoma. *World Journal of Surgical Oncology*, *10*(1), 1. https://doi.org/10.1186/1477-7819-10-126

Edge, S. B., & Compton, C. C. (2010). The American Joint Committee on Cancer: the 7th Edition of the AJCC Cancer Staging Manual and the Future of TNM. *Annals of Surgical Oncology*, *17*(6), 1471–1474. https://doi.org/10.1245/s10434-010-0985-4

Er, H. Ç., Erden, A., Küçük, N. Ö., & Geçim, E. (2014). Correlation of minimum apparent diffusion coefficient with maximum standardized uptake on fluorodeoxyglucose PET-CT in patients with rectal adenocarcinoma. *Diagnostic and Interventional Radiology*, *20*(2), 105.

European crude and age adjusted incidence by cancer, years of diagnosis 2000 and 2007 Analisys based on 83 population-based cancer registries *. (2014). http://www.rarecarenet.eu/rarecarenet/images/indicators/Incidence.pdf

Fraum, T. J., Fowler, K. J., & McConathy, J. (2016). PET/MRI: Emerging Clinical Applications in Oncology. *Acad Radiol*, *23*(7), 220–2236. https://doi.org/10.1016/j.ejrad.2015.04.010

Fruehwald-Pallamar, J., Czerny, C., Mayerhoefer, M. E., Halpern, B. S., Eder-Czembirek, C., Brunner, M., Schuetz, M., Weber, M., Fruehwald, L., & Herneth, A. M. (2011). Functional imaging in head and neck squamous cell carcinoma: Correlation of PET/CT and diffusion-weighted imaging at 3 Tesla. *European Journal of Nuclear Medicine and Molecular Imaging*, *38*(6), 1009–1019. https://doi.org/10.1007/s00259-010-1718-4

Gong, J., Wang, N., Bian, L., Wang, M., Ye, M., Wen, N., Fu, M., Fan, W., & Meng, Y. (2019). Cervical cancer evaluated with integrated 18F-FDG PET/MR. *Oncology Letters*, 1815–1823. https://doi.org/10.3892/ol.2019.10514

Grégoire, V., Lefebvre, J. L., Licitra, L., & Felip, E. (2010). Squamous cell carcinoma of the head and neck: EHNS-ESMO-ESTRO clinical practice guidelines for diagnosis, treatment and follow-up. *Annals of Oncology*, *21*(SUPPL. 5), 184–186. https://doi.org/10.1093/annonc/mdq185

Haerle, S. K., Huber, G. F., Hany, T. F., Ahmad, N., & Schmid, D. T. (2010). Is there a correlation between 18F-FDG-PET standardized uptake value, T-classification, histological grading and the anatomic subsites in newly diagnosed squamous cell carcinoma of the head and neck? *European Archives of Oto-Rhino-Laryngology*, *267*(10), 1635–1640. https://doi.org/10.1007/s00405-010-1348-2

Han, M., Kim, S. Y., Lee, S. J., & Choi, J. W. (2015). The Correlations Between MRI Perfusion , Diffusion Parameters , and 18 F-FDG PET Metabolic Parameters in Primary Head-and-Neck Cancer A Cross-Sectional Analysis in Single Institute. *Medicine*, *94*(47), 1–7. https://doi.org/10.1097/MD.0000000000002141

Hayashida, Y., Hirai, T., Morishita, S., Kitajima, M., Murakami, R., Korogi, Y., Makino, K., Nakamura, H., Ikushima, I., Yamura, M., Kochi, M., Kuratsu, J. -i., & Yamashita, Y. (2006). Diffusion-weighted Imaging of Metastatic Brain Tumors: Comparison with Histologic Type and Tumor Cellularity. *American Journal of Neuroradiology*, *27*(7), 1419 LP – 1425. http://www.ajnr.org/content/27/7/1419.abstract

Herneth, A. M., Guccione, S., & Bednarski, M. (2003). Apparent diffusion coefficient: A quantitative parameter for in vivo tumor characterization. *European Journal of Radiology*, *45*(3), 208–213. https://doi.org/10.1016/S0720-048X(02)00310-8

Ito, K., Kato, T., Ohta, T., Tadokoro, M., Yamada, T., Ikeda, M., Nishino, M., Ishigaki, T., Ito, K., & Gambhir, S. (1996). Fluorine-18 fluoro-2-deoxyglucose positron emission

tomography in recurrent rectal cancer: relation to tumour size and cellularity. *European Journal of Nuclear Medicine*, *23*(10), 1372–1377. https://doi.org/10.1007/BF01367594

Jeh, S. K., Kim, S. H., Kim, H. S., Kang, B. J., Jeong, S. H., Yim, H. W., & Song, B. J. (2011). Correlation of the apparent diffusion coefficient value and dynamic magnetic resonance imaging findings with prognostic factors in invasive ductal carcinoma. *Journal of Magnetic Resonance Imaging : JMRI*, *33*(1), 102–109. https://doi.org/10.1002/jmri.22400

Jeong, J. H., Cho, I. H., Chun, K. A., Kong, E. J., Kwon, S. D., & Kim, J. H. (2016). Correlation Between Apparent Diffusion Coefficients and Standardized Uptake Values in Hybrid 18F-FDG PET/MR: Preliminary Results in Rectal Cancer. *Nuclear Medicine and Molecular Imaging*, *50*(2), 150–156. https://doi.org/10.1007/s13139-015-0390-9

Karan, B., Pourbagher, A., & Torun, N. (2016). Diffusion-weighted imaging and 18F-fluorodeoxyglucose positron emission tomography/computed tomography in breast cancer: Correlation of the apparent diffusion coefficient and maximum standardized uptake values with prognostic factors. *Journal of Magnetic Resonance Imaging*, *43*(6), 1434–1444. https://doi.org/10.1002/jmri.25112

Kato, F., Kudo, K., Yamashita, H., Baba, M., Shimizu, A., Oyama-Manabe, N., Kinoshita, R., Li, R., & Shirato, H. (2019). Predicting metastasis in clinically negative axillary lymph nodes with minimum apparent diffusion coefficient value in luminal A-like breast cancer. *Breast Cancer*, *26*(5), 628–636. https://doi.org/10.1007/s12282-019-00969-0

Kim, Y. Il, Paeng, J. C., Cheon, G. J., Suh, K. S., Lee, D. S., Chung, J. K., & Kang, K. W. (2016). Prediction of posttransplantation recurrence of hepatocellular carcinoma using metabolic and volumetric indices of 18F-FDG PET/CT. *Journal of Nuclear Medicine*, *57*(7), 1045–1051. https://doi.org/10.2967/jnumed.115.170076

King, A. D., & Thoeny, H. C. (2016). Functional MRI for the prediction of treatment response in head and neck squamous cell carcinoma: Potential and limitations. *Cancer Imaging*, *16*(1), 1–8. https://doi.org/10.1186/s40644-016-0080-6

Lambregts, D. M. J., Beets, G. L., Maas, M., Curvo-Semedo, L., Kessels, A. G. H., Thywissen, T., & Beets-Tan, R. G. H. (2011). Tumour ADC measurements in rectal cancer: effect of ROI methods on ADC values and interobserver variability. *European Radiology*, *21*(12), 2567–2574. https://doi.org/10.1007/s00330-011-2220-5

Miccò, M., Vargas, H. A., Burger, I. A., Kollmeier, M. A., Goldman, D. A., Park, K. J., Abu-

Rustum, N. R., Hricak, H., & Sala, E. (2014). Combined pre-treatment MRI and 18F-FDG
PET/CT parameters as prognostic biomarkers in patients with cervical cancer. *European
Journal of Radiology*, *83*(7), 1169–1176. https://doi.org/10.1016/j.ejrad.2014.03.024

Min, M., Lee, M. T., Lin, P., Holloway, L., Wijesekera, D. J., Gooneratne, Di., Rai, R., Xuan,
W., Fowler, A., Forstner, Di., & Liney, G. (2016). Assessment of serial multi-parametric
functional MRI (diffusion-weighted imaging and R2) with 18F-FDG-PET in patients with
head and neck cancer treated with radiation therapy. *British Journal of Radiology*,
89(1058), 1–9. https://doi.org/10.1259/bjr.20150530

Morand, G. B., Vital, D. G., Kudura, K., Werner, J., Stoeckli, S. J., Huber, G. F., & Huellner, M.
W. (2018). Maximum Standardized Uptake Value (SUVmax) of Primary Tumor Predicts
Occult Neck Metastasis in Oral Cancer. *Scientific Reports*, *8*(1), 11817.
https://doi.org/10.1038/s41598-018-30111-7

Nakajo, M., Nakajo, M., Kajiya, Y., Tani, A., Kamiyama, T., Yonekura, R., Fukukura, Y.,
Matsuzaki, T., Nishimoto, K., Nomoto, M., & Koriyama, C. (2012). FDG PET/CT and
diffusion-weighted imaging of head and neck squamous cell carcinoma: Comparison of
prognostic significance between primary tumor standardized uptake value and apparent
diffusion coefficient. *Clinical Nuclear Medicine*, *37*(5), 475–480.
https://doi.org/10.1097/RLU.0b013e318248524a

Nakamatsu, S., Matsusue, E., Miyoshi, H., Kakite, S., Kaminou, T., & Ogawa, T. (2012).
Correlation of apparent diffusion coefficients measured by diffusion-weighted MR imaging
and standardized uptake values from FDG PET/CT in metastatic neck lymph nodes of head
and neck squamous cell carcinomas. *Clinical Imaging*, *36*(2), 90–97.
https://doi.org/10.1016/j.clinimag.2011.05.002

Nerad, E., Delli Pizzi, A., Lambregts, D. M. J., Maas, M., Wadhwani, S., Bakers, F. C. H., van
den Bosch, H. C. M., Beets-Tan, R. G. H., & Lahaye, M. J. (2019). The Apparent Diffusion
Coefficient (ADC) is a useful biomarker in predicting metastatic colon cancer using the
ADC-value of the primary tumor. *PLOS ONE*, *14*(2), e0211830.
https://doi.org/10.1371/journal.pone.0211830

Núñez, D. A., Medina, A. L., Iglesias, M. M., Gomez, F. S., Dave, A., Hatzoglou, V., Paudyal,
R., Calzado, A., Deasy, J. O., Shukla-Dave, A., & Muñoz, V. M. (2017). Multimodality
functional imaging using DW-MRI and 18 F-FDG-PET/CT during radiation therapy for

human papillomavirus negative head and neck squamous cell carcinoma: Meixoeiro Hospital of Vigo Experience . *World Journal of Radiology*, *9*(1), 17. https://doi.org/10.4329/wjr.v9.i1.17

Onal, C., Reyhan, M., Parlak, C., Guler, O. C., & Oymak, E. (2013). Prognostic value of pretreatment 18F-fluorodeoxyglucose uptake in patients with cervical cancer treated with definitive chemoradiotherapy. *International Journal of Gynecological Cancer : Official Journal of the International Gynecological Cancer Society*, *23*(6), 1104–1110. https://doi.org/10.1097/IGC.0b013e3182989483

Pace L, Nicolai E, Aiello M, Catalano OA, S. M. (2013). Whole-body PET/MRI in oncology: current status and clinical applications. *Transl Imaging.*, *1*(1), 31–44.

Pak, K., Cheon, G., Nam, H., Kim, S., Med, K. K.-J. N., & 2014, U. (2014). Prognostic value of metabolic tumor volume and total lesion glycolysis in head and neck cancer: a systematic review and meta-analysis. *THE JOURNAL OF NUCLEAR MEDICINE*, *55*(6), 1–7. http://www.academia.edu/download/46307953/Prognostic_Value_of_Metabolic_Tumor_V olu20160607-17979-obn7np.pdf

Queiroz, M. A., Hüllner, M., Kuhn, F., Huber, G., Meerwein, C., Kollias, S., von Schulthess, G., & Veit-Haibach, P. (2014). Use of diffusion-weighted imaging (DWI) in PET/MRI for head and neck cancer evaluation. *European Journal of Nuclear Medicine and Molecular Imaging*, *41*(12), 2212–2221. https://doi.org/10.1007/s00259-014-2867-7

Rasmussen, J. H., Nørgaard, M., Hansen, A. E., Vogelius, I. R., Aznar, M. C., Johannesen, H. H., Costa, J., Engberg, A. M. E., Kjær, A., Specht, L., & Fischer, B. M. (2017). Feasibility of multiparametric imaging with PET/MR in head and neck Squamous cell carcinoma. *Journal of Nuclear Medicine*, *58*(1), 69–74. https://doi.org/10.2967/jnumed.116.180091

S., D., Z., W., Y., W., W., Z., J., L., N., D., B., Z., & J., Y. (2017). Meta-analysis of the correlation between apparent diffusion coefficient and standardized uptake value in malignant disease. *Contrast Media and Molecular Imaging*, *2017*(no pagination), 4729547. http://www.epistemonikos.org/documents/2ffc3010315c57bfa650e08188580270f3fc4105

Sakane, M., Tatsumi, M., Kim, T., Hori, M., Onishi, H., Nakamoto, A., Eguchi, H., Nagano, H., Wakasa, K., Hatazawa, J., & Tomiyama, N. (2015). Correlation between apparent diffusion coefficients on diffusion-weighted MRI and standardized uptake value on FDGPET/ CT in pancreatic adenocarcinoma. *Acta Radiologica*, *56*(9), 1034–1041.

https://doi.org/10.1177/0284185114549825

Siegel, R., Miller, K. D., & Ahmedin, J. (2017). Cancer Statistics. *Ca Cancer Journal*, *67*(1), 7–30. https://doi.org/10.3322/caac.21387.

Sridhar P, Mercier G, Tan J, et al. (2014). FDG PET metabolic tumor volume seg- mentation and pathologic volume of primary human solid tumors. *AJR Am JRoentgenol.*, *202*, 1114–1119.

Srinivasan, A., Dvorak, R., Perni, K., Rohrer, S., & Mukherji, S. K. (2008). Differentiation of benign and malignant pathology in the head and neck using 3T apparent diffusion coefficient values: Early experience. *American Journal of Neuroradiology*, *29*(1), 40–44. https://doi.org/10.3174/ajnr.A0743

Surov, A., Meyer, H. J., & Wienke, A. (2017). Correlation between apparent diffusion coefficient (ADC) and cellularity is different in several tumors: a meta-analysis. *Oncotarget*, *8*(35), 59492–59499. https://doi.org/10.18632/oncotarget.17752

Surov, A., Stumpp, P., Meyer, H. J., Gawlitza, M., Höhn, A.-K., Boehm, A., Sabri, O., Kahn, T., & Purz, S. (2016). Simultaneous 18F-FDG-PET/MRI: Associations between diffusion, glucose metabolism and histopathological parameters in patients with head and neck squamous cell carcinoma. *Oral Oncology*, *58*, 14–20. https://doi.org/10.1016/J.ORALONCOLOGY.2016.04.009

Toth, Z., Lukacs, G., Cselik, Z., Bajzik, G., Egyed, M., Vajda, Z., Borbely, K., Hadjiev, J., Gyarmati, T., Emri, M., Kovacs, A., & Repa, I. (2018). [Hungarian clinical application opportunities of PET/MR imaging and first experiences]. *Orvosi hetilap*, *159*(34), 1375–1384. https://doi.org/10.1556/650.2018.31141

Vandecaveye, V., Keyzer, F. De, Poorten, V. Vander, Dirix, P., Verbeken, E., Nuyts, S., & Hermans, R. (2009). Head and Neck Squamous Cell Carcinoma : Value of Diffusion-weighted MR Imaging for Nodal STAGING. *Radiology*, *251*(1), 134–146.

Varoquaux, A., Rager, O., Lovblad, K. O., Masterson, K., Dulguerov, P., Ratib, O., Becker, C. D., & Becker, M. (2013). Functional imaging of head and neck squamous cell carcinoma with diffusion-weighted MRI and FDG PET/CT: Quantitative analysis of ADC and SUV. *European Journal of Nuclear Medicine and Molecular Imaging*, *40*(6), 842–852. https://doi.org/10.1007/s00259-013-2351-9

Xu, C., Li, H., Seng, D., & Liu, F. (2020). Significance of SUV Max for Predicting Occult

Lymph Node Metastasis and Prognosis in Early-Stage Tongue Squamous Cell Carcinoma. *Journal of Oncology*, *2020*. https://doi.org/10.1155/2020/6241637

Yamauchi H, S. A. (2014). Diffusion imaging of the head and neck. *Curr Radiol Rep. 2014;2:49*, *2*(49).

Yang, Z., Wu, J. R., Wei, L. L., Liao, G. X., Yang, C. J., Jin, G. Q., Xiao, G. Y., & Su, D. K. (2019). High standardized uptake values of 18F-FDG PET/CT imaging but not MRI correlates to pathology findings in patients with cervical cancer. *Hellenic Journal of Nuclear Medicine*, 96–102. https://doi.org/10.1967/s002449911001

Yildirim, I. O., Ekici, K., Doğan, M., Temelli, Ö., Kekilli, E., Saglık, S., Erbay, F., & Comak, A. (2017). Can diffusion weighted magnetic resonance imaging (DW-MRI) be an alternative to18f-FDG PET/CT (18f fluorodeoxyglucose positron emission tomography) in nasopharyngeal cancers? *Biomedical Research (India)*, *28*(9), 4255–4260.

Yu, Y. Y., Zhang, R., Dong, R. T., Hu, Q. Y., Yu, T., Liu, F., Luo, Y. H., & Dong, Y. (2019). Feasibility of an ADC-based radiomics model for predicting pelvic lymph node metastases in patients with stage IB–IIA cervical squamous cell carcinoma. *The British Journal of Radiology*, *92*(1097), 20180986. https://doi.org/10.1259/bjr.20180986

Zhang, S. C., Bao, Y. Y., Zhou, S. H., & Shang, D. S. (2016). Application value of diffusion weighted magnetic resonance imaging in head and neck cancer. *International Journal of Clinical and Experimental Medicine*, *9*(8), 16747–16752.

Zheng, D., Niu, L., Liu, W., Zheng, C., Yan, R., Gong, L., Dong, Z., Fei, J., & Li, K. (2019). Relationship between the maximum standardized uptake value of fluoro-2-deoxyglucose-positron emission tomography/computed tomography and clinicopathological characteristics in tongue squamous cell carcinoma. *Journal of Cancer Research and Therapeutics*, *15*(4), 842–848. https://doi.org/10.4103/jcrt.JCRT

ETHICAL APPROVAL AND CONSENT TO PARTICIPATE.

Regional and Local Research Ethics Committee (CCRLREC), Doctoral School of Health Sciences, University of Pecs, and Somogy Megyei Kaposi Mor Educational Hospital, Pecs, Hungary (Approval Number: IG/04866.000/2020). The requirement of the informed consent was waived and confirmed by the (CCRLREC) due to the retrospective nature, and all methods were carried out following the relevant guidelines and regulations (Declaration of Helsinki).

SOMOGY MEGYEI
KAPOSI MÓR OKTATÓ KÓRHÁZ

Dr. Moizs Mariann PhD
főigazgató
7400 Kaposvár, TalliánGy. u. 20-32.

TAM

TAM

☎ 82/501-301   📠 82/413-122   ✉ foigtitk@kmmk.hu

Omar Freihat
részére

Ikt.sz.: IG/~~...~~ -~~...~~/2020
Tárgy: Kutatási kérelem elbírálása
Ügyintéző: Dr. Zóka Péter

Tisztelt Omar Freihat!

A Somogy Megyei Kaposi Mór Oktató Kórházhoz benyújtott kutatási kérelmét etikai, szakmai, és adatvédelmi szempontból megvizsgáltam.

„A diffúzió súlyozott mágneses rezonanciás képalkotás és a 18F-FDG PET szerepe a fej-nyaki daganatok diagnosztikájában" témájú kutatási kérelmét engedélyezem.

Tájékoztatom, hogy a Somogy Megyei Kaposi Mór Oktató Kórháznak az engedélyhez vagy bejelentéshez kötött kutatások rendjéről szóló szabályzata, az egészségügyi és a hozzájuk kapcsolódó személyes adatok kezeléséről és védelméről szóló jogszabályok, valamint intézményi szabályzatok betartására köteles.

Elkészített dolgozatából egy példányt az intézmény Dr. Arató Miklós Orvosi Könyvtárában köteles elhelyezni.

Kaposvár, 2020. július 24.

Dr. Moizs Mariann PhD
főigazgató

Másolatban kapja:
- Dr. Bajzik Gábor centrumvezető főorvos

110

APPENDIX 5:

SUBMISSION OF THE DOCTORAL DISSERTATION AND DECLARATION OF THE ORIGINALITY OF THE DISSERTATION.

Appendix 7

SUBMISSION OF THE DOCTORAL DISSETRTATION AND DECLARAITION OF
THE ORIGINALITY OF THE DISSERTATION
The undersigned
name: Omar Mahmoud Ahmad Freihat
maiden name: Mahmoud
mother's maiden name: Sabah Bani Nasr
place and time of birth: Ajloun/ Jordan
on this day submitted my doctoral dissertation entitled " **PET/CT and PET/MR based**
treatment modalities in the modern oncology*"*

to the
programme/topic area: Oncology / Diagnostic medical imaging

of the Health sciences Doctoral School.
Names of the consultant(s):
Dr. Cselik Zsolt / Dr. Arpad Kovacs …………………………………...
At the same time I declare that
- I have not submitted my doctoral dissertation to any other Doctoral School (neither in
this country nor abroad),
- my application for degree earning has not been rejected in the past two years,
- in the past two years I have not had unsuccesful doctoral procedures,
- my doctoral degree has not been withdrawn in the past five years,
- my dissertation is independent work, I have not presented others' intellectual work as
mine, the references are definite and full, on preparation of the dissertation I have not
used false or falsified data.

Dated: 17/05/2021

signed by candidate

supervisor   co-supervisor

12. ACKNOWLEDGMENT: